ENV Report 38

Interim Report For The Upper Mississippi River — Illinois Waterway System Navigation Study

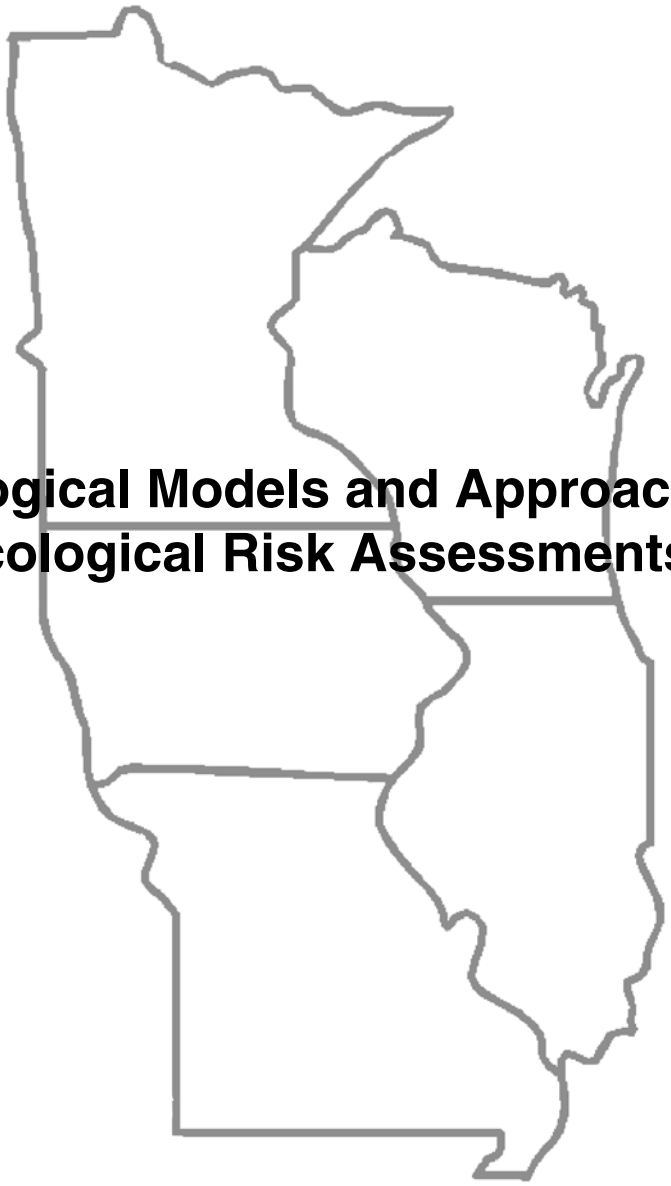

Ecological Models and Approach to Ecological Risk Assessments

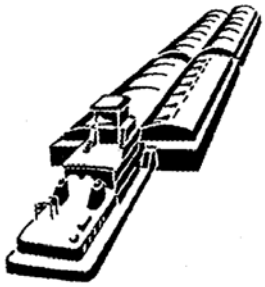

US Army Corps of Engineers®

September 2003

Rock Island District
St. Louis District
St. Paul District

Upper Mississippi River - Illinois Waterway
System Navigation Study

ENV Report 38
September 2003

Ecological Models and Approach to Ecological Risk Assessments

Steven M. Bartell, Kym Rouse Campbell, Erin M. Miller, and Shyam K. Nair

The Cadmus Group, Inc.
136 Mitchell Road
Oak Ridge, TN 37830

Elly P. H. Best

Environmental Laboratory
U.S. Army Engineer Research and Development Center
3909 Halls Ferry Road
Vicksburg, MS 39180-6199

David J. Schaeffer

EcoHealth Research, Inc.
701 Devonshire Drive
Champaign, IL 61820

Interim report

Prepared for U.S. Army Engineer District, Rock Island
Rock Island, IL 61204-2004
U.S. Army Engineer District, St. Louis
St. Louis, MO 63103-2833
U.S. Army Engineer District, St. Paul
St. Paul, MN 55101-1638

ABSTRACT: The Navigation Study being performed by the U.S. Army Corps of Engineers is assessing the potential environmental impacts associated with anticipated increases in commercial navigation traffic on the Upper Mississippi River-Illinois Waterway System. Each Navigation Study ecological risk assessment addresses a time period beginning with the present condition (defined as 2000) and continuing through the year 2050, in 10-year increments. Upon completion, the assessments will fulfill a requirement of the National Environmental Policy Act of 1969, and a subsequent Environmental Impact Statement, summarizing the results of each risk assessment, will be prepared. This report describes the overall approach adopted for performing the environmental assessments and presents several ecological models that were instrumental in their completion. The report also briefly outlines several hydraulic and hydrodynamic models necessary for the assessments and discusses their integration with the ecological models to estimate ecological impacts. Specific assessment results for each of the component ecological risk assessments (fish, submerged aquatic plants, and freshwater mussels) for future traffic scenarios are presented in separate reports of the Navigation Study series of technical publications.

Contents

List of Figures

List of Tables

Preface

The work reported herein was conducted as part of the Upper Mississippi River - Illinois Waterway (UMR-IWW) System Navigation Study. The information generated for this interim effort will be considered as part of the plan formulation process for the System Navigation Study.

The UMR-IWW System Navigation Study is being conducted by the U.S. Army Engineer Districts of Rock Island, St. Louis, and St. Paul under the authority of Section 216 of the Flood Control Act of 1970. Commercial navigation traffic is increasing and, in consideration of existing system lock constraints, will result in traffic delays that will continue to grow in the future. The system navigation study scope is to examine the feasibility of navigation improvements to the Upper Mississippi River and Illinois Waterway to reduce delays to commercial navigation traffic. The study will determine the location and appropriate sequencing of potential navigation improvements on the system, prioritizing the improvements for the 50-year planning horizon from 2000 through 2050. The final product of the System Navigation Study is a Feasibility Report which is the decision document for processing to Congress.

This report was written by Steven M. Bartell, Kym Rouse Campbell, Erin M. Miller, and Shyam K. Nair, The Cadmus Group, Inc.; Elly P.H. Best, formerly of American Science Corporation, now with Environmental Laboratory (EL), U.S. Army Engineer Research and Development Center (ERDC), and David J. Schaeffer, EcoHealth Research, Inc.

The development of each of the Navigation Study ecological risk assessments resulted from the participation of many individuals from government, academia, and the private sector in workshops, meetings, discussions, and correspondence. Developers of the fish assessment methodology included Tom Keevin, Steve Gutreuter, Dan Wilcox, Dave Schaeffer, John Dettmers, Ken Barr, John Barko, Al Jensen, and Webb Van Winkle, as well as input from members of the Navigation Environmental Coordinating Committee. The plant modeling and assessment approaches were developed from the inputs of John Barko, William Boyd, Dan Wilcox, Dave Soballe, Sarah Lubinski, Mike Stewart, and Steve Carpenter. The mussel assessment approaches were developed in large part through the active participation of Scott Whitney, Drew Miller, and Tom Keevin. The development of the methods and approaches for characterizing the commercial traffic, associated physical forces, river hydrodynamics, and river sediments resulted mainly from the continuing efforts of Sandra Knight, Steve Maynord, Ron Copeland, Tom Pokrefke, Charlie Berger, Rebecca Seal, and

David Abraham. The ongoing development of the overall system model and its integration with a geographic information system results mainly from the efforts of Sandra Knight, Rose Kress, Salvador Rivera, Scott Bourne, and the Model Integration and Simulation Team. The overall risk assessment methodology was made possible by the continued support and encouragement of Ken Barr, John Barko, and Jeff Holland. Thanks to Glenn Cada, Al Jensen, Steve Carpenter, and Ann Kimber for helpful review comments on an earlier version of this report.

Mr. Robert C. Gunkel, Jr., EL, ERDC, was responsible for coordinating the necessary activities leading to publication. Dr. Elizabeth C. Fleming was Acting Director, EL.

COL James R. Rowan was Commander and Executive Director of ERDC. Dr. James R. Houston was Director.

Summary

The Navigation Study being performed by the U.S. Army Corps of Engineers (USACOE) is assessing the potential environmental impacts associated with anticipated increases in commercial navigation traffic on the Upper Mississippi River-Illinois Waterway (UMR-IWW) System. Each Navigation Study ecological risk assessment addresses a time period beginning with the present condition (defined as 2000) and continuing through the year 2050, in 10-year increments. Upon completion, the assessments will fulfill a requirement of the National Environmental Policy Act (NEPA) of 1969, and a subsequent Environmental Impact Statement (EIS), summarizing the results of each risk assessment, will be prepared. This report describes the overall approach adopted for performing the environmental assessments and presents several ecological models that were instrumental in their completion. The report also briefly outlines several hydraulic and hydrodynamic models necessary for the assessments and discusses their integration with the ecological models to estimate ecological impacts. Specific assessment results for each of the component ecological risk assessments (fish, submerged aquatic plants, and freshwater mussels) for future traffic scenarios are presented in separate reports of the Navigation Study series of technical publications.

In designing each of the Navigation Study ecological risk assessments, participants anticipated that environmental impacts will be interpreted by the regulatory community [e.g., U.S. Environmental Protection Agency (USEPA)] primarily in the context of ecological risk. An ecological risk is the conditional probability of a specified ecological event occurring, coupled with some statement of its consequences (Campbell and Bartell 1998). The Navigation Study environmental assessments were, therefore, organized according to the framework recommended in the Guidelines for Ecological Risk Assessment (USEPA 1998). The ecological risk assessment process consists of three steps: problem formulation, analysis (characterization of exposure and characterization of ecological effects), and risk characterization. Completing each step might require the collection of new data and information.

The problem formulation component of each of the Navigation Study ecological risk assessments consists of developing a conceptual model of the entire assessment process. The conceptual model outlines the nature and sources of stress to the ecological resources, identifies the ecological resources potentially at risk, specifies the ecological impacts of concern regarding these resources, identifies relevant data and information, and suggests models and methods of analysis that can be used to estimate risks. The problem formulation

step emphasizes the need for discussion and participation among risk managers, risk assessors, and stakeholders in developing the overall design for risk assessment. In addition to the overall conceptual model, the conceptual model outlining each Navigation Study ecological risk assessment evolved through a series of meetings and workshops and continues to be evaluated by members of the Navigation Study's Model Integration and Simulation Team (MIST). Regular meetings with the Navigation Environmental Coordination Committee (NECC) provide opportunities for review and comments from representatives of state governments, other governmental agencies, environmental organizations, and the concerned public. The overall conceptual model is summarized below and is presented in detail in the body of this report.

In each ecological risk assessment, the ecological stressors take the form of the physical forces produced directly by commercial vessels navigating the UMR-IWW System and indirect effects that result from these forces. To characterize current commercial traffic intensity, a baseline number of vessels passing through each pool for each month was developed using 1992 lockage data. Existing fleet data were also analyzed to construct a data set that describes, by pool and by month, the relative distribution of vessels across categories of vessel direction, size, speed, load, and whether or not the vessel had a Kort nozzle. This classification scheme produced 108 possible configurations of commercial vessels operating on the UMR-IWW System. Future traffic scenarios were developed for the years 2000 through 2050, in ten-year increments, by USACOE economists based on economic considerations. In developing and assessing future traffic scenarios, the current fleet configuration were assumed to apply through the year 2050.

The direct hydrodynamic forces imposed by operating commercial vessels include increases in river current velocity, return currents, or drawdown; pressure changes and shear stresses associated with the propeller jet; shear stresses on the bed sediments beneath the vessel; and bed shear stresses extending to the channel borders and backwaters. The risk assessments do not specifically address the recognized direct physical impacts of vessels in turning basins or fleeting areas where, for example, turning propellers might mechanically disrupt sediments, uproot aquatic plants, or damage mussel beds. The primary indirect effect in the assessments of the effects of navigating commercial vessels is sediment resuspension. The analysis of exposure consists of performing laboratory experiments on physical replicas of river segments; making direct measurements on selected pools; and developing mathematical models to quantify the frequency, magnitude, extent, and duration of the hydrodynamic forces.

To characterize exposure (first part of the analysis step) across the UMR-IWW System, each pool has been spatially subdivided into cells. Each cell references a 3-dimensional location within a geographic information system (GIS) data file that describes the bathymetry of the pool and is assigned a unique identification code in relation to its pool location in river miles and distance of its center point left or right of the sailing line. A pool can consist of thousands of cells depending on overall pool dimensions, which vary with seasonal changes in river discharge and stage height. An exposure profile has been developed for each cell by executing the physical forces models for all 108 possible vessel configurations, for three different discharge regimes, and for three sailing line

positions. The results for each cell are stored as a series of coverages using a GIS.

Characterizing the ecological effects in the risk assessment, the second component of the analysis step, produced a set of possible adverse effects that includes commercial traffic-induced increases in fish early life stage mortality, degradation or loss of fish spawning habitat, physical breakage of submerged aquatic vegetation, impacts on the growth and reproduction of submerged aquatic vegetation, and impacts on the growth and reproduction of freshwater mussels. The increased likelihood of direct entrainment of fish larvae into the propeller jets of commercial vessels poses a risk of incremental increases in fish mortality. Vessel-induced changes in current velocities or alterations in sediment substrate might reduce the quantity and quality of suitable habitat for certain spawning guilds of fish in the UMR-IWW System. Sudden increases (or shifts in direction) of current velocity or increased wave heights resulting from vessel passage might physically uproot or break submerged aquatic plants. Incremental increases in suspended sediment concentrations resulting from increased commercial traffic might reduce the available light within the water column to the extent that species of submerged aquatic vegetation become limited by light, and photosynthesis is reduced. Reduced photosynthesis implies less carbohydrates available for allocation to growth and vegetative reproduction. Increased suspended sediments might also impair the filter feeding capabilities of freshwater mussels, including several threatened and endangered species that inhabit the UMR-IWW System, which would affect mussel growth and reproduction. The quantification of these ecological effects in relation to anticipated increases in commercial navigation traffic is the objective of each of the Navigation Study ecological risk assessments.

The risk assessments, as currently designed, do not examine possible indirect ecological effects. For example, an obligate life stage of freshwater mussels requires a period of attachment to fish; therefore, traffic-related reductions in fish abundance or diversity could, in theory, have an indirect negative impact on mussel survival. Several fish species utilize submerged aquatic vegetation for spawning, foraging, or protection from piscivores, and traffic-related reductions in submerged aquatic vegetation might also indirectly affect these aspects of fish ecology in the UMR-IWW System. However, in designing the Navigation Study ecological risk assessments, it was recognized that addressing indirect impacts was not possible given the sparse nature of ecological information, available time, and resources. The consideration of indirect impacts was deferred to future assessments and will depend, in part, on the results of the current assessments of direct effects.

In order to assess the ecological risks associated with the incremental increase in commercial navigation traffic on fish, 30 fish species that inhabit the UMR-IWW System were selected as a result of numerous meetings and workshops held throughout the Navigation Study. The fish species selected for the ecological risk assessment include species that have different life history strategies as well as species important to both the commercial and recreational fishery, important forage species, and species listed as threatened, endangered, or other similar category.

Potential impacts or risks posed by commercial vessels on fish larvae were assessed using the Conditional Entrainment Mortality (CEM) model (Boreman et al. 1981), which is a standard modeling approach for evaluating fish entrainment by power plant water intakes. The CEM model estimates the number of fish larvae that are drawn through and subsequently killed by the propeller jets of commercial vessels traversing each pool on the UMR-IWW System during the spawning season. Using published models, the results of the entrainment mortality calculations are extrapolated to estimates of future lost adults, recruitment forgone, and production forgone.

The Equivalent Adults Lost (EAL) model (Horst 1975, Goodyear 1978) extrapolates the calculated larval entrainment mortalities to the number of adult individuals lost from the future population. The EAL model essentially compares the incremental entrainment mortalities to natural mortalities suffered by larvae and juvenile life stages.

The Recruitment Forgone (RF) model (Jensen 1990) represents a more complex extrapolation of entrainment mortalities to lost future recruits. It addresses fish growth in addition to simply adding to natural mortality. The RF model is important in evaluating the implications of larval entrainment of individuals that fail to recruit to commercial and recreational fisheries in the UMR-IWW System.

The Production Forgone (PF) model (Rago 1984, Jensen et al. 1988) is analogous to the RF model, except that lost future biomass is estimated instead of individual recruits or adults. This model is important for assessing risks posed by commercial vessels on the biomass of important forage species [e.g., gizzard shad (*Dorosoma cepedianum*)], which may indirectly determine the population sizes of future commercial or recreational fisheries on the UMR-IWW System.

Fish spawning habitat suitability index (HSI) models have been developed for fish species representative of different spawning guilds for the UMR-IWW System. The HSI models are structured as a series of abiotic values describing different aspects of potential spawning habitat. Spawning index (*SI*) values are specified over the [0,1] interval, with a value of 0 meaning unsuitable spawning habitat and a value of 1 corresponding to optimal spawning habitat. For the UMR-IWW System, spawning habitat variables that were considered include water depth, current velocity, water level fluctuation, scour depth, vessel-induced changes in current velocity, and substrate size.

A combined phenological event and physiological model for growth and vegetative reproduction of submerged aquatic vegetation was adapted for sago pondweed (*Potamogeton pectinatus*) and American wild celery (*Vallisneria americana*), two representative species of the different growth forms that typify submerged aquatic vegetation growing in the main channel and main channel borders of the UMR-IWW System. Backwaters were not considered in the risk assessment. The two models were used to estimate the potential impacts of navigation-induced increases in suspended sediment concentrations on underwater light available for photosynthesis and biomass formation by these two aquatic plant species. In addition, a simple rule-based model was developed to identify combinations of traffic intensity, location of plants (including

potential plant habitat), and hydrodynamic conditions that might result in physical breakage of submerged aquatic plants.

A bioenergetics model for the threeridge mussel (*Amblema plicata*) was developed and implemented for locations of known mussel beds in the UMR-IWW System. The threeridge mussel was selected to represent the freshwater mussel community in the UMR-IWW System. It is one of the most common species and is widespread throughout the UMR-IWW System (USGS 1999). Additionally, it is one of the most important commercially-harvested species. The bioenergetics model was used to assess the potential impacts of navigation-induced increases in suspended sediment concentrations on the growth and reproduction of freshwater mussels.

Characterization of potential ecological risks posed by commercial traffic on the UMR-IWW System, the third step in the risk assessment process, is performed by integrating the ecological models with models that quantify the magnitude, extent, and duration of the physical forces produced by commercial vessels. The projected traffic scenarios that estimate the average number of vessels passing daily through each pool provide the initial conditions (e.g., vessels/day, vessel and barge configuration, direction, speed, draft) that drive the hydrodynamic forces models. Integration of the hydrodynamic forces models and the ecological models occurs by using the results of the hydrodynamic forces models as inputs to the ecological models.

One key aspect of ecological risk assessment that distinguishes this process from more historical environmental assessments performed under the NEPA is the explicit identification and quantification of uncertainties that enter into the analysis. Once quantified, these uncertainties are included in the assessment calculations to produce probabilistic estimates of ecological impacts (i.e., risks). In each of the Navigation Study ecological risk assessments, uncertainties enter the analysis in the form of bias and imprecision in the estimates of future traffic intensity, in the characterization of physical forces generated by specific vessel configurations, and in the ecological responses to those forces produced by the ecological models. Uncertainties also take the form of the simplifications and assumptions that are inherent in the modeling process. Another important aspect of the risk assessment process is that the resulting risk estimates can be analyzed using numerical methods to identify and rank-order the contributions of specific sources of uncertainty to the overall assessment results. Such analyses can be used to design additional studies or identify additional data collection that will provide the greatest return in reducing bias and imprecision per unit investment of future Navigation Study resources.

Upon completion of each of the Navigation Study ecological risk assessments, a set of integrated hydrodynamic and ecological models will have been developed, implemented, and evaluated for the UMR-IWW System. This integrated "system model" will provide USACOE planning personnel, resource managers, and decision makers with additional capabilities to characterize ecological impacts, calculate risks, and answer questions. For example, questions can be answered in relation to site-specific modifications or additions of navigation infrastructure, exploration of alternative plans for operation and maintenance, and other resource management challenges.

1 Introduction

The Mississippi River is an integral part of American heritage, a unique resource, and the best example of a multi-purpose river in the United States. The Mississippi River, with a drainage basin of nearly 4 million km^2, is one of the largest and most productive ecosystems in the world (Holland-Bartels et al. 1990b). The river above the confluence of the Ohio River is commonly called the UMR (Figure 1) and includes nearly 500,000 km^2 of watershed (Holland-Bartels et al. 1990b). The UMR, including the IWW and several important tributaries (Figure 1), is designated both a nationally-significant ecosystem and a nationally-significant navigation system. It is the only inland river in the United States to have such a designation. Many national wildlife refuges exist along the river corridor. The Mississippi Flyway is the migration corridor for 40% of North America's waterfowl and shorebirds, as well as an important flyway for raptors and neotropical songbirds. A total of 50 species of freshwater mussels have been recorded in the river system. In addition, the Mississippi River System is noteworthy among the world's large temperate rivers because it supports an unusually large number of fish species. Historically, at least 150 species of fish have been reported in the UMR (Gutreuter 1997).

The history of navigation on the UMR-IWW System began in the 1820s, when Congress authorized navigation improvements by the USACOE (Fremling and Claflin 1984). These improvements included the removal of snags and other obstructions in several locations of the Mississippi River and the construction of a canal connecting Lake Michigan to the Illinois River. Several navigation improvement projects, such as the excavation of rocks, closing off sloughs, construction of the 4.5-foot navigation channel, and construction of the 6-foot navigation channel, continued throughout the early 1900s (Fremling and Claflin 1984). Projects creating the current 9-foot navigation channel were authorized in the 1930s, and by 1940, most had been completed by the USACOE (Fremling and Claflin 1984). Twenty-nine locks and dams on the Mississippi River and eight on the Illinois River replaced rapids and falls with a series of terraced pools for commercial and recreational traffic (Figure 1). Habitats in a typical pool include a braided channel in the upper pool, a lotic area (e.g., flowing water) at the head of the pool, and a lentic environment (e.g., standing water) above the impounding lock and dam (Van Vooren 1983).

Commercial barge traffic transports a wide variety of essential goods on the UMR-IWW System. Agricultural commodities, petroleum products, and coal are the leading cargoes, with farm products accounting for approximately half of the total tonnage shipped. Estimates indicate that the transport of commodities on the river system could significantly increase in the future (Holland 1986,

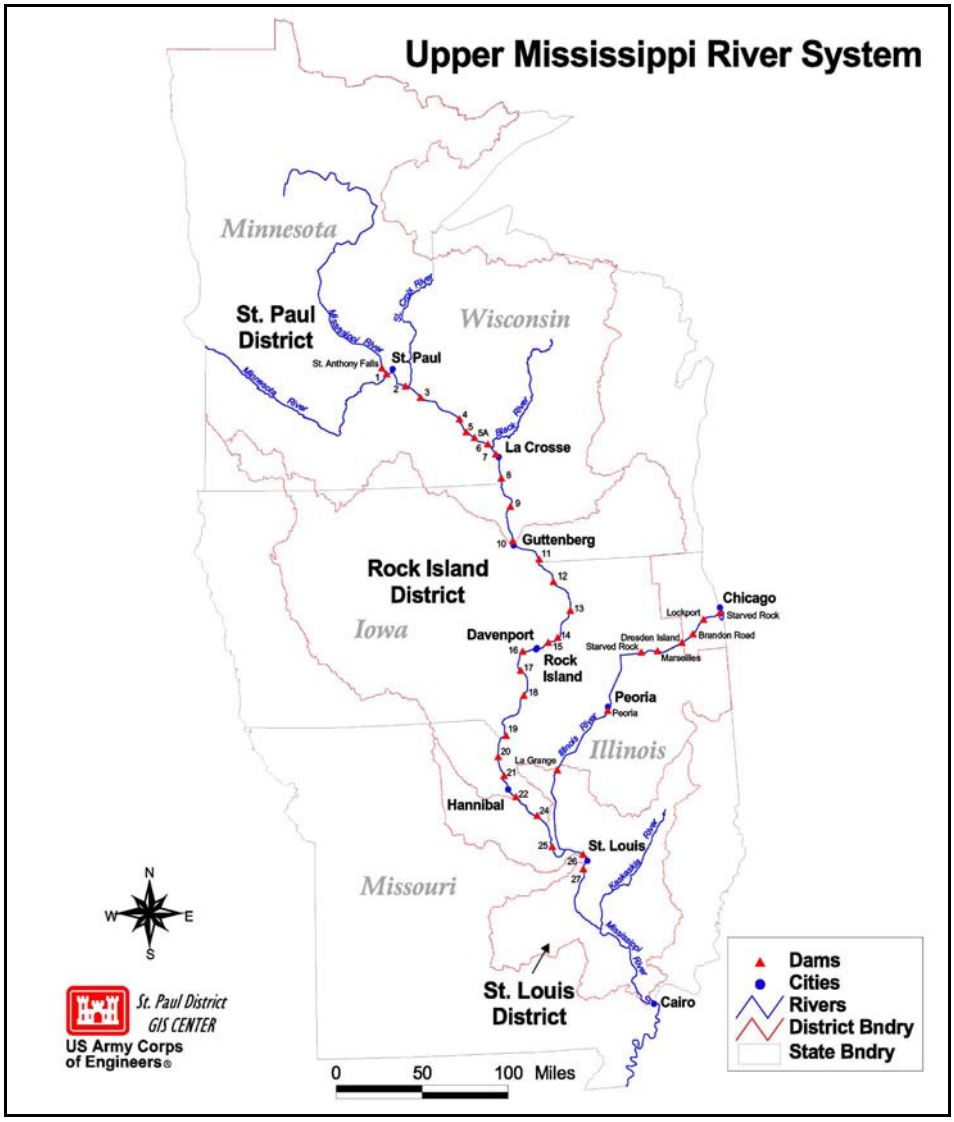

Figure 1. The Upper Mississippi River-Illinois Waterway System, the pool upstream from the dam has the same number or name as the dam

Holland-Bartels et al. 1990a). In the UMR-IWW System, a typical commercial "tow" consists of a tow boat and 15 barges with the configuration of 3 barges wide by 5 barges long (Holland 1986).

The UMR-IWW System Navigation Study being performed by the USACOE assesses the potential environmental impacts associated with anticipated increases in commercial navigation traffic. The assessments address a time period beginning with the year 2000 through the year 2050, in 10-year increments. Traffic projections have been developed by USACOE economists for the future (2000, 2010, 2020, 2030, 2040, and 2050). The conditions that would occur without any major improvements to the UMR-IWW System are referred to as the "without-project" conditions. Future traffic projections have also been developed for various navigation improvement alternatives, one of which will ultimately become the selected National Economic Development

(NED) Plan, for the years 2000-2050. Traffic that actually occurred on the river system in 1992 can be used as the baseline for comparison.

Upon completion, the assessments will fulfill a requirement of the NEPA of 1969, and a subsequent EIS summarizing the results of the assessments will be prepared. Results of the Navigation Study will be of importance in planning for any future modifications or additions to the infrastructure (e.g., locks and dams) that support commercial navigation.

This report describes the overall approach adopted for performing the environmental assessments and presents several of the ecological models that were used. The models are presented in detail, including statements of their relative strengths, limitations, and key underlying assumptions. The report also briefly outlines several hydraulic and hydrodynamic models necessary for the risk assessments. These models were integrated with the ecological models to ultimately estimate ecological impacts. Results of model applications to the UMR-IWW System future commercial traffic scenarios are not included as part of this report. Specific assessment results for each of the component ecological risk assessments (fish, submerged aquatic plants, and freshwater mussels) for future traffic scenarios are presented in separate reports of the Navigation Study series of technical publications.

Ecological risk assessment is becoming a common framework for assessing environmental impacts in relation to many environmental laws in the United States (e.g., Bartell et al. 1992). An ecological risk is the conditional probability of a specified ecological event occurring, coupled with some statement of its consequences (Campbell and Bartell 1998). In designing each of the Navigation Study ecological risk assessments, technical and planning personnel also recognized that environmental impacts will be interpreted by the regulatory community (e.g., USEPA) primarily in the context of ecological risk. The environmental assessments of the Navigation Study were, therefore, organized according to the framework contained in the Guidelines for Ecological Risk Assessment developed by the USEPA (USEPA 1998).

Chapter 2 briefly describes the ecological risk assessment process, specifically in relation to the potential impacts of commercial vessels on selected ecological resources in the UMR-IWW System. Chapter 2 also addresses the nature and sources of uncertainty that enter into the risk assessments. Clearly, any ecological assessment of this magnitude and complexity is subject to bias and imprecision. Example sources of uncertainty include background variability in the distribution and abundance of ecological resources in the UMR-IWW System, estimates of future traffic intensity and its spatial-temporal distribution in the system, and estimates of initial conditions and parameter values for the ecological and physical forces models. A major concern is that unacceptably high estimates of risk might result more from the high degrees of uncertainty entering the analyses, rather than from the actual magnitude of physical impacts produced by commercial vessels. Uncertainty propagation methods allow for the propagation of the uncertainties in the input parameters and models to the final estimate of the desired endpoint (e.g., risk). These methods are able to exclude single-point, extreme predictions that result when extreme values of the input parameters are used for model simulations with the objective of obtaining a

worst-case or conservative estimate of an ecological impact. However, such uncertainty propagation tools are computationally intensive. Therefore, the analyses in this study were conducted to obtain conservative, non-conservative, and central estimates of the impacts. Simulations in the uncertainty analysis framework were conducted later to compare the single-point predictions with the confidence intervals and central estimates developed from the uncertainty propagation methods.

Chapter 3 presents a detailed description of the ecological models developed and implemented to assess the impacts of commercial traffic on fish, submerged aquatic vegetation, and freshwater mussels. The strengths, limitations, and underlying assumptions important to each model are presented. However, comprehensive and detailed derivations of model input data and parameter estimates are presented in each individual ecological risk assessment that presents the results of applying these models to future scenarios of traffic increases on the UMR-IWW System.

Chapter 4 addresses the evaluation of performance of the ecological models and outlines approaches for ecological model verification, calibration, and validation that are planned in support of each of the Navigation Study ecological risk assessments. The fundamental structure of the ecological models, combined with the typically sparse nature of ecological data for much of the UMR-IWW System, poses considerable challenges to evaluating the accuracy and precision of the model calculations.

Chapter 5 discusses the integration of the ecological models with the hydrodynamic and hydraulic models to estimate ecological risks. In many instances, the direct measurement of physical forces (e.g., shear stresses, entrainment velocities), produced by moving commercial vessels remains extremely difficult, unacceptably dangerous, or impossible. Mathematical models have been developed to estimate these and other forces, as well as sediment resuspension, for vessels traveling through pools on the UMR-IWW System. One requisite to performing the ecological risk assessments lies in establishing the mathematical and data input connections between the physical forces models and the ecological models. This chapter briefly describes several physical forces models critical to the overall assessment and discusses the mechanics of integrating their calculations as inputs to the ecological models.

Chapter 6 completes this report by considering the ecological risk assessment process from the perspectives of risk-based decision making in relation to avoiding, minimizing, and mitigating ecological impacts associated with increased commercial navigation on the UMR-IWW System. From the beginning, it has been envisioned that one valuable by-product of the Navigation Study ecological risk assessments would be the development of an integrated system model that could be used as a general planning tool by USACOE personnel. For example, the system model might be used to evaluate the ecological implications of alternatives for operations and maintenance of the navigation infrastructure or for assessing the ecological effects anticipated for specific new construction or renovation projects. Chapter 6 discusses the possibilities of such a system model.

2 Ecological Risk Assessment

An ecological risk is the probability of a specified adverse ecological impact, combined with some statement concerning its consequences or significance (Bartell 1996). Risk can be defined for *k* adverse effects associated with *j* exposures to *i* stressors as:

$$Risk = \sum_k C_{(Ak)} \sum_j \sum_i P\left(A_k \setminus E_{ji}\right) P\left(E_{ji} \setminus S_i\right) P\left(S_i\right) \qquad \text{(Eq. 1)}$$

where,

A_k = adverse effect k,

C_k = consequences of A_k,

$P(A_k \setminus E_{ji})$ = probability of A_k given exposure E_j and stressor S_i,

$P(E_{ji} \setminus S_i)$ = probability of exposure E_j given stressor S_i, and

$P(S_i)$ = probability of stressor S_i.

For the Navigation Study ecological risk assessments, this model simplifies, in part, because $P(S_i)$ is assumed to be 1.0, that is, commercial vessels will continue to operate on the UMR-IWW System. In this analysis, the dimensionality of k is defined by the number of ecological impacts of concern. The term, $P(E_{ji} \setminus S_i)$, reinforces the fact that the presence of the stressor does not strictly imply exposure. Physical and biological processes with their associated relevant spatial-temporal scales (including natural fluctuations or variability) require that exposure be considered in a statistical sense for risk assessment. The relationships between exposure and adverse ecological effects are also probabilistic (or at least uncertain), as reflected in the term, $P(A_k \setminus E_{ji})$. Finally, the general risk model explicitly includes the consequences of the adverse effect(s) as fundamental to risk assessment. Thus, the general model more than hints at the need for close collaboration and communication among risk assessors and risk managers throughout the risk assessment process. The generalized model for risk is offered as a standard against which developing approaches for specific assessments can be evaluated, in this case for assessing risks posed by commercial navigation.

A simpler model was offered by Kaplan and Garrick (1981), who defined risk more generally as:

$$Risk = F\{x_i, p_i, s_i\} \qquad \text{(Eq. 2)}$$

In this model, risk is conceived as a functional integration of three components: x_i, which identifies a potential impact; p_i, which estimates the probability of occurrence of x_i; and s_i, which measures the significance of the impact, if it should occur. This model simply addresses the questions: What can happen? How likely is it to happen? And, what are the implications if it does? Though simpler than Equation 1, this model captures the key concepts of risk assessment and provides the conceptual basis for each of the Navigation Study ecological risk assessments.

This report is organized according to the framework recommended in the Guidelines for Ecological Risk Assessment (USEPA 1998). The USEPA Guidelines were developed to promote consistent approaches to ecological risk assessments, identify key issues, and define terminology (Bartell 1996). They represent a step towards developing guidelines for incorporating ecological principles into USEPA decisions (USEPA 1998). The Guidelines identify three components of an ecological risk assessment: problem formulation, analysis (characterization of exposure and characterization of ecological effects), and risk characterization (USEPA 1998) (Figure 2).

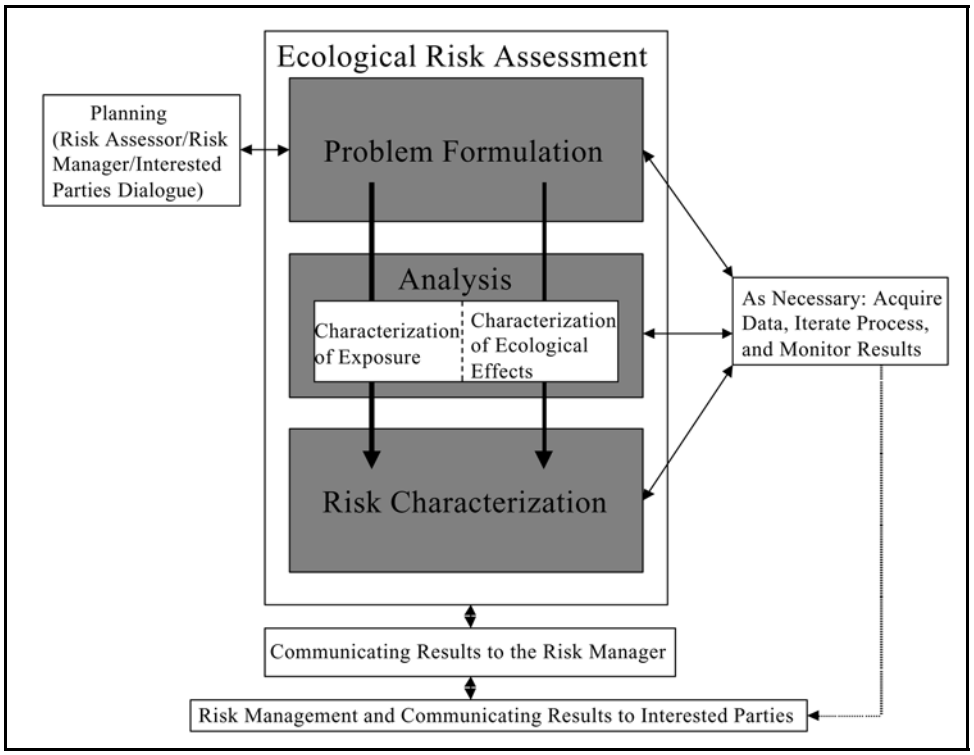

Figure 2. Schematic outline of the ecological risk assessment process, redrawn from USEPA (1998)

Problem Formulation

In addition to developing an overall conceptual model, the problem formulation component of each of the Navigation Study ecological risk assessments consists of developing a conceptual model of the entire assessment

process (Figure 3). The conceptual model outlines the nature and sources of stress to ecological resources, identifies ecological resources potentially at risk, specifies the ecological impacts of concern regarding these resources, identifies relevant data and information, and suggests models and methods of analysis that can be used to estimate risks. The problem formulation step emphasizes the need for discussion and participation among risk managers, risk assessors, and stakeholders in developing the overall design for risk assessment. The overall conceptual model outlining each of the Navigation Study ecological risk assessments evolved through a series of technical meetings and workshops and continues to be evaluated by members of the Model Integration and Simulation Team (MIST) (Figure 3). Regular meetings with the Navigation Environmental Coordinating Committee (NECC) provide opportunities for review and comments from representatives of state governments, other governmental agencies, environmental organizations, and the concerned public.

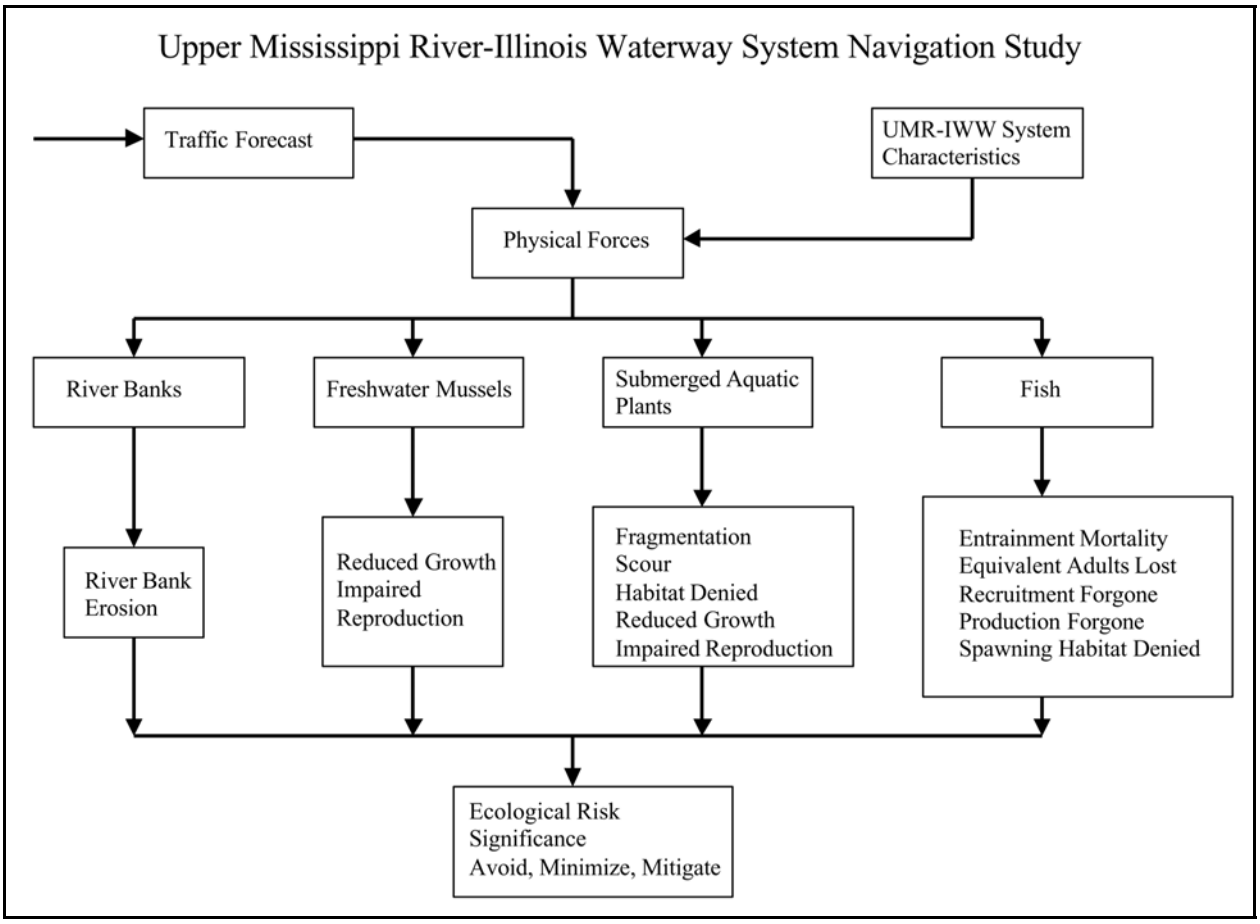

Figure 3. Overall conceptual model showing components of the Navigation Study environmental assessment

Analysis–Characterization of Exposure

In each ecological risk assessment, the ecological stressors take the form of the physical forces produced directly by commercial vessels navigating the

UMR-IWW System and indirect effects that result from these forces. To characterize current commercial traffic intensity, a baseline number of vessels passing through each pool each month was developed using 1992 lockage data. Existing fleet data were also analyzed to construct a data set that describes, by pool and by month, the relative distribution of vessels across categories of vessel direction, size, speed, load, and whether or not the vessel had a Kort nozzle. This classification scheme produced 108 possible configurations of commercial vessels operating on the UMR-IWW System under three water discharge regimes, and three sailing line positions. Future traffic scenarios were developed for the years 2000 through 2050 based on economic considerations. In developing and assessing future traffic scenarios, the current fleet configurations were assumed to apply through the year 2050.

The direct physical (or hydrodynamic) forces imposed by operating commercial vessels include increases in river current velocity, return currents, or drawdown; pressure changes and shear stresses associated with the propeller jet; shear stresses on the bed sediments beneath the vessel; and bed shear stresses extending to the channel borders and backwaters. The risk assessments do not specifically address the recognized direct physical impacts of vessels in turning basins or fleeting areas where, for example, turning propellers might mechanically disrupt sediments. The primary indirect effect identified in assessing the effects of navigating commercial vessels is sediment resuspension. The analysis of exposure consists of performing laboratory experiments on physical replicas of river segments; making direct measurements on selected pools; and developing mathematical models to quantify the frequency, magnitude, extent, and duration of the physical forces.

To analyze exposure across the UMR-IWW System, each pool has been spatially subdivided into cells. Each cell references a 3-dimensional location with a GIS data file that describes the bathymetry of the pool and is assigned a unique identification code in relation to its pool location in river miles and distance of its center point left or right of the sailing line (e.g., 135R5250 = 135 m to the right of the sailing line at River Mile 525.0). Cell dimensions are 10-m wide by 0.5-miles in length in the Long Term Resource Monitoring Program (LTRMP) trend pools (UMR Pools 4, 8, 13, and 26, and the IWW LaGrange Pool) and extend from the water surface to the river bottom. In the non-trend pools, cell dimensions are 10-m wide by 1.0-miles in length. A pool can consist of thousands of cells depending on overall pool dimensions, which vary with seasonal changes in river discharge and stage height. An exposure profile has been developed for each cell by executing the physical forces models for all 108 possible vessel configurations, three water stage heights, and three sailing line positions. The results for each cell are stored as a series of GIS coverages.

Analysis–Characterization of Ecological Effects

The analysis of the ecological effects components in each of the risk assessments produced a set of possible adverse effects that includes commercial traffic-induced increases in fish early life stage mortality, degradation or loss of fish spawning habitat, physical breakage of submerged aquatic vegetation,

impacts on the growth and reproduction of submerged aquatic vegetation, and impacts on the growth and reproduction of freshwater mussels. The increased likelihood of direct entrainment of fish larvae into the propeller jets of commercial vessels poses a risk of incremental increases in fish mortality. Vessel-induced changes in current velocities or alterations in sediment substrate might reduce the quantity and quality of suitable habitat for certain spawning guilds of fish in the UMR-IWW System. Sudden increases (or shifts in direction) of current velocity or increased wave heights resulting from vessel passage might physically uproot or break submerged aquatic plants. Incremental increases in suspended sediment concentrations resulting from increased commercial traffic might reduce the available light within the water column to the extent that species of submerged aquatic vegetation become light-limited and photosynthesis is inhibited or reduced. Reduced photosynthesis implies less carbohydrates available for allocation to growth and vegetative reproduction. Increased suspended sediments might also impair the filter feeding capabilities of freshwater mussels, including several threatened and endangered species that inhabit the UMR-IWW System, which would affect mussel growth and reproduction. The quantification of these ecological effects in relation to anticipated increases in commercial navigation traffic is the objective of each of the Navigation Study ecological risk assessments.

The risk assessments, as currently designed, do not examine possible indirect ecological impacts. For example, an obligate life stage of freshwater mussels requires a period of attachment to fish; therefore, traffic related reductions in fish abundance or diversity could, in theory, have an indirect negative impact on mussel survival. Several fish species utilize submerged aquatic vegetation for spawning, foraging, or protection from piscivores, and traffic-related reductions in submerged aquatic vegetation might also indirectly affect these aspects of fish ecology in the UMR-IWW System. However, in developing the Navigation Study, it was recognized that addressing indirect impacts was not possible given the sparse nature of ecological information, available time, and resources. The consideration of indirect impacts was deferred to future assessments and will depend, in part, on the results of the current assessment of direct impacts.

Risk Characterization

Characterization of the potential ecological risks posed by commercial traffic on the UMR-IWW System, the third step in the risk assessment process, is performed by integrating the ecological models with models that quantify the magnitude, extent, and duration of the hydrodynamic forces produced by commercial vessels. The future traffic scenarios that estimate the average number of vessels passing daily through each pool provide the initial conditions (e.g., vessels/day, vessel and barge configuration, direction, speed, draft) that drive the physical forces models. Model integration occurs in the sense that the results of the physical and hydrodynamic forces models serve as inputs to the ecological models.

One key aspect of ecological risk assessment that distinguishes this process from more historical environmental assessments performed under the NEPA is

the explicit identification and quantification of uncertainties that enter into the analysis. Once quantified, these uncertainties are included in the assessment calculations to produce probabilistic estimates of ecological impacts (i.e., risks). In the Navigation Study ecological risk assessments, uncertainties enter the analysis in the form of bias and imprecision in the estimates of future traffic intensity, in the characterization of physical forces generated by specific vessel configurations, and in the ecological responses to those forces produced by the ecological models. Uncertainties also take the form of the simplifications and assumptions that are inherent in the modeling process. Another important aspect of the risk assessment process is that the resulting risk estimates can be analyzed using numerical methods to identify and rank-order the contributions of specific sources of uncertainty to the overall assessment results. Such analyses can be used to design additional studies or identify additional data collection that will provide the greatest return in reducing bias and imprecision per unit investment of future Navigation Study resources.

Characterizing Uncertainty

Bias and imprecision are anticipated for each general component of the Navigation Study ecological risk assessments: traffic projections, physical forces models, and ecological models. The nature and sources of bias and imprecision associated with each aspect of the UMR-IWW System risk assessments will be addressed during the Navigation Study. Where possible, uncertainties will be quantified, incorporated into the calculations of ecological impacts, and included in the presentation of results. The description, quantification, and propagation of uncertainties through the analyses differentiates risk assessment from more traditional NEPA environmental impact assessments.

At least two types of uncertainty are inherent to the assessment process: model uncertainty and uncertainty about the model parameter values. The following sections briefly describe these kinds of uncertainty and how they pertain to different components of each of the Navigation Study ecological risk assessments.

Model uncertainty

Model uncertainty results from the incomplete understanding of the phenomenon being modeled and the necessary simplifications, assumptions, and formulations used to derive the model. Model uncertainty can also result from arbitrary choices of how much (or how little) detail to explicitly include in the model (i.e., aggregation error). Uncertainty in mathematical structure might include, for example, the assumed linear relationships that describe the different components of the fish spawning HSI models in relation to changes in current velocity or alteration of sediment substrate. When attempting to evaluate uncertainty in models, addressing the following questions prove useful:

- Have the necessary and sufficient system components and processes been identified and incorporated into the model?

- Have the mathematical equations that constitute the model been formulated in a manner consistent with the data and process-level understanding of the physical or ecological phenomenon of interest?

- If there are alternative models, what are the significant differences in model structure or data sets used for model development?

Parameter uncertainty

Parameter uncertainty refers to the accuracy and precision of the values used to calculate model results. Uncertainty in model parameters can result from the absence of directly-applicable data, the variability in available data, inappropriate sampling, and/or incorrect data analysis and interpretation. Parameter uncertainty will, of course, influence the accuracy and precision of any model estimate throughout the assessments; increasingly uncertain model parameter values can impact the accuracy and precision of all models used in the assessments. Therefore, describing and quantifying uncertainty associated with model parameters is an important part of the risk assessment process.

To characterize uncertainties in model parameters, available data and information will be reviewed. Clearly, species-specific and site-specific data, whenever available, should be used to quantify parameter uncertainty. In their absence, professional judgment might be used to formally characterize uncertainty associated with model parameters. The nature and sources of uncertainties associated with parameter estimates will be documented as part of the Navigation Study risk assessment process.

Quantifying Uncertainty

Bias and imprecision associated with model parameter estimates and initial conditions will be addressed by defining input parameters as statistical distributions where logical. Distributions will be developed on the basis of existing data and professional judgment. The selection of parameter distribution types (e.g., normal, lognormal, exponential, triangular, etc.) will follow a sequential prescription: if data are sufficient, the "best-fit" distribution will be used to characterize the parameter value; if only a range of possible values is available, a uniform distribution will be developed; if data permit estimation of a range and some central tendency, a triangular distribution will be selected. A distribution may also be defined for a given model input if physical, hydrological, hydraulic, or biological theory or empiricism justifies or determines its selection.

Propagating Uncertainties

Monte Carlo simulations will be used to propagate uncertainties through the models primarily to compare the single-value modeled impacts with distributions of estimated impacts produced by these methods of uncertainty propagation. It is well known that single-value estimates, made with conservative estimates of

input parameters, yield results that can be extremely and unrealistically conservative. The Monte Carlo simulations would permit the determination of the degrees of conservatism reflected in the single-value estimates. The number of simulations and the sampling procedure (i.e., simple random and stratified random) will be determined by the particular model and scenario. Results of the Monte Carlo simulations will be summarized as distributions of possible impact or risk. These distributions will be used to present the selected impact results in a probabilistic framework consistent with quantitative risk assessment (e.g., Bartell et al. 1992, Bartell 1996).

3 Ecological Models for Risk Characterization

To successfully realize the objectives of each of the Navigation Study ecological risk assessments, methods, tools, and ecological models were developed to translate the current and future traffic scenarios into estimates of associated ecological impacts on fish, fish spawning habitat, submerged aquatic vegetation, and freshwater mussels. The models complement laboratory and field studies of commercial impacts on these ecological resources.

Larval Fish Entrainment Models

In order to assess the ecological risks to fish associated with the incremental increase in commercial navigation traffic, 30 fish species that inhabit the UMR-IWW System were selected (Table 1). This list of 30 species was assembled as a result of numerous meetings and workshops held throughout the Navigation Study period. The fish species selected for the ecological risk assessment include species that have different life history strategies as well as species important to both the commercial and recreational fishery, important forage species, and species listed as threatened, endangered, or in another similar category.

The following sections describe the models that have been used to assess the incremental ecological risks posed by projected increases in commercial navigation traffic on fish of the UMR-IWW System. These models include the CEM model (Boreman et al. 1981), the EAL model (Horst 1975, Goodyear 1978), the RF model (Jensen 1990), and the PF model (Rago 1984, Jensen et al., 1988). These models have been the subject of intensive discussion and debate, as well as follow-up implementation and evaluation since the inception of the Navigation Study technical working groups on larval, juvenile, and adult fish. Alternative models were identified and discussed, including individual-based models, demographic population models, bioenergetic- based models, and comprehensive ecosystem models. However, it was recognized that the data requirements for these kinds of models realistically prohibited their implementation for an assessment of this magnitude (i.e., 30 fish species, 30+ pools, multiple years, multiple traffic alternatives).

The following descriptions outline the basic purpose, mathematical structure, and underlying assumptions of the four models that are being used to assess risks

Table 1
Fish Species Selected to Assess the Ecological Risks Associated With the Incremental Increase in Commercial Navigation Traffic

Scientific Name	Common Name	Category[1]
Family Acipenseridae - Sturgeons		
Scaphirhynchus platorynchus	Shovelnose sturgeon	Commercial
Scaphirhynchus albus	Pallid sturgeon	Listed
Acipenser fulvescens	Lake sturgeon	Listed
Family Polyodontidae - Paddlefishes		
Polyodon spathula	Paddlefish	Commercial, Listed
Family Lepisosteidae - Gars		
Lepisosteus platostomus	Shortnose gar	Commercial
Family Amiidae - Bowfins		
Amia calva	Bowfin	Commercial
Family Clupeidae - Herrings		
Dorosoma cepedianum	Gizzard shad	Forage
Family Hiodontidae - Mooneyes		
Hiodon alosoides	Goldeye	Listed
Hiodon tergisus	Mooneye	Commercial
Family Esocidae - Pikes		
Esox lucius	Northern pike	Recreational, Listed
Family Cyprinidae - Minnows		
Cyprinus carpio	Common carp	Commercial
Notropis atherinoides	Emerald shiner	Forage
Family Catostomidae - Suckers		
Carpiodes carpio	River carpsucker	Commercial
Cycleptus elongatus	Blue sucker	Listed
Ictiobus bubalus	Smallmouth buffalo	Commercial
Ictiobus cyprinellus	Bigmouth buffalo	Commercial
Minytrema melanops	Spotted sucker	Commercial
Moxostoma macrolepidotum	Shorthead redhorse	Commercial
Family Ictaluridae - Catfishes		
Ictalurus punctatus	Channel catfish	Commercial, recreational
Ictalurus furcatus	Blue catfish	Commercial, recreational
Pylodictis olivaris	Flathead catfish	Commercial, recreational
Family Moronidae - Temperate Basses		
Morone chrysops	White bass	Recreational
Family Centrarchidae - Sunfishes		
Lepomis macrochirus	Bluegill	Forage, recreational
Micropterus dolomieu	Smallmouth bass	Recreational
Micropterus salmoides	Largemouth bass	Recreational
Pomoxis annularis	White crappie	Recreational
Pomoxis nigromaculatus	Black crappie	Recreational
Family Percidae - Perches		
Stizostedion canadense	Sauger	Recreational
Stizostedion vitreum	Walleye	Recreational
Family Sciaenidae - Drums		
Aplodinotus grunniens	Freshwater drum	Commercial, recreational

[1] Commercial = Of commercial importance
Recreational = Of recreational importance
Listed = State or federal listed as threatened, endangered, candidate for listing, need of management, etc.

posed by navigation traffic on fish in the UMR-IWW System. Discussions concerning the feasibility of implementation, as well as strengths and limitations of these models, are reserved for Chapter 4.

The Conditional Entrainment Mortality model

The Conditional Entrainment Mortality model (Boreman et al. 1981) has been adapted to estimate the mortality suffered by larval fish as a function of increased commercial traffic on the UMR-IWW System. This model is also known as the Empirical Transport model or the Proportional Mortality model. The CEM model has been used mainly to estimate larval fish mortality associated with entrainment by the water intake structures that are part of the cooling systems of electric power generating facilities (e.g., Boreman et al. 1981, Boreman and Goodyear 1988). Adapting this model for the assessment of fish entrainment by commercial traffic required quantification of the volumes of water entrained through the propellers of different commercial vessels and barge configurations that operate on the UMR-IWW System.

Fish mortality due to entrainment in the propeller zone of a passing vessel can be expressed as the fraction of the initial population (or life stage) that would die assuming no other sources of mortality. For a group of fish vulnerable to entrainment, the CEM rate, m_T, can be defined as (Boreman et al. 1981):

$$m_T = 1 - \sum_{s=1}^{S} R_s \prod_{j=0}^{J} \prod_{l=1}^{L} \sum_{k-1}^{K} D_{lk} \exp\left(-E_{s+j,lk}\, C_{jl}\, t_j\right) \qquad \text{(Eq.3)}$$

where,

R_s = the proportion of total eggs spawned in months over the entire spawning season, S,

j = the age group of individuals for J-age groups within each life stage,

l = life stage of L total life stages addressed by the model application,

k = one of K total regions within the water body subjected to entrainment,

$D_{l,k}$ = the proportion of age-j organisms initially occurring in region k,

$E_{s+j,l,k}$ = the instantaneous entrainment mortality rate constant (time^{-1}) of life stage-l organisms in region k during time step $s + j$,

$C_{j,l}$ = the fraction of age-j organisms in life stage l, and

t_j = the duration of age-j.

Several simplifying assumptions were made that reduced the complexity of implementing Equation 3 for this assessment. All organisms within each life stage were assumed to be of equal age; therefore, j equaled 1. The entrainment calculations focused on the navigation channel as the single region within each UMR-IWW System pool; therefore, k was also 1, and D_{lk} dropped out of the model. Finally, all age-j organisms were assumed to be in the same life stage: C_{jl}

equaled 1. Entrainment was calculated each month of the spawning season for each of the selected fish species. Therefore, R_s defined the fraction of total spawning that occurred in month s, and t_j was defined correspondingly as the number of days in each month of the spawning season for each species (Boreman et al. 1981). The reduced form of Equation 3 used in the calculations was thus:

$$m_T = 1 - \sum_{s=1}^{S} R_s \exp\left(-E_{s+j}, t_j\right) \qquad \text{(Eq. 4)}$$

In the assessment, E_{s+j} defined the instantaneous entrainment mortality rate constant for each life stage and specified time interval (e.g., month). The instantaneous constant, E, is a function of the amount of water entrained by the propellers per unit time in relation to the volume of river (i.e., hydraulic classification pool volume), the susceptibility of the fish (life stage) to entrainment, and mortality subsequent to entrainment. In general form it is:

$$E = Q\, w\, f / V \qquad \text{(Eq. 5)}$$

where, Q is the volumetric flow through the propeller(s), w is the ratio of the average concentration of the fish life stage in the entrained water to the average concentration in the river volume, f is the fraction of entrained organisms killed as a result, and V is the volume of the river pool being modeled. In the adaptation used to assess navigation impacts on fish life stages, Equation 5 was re-formulated as:

$$E_i = n\, R\, w_i\, f_i\, t_i \qquad \text{(Eq. 6)}$$

where, $R = Q/V$, and n specifies the number of tows passing through the pool per day. The parameter, w_i, estimates the relative concentration of life stage i individuals in the zone of entrainment compared to the concentration of individuals in the remainder of the main channel. The f_i value defines the fraction of individuals entrained that are killed for life stage i. In this assessment, $i = 1$ for the larval stage, 2 for young-of-the-year, and 3 for adult fish. The parameter, t_i, is the duration of life stage i (days).

The flow rates (Q) through propellers were determined from the work of Maynord (1999) and Holley (1997). Fleet characteristics were summarized for the 1992 baseline traffic condition using lockage records. The expected value and variance of the entrainment rate for vessels on each pool and for each month were estimated as a function of the size, speed, direction, and draft depth of the vessel and its barges. The total volume of water entrained per day was calculated as the product of Q times the number of seconds required for a vessel to traverse the pool of interest. This volume was calculated using three combinations of estimated entrainment rates and vessel speeds (relative to the water): mean value of Q and vessel speed (i.e., the expected vessel), the mean + 1 standard deviation (SD) of Q plus the mean - 1 SD of velocity (e.g., a slow moving vessel that entrained a large volume), and the mean - 1 SD of Q with the mean + 1 SD of

velocity (e.g., an efficient vessel moving quickly and entraining comparatively smaller volumes). Of the possible combinations of estimated Q and reported velocities, the last two consistently provided the highest and lowest projected entrainment volumes.

In addition, the DIFFLARV model (Holley 1997) serves as an independent check on the assumption that the river segment traversed by a commercial vessel is completely mixed before the next vessel passes. This model was developed to estimate what fraction of water entrained by a vessel was previously entrained by the immediately preceding vessel. Caution was taken in developing and applying the CEM model to avoid killing the same individuals more than once. Analysis of the DIFFLARV model simulations of selected intensive traffic scenarios suggested that entrainment of water by successive vessels is, at most, a few percent given the expected traffic densities. As new traffic projections were developed, the DIFFLARV model was used to re-evaluate the underlying assumption of complete channel mixing between successive vessel passages.

Pool volumes (V) were estimated using changes in bathymetry associated with seasonal differences in discharge and corresponding stage height. Analyses of existing data were used to estimate the 10^{th}, 50^{th}, and 90^{th} percentiles of discharge for pools on the UMR-IWW System, and these percentiles defined low, medium, and high stage heights and their corresponding pool volumes. The seasonally-dependent probability of these stage heights was estimated for each pool (Kevin Landwehr, USACOE, Rock Island District, pers. comm.), and a monthly expected value of pool volume was calculated for use in estimating R in the CEM model.

A w_i value was estimated for each life stage of each species for each month of the year. The w_i values were derived from the life history information for each species discussed during workshops or obtained from the literature. The w_i value is 0 if the life stage for that particular species does not occur in the main channel in that particular month. The w_i value is 0.25 if the average concentration of the life stage of that particular species in the main channel to the average concentration in the main channel river volume for that month is very small, such as what occurs for some bottom-dwelling species or species that spend a majority of time in the backwaters (i.e., larvae of a particular species is usually found in the backwaters; however, larval density data indicate that they are flushed into the main channel and are present at low densities during the spawning season). w_i is 0.50 if the average concentration of the life stage of that particular species in the main channel to the average concentration in the main channel river volume for that month is fairly low (this value also applied to some species closely associated with the river bottom). Lastly, w_i is 1.0 if the concentration of that particular life stage for a species in a given month is evenly distributed across the main channel (i.e., larvae of main-channel spawners).

Equation 6 demonstrates that E_i varies in direct proportion to the value of f_i. Thus, the assessment of entrainment mortality is sensitive to the estimate of the f_i parameter. Experimental results reported by Killgore et al. (1997) were analyzed to provide realistic estimates of f_i values for the 30 species of concern in the UMR-IWW System Navigation Study Fish Ecological Risk Assessment [Steve Maynord and Jack Killgore, USACOE, Waterways Experiment Station (WES),

Vicksburg, MS, pers. corres.]. Killgore et al. (1997) performed laboratory experiments on four species of larval fish (shovelnose sturgeon, lake sturgeon, paddlefish, and blue sucker) and one species of juvenile fish (common carp) to determine the percent mortality (initial and delayed) resulting from entrainment through the propeller zone. It was suggested that the experimental mortality results might reasonably be examined in relation to shear stresses calculated for the propeller entrainment zones. Experiments were performed under different shear stresses that were determined largely by the selected propeller revolutions per minute. Based on the analyses of the experimental results (Killgore et al. 1997), regression models were developed for fish larvae classified according to size.

For small larvae (<10 mm in total length):

$$f_i = 0.008\ (S) + 45.45, \qquad df = 11,\ R^2 = 0.35 \qquad \text{(Eq. 7)}$$

For large (>10 mm in total length) larvae of lentic fish:

$$f_i = 0.018\ (S) - 2.12, \qquad df = 18,\ R^2 = 0.83 \qquad \text{(Eq. 8)}$$

For large (>10 mm in total length) larvae of lotic fish:

$$f_i = 0.009\ (S) + 13.12, \qquad df = 7,\ R^2 = 0.86 \qquad \text{(Eq. 9)}$$

where, S = shear stress (dynes/cm^2).

Shear stress values were calculated for all 108 possible vessel configurations used in the larval entrainment calculations. Larvae of the 30 species of interest were classified, using published larval length values or lengths estimated from age-length regressions, as small, larger lentic, or larger lotic larvae. Finally, values of f_i were calculated for all 30 species using the appropriate regression equations (Equations 7-9) for all 108 vessel configurations.

The resulting f_i values distributed among the 108 possible vessel types and their corresponding shear stresses are illustrated in Figures 4-6. The values range from approximately 0.1 to 1.0 for the three larvae types. The modal value of f_i for small larvae was estimated as approximately 0.65, with a range of 0.5 to 1.0 (Figure 4). The f_i values for large, lentic larvae, estimated from propeller shear forces, range from 0.1 to 1.0, with a modal value of approximately 0.35 (Figure 5). The f_i values calculated for large, lotic larvae range from 0.2 to 0.75 with a modal value of approximately 0.33 (Figure 6).

The f_i values selected from these distributions in assessing alternative traffic scenarios vary in relation to the relative frequency of the 108 different vessel configurations reported for each month and pool of the UMR-IWW System. These relative frequencies were determined from 1992 lockage data and were assumed to remain constant over the project period (e.g., years 2000-2050).

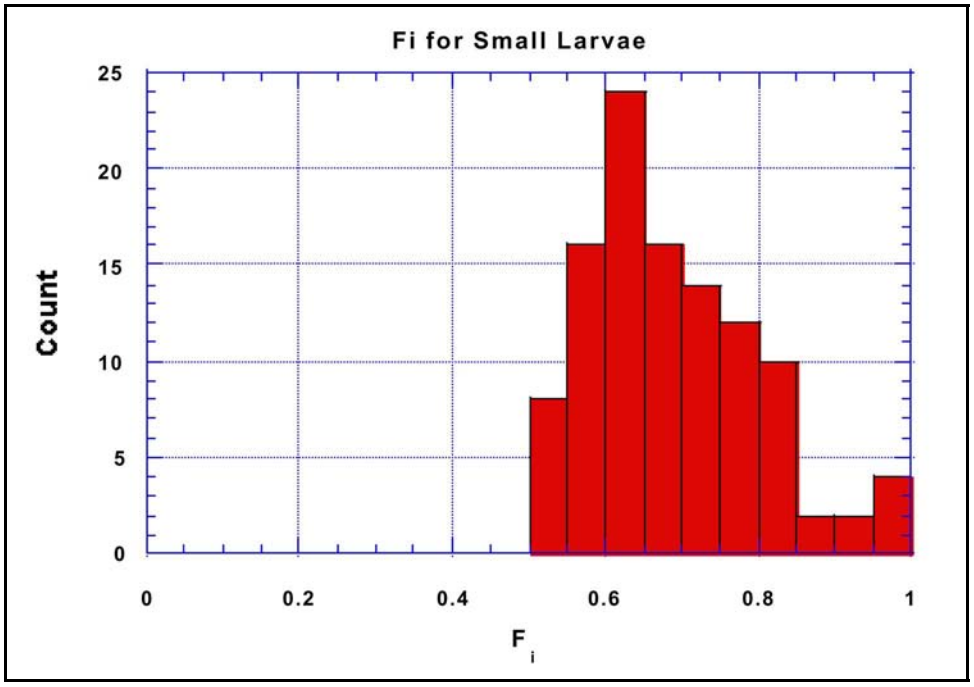

Figure 4. The distribution of f_i for small larvae (<10 mm in total length)

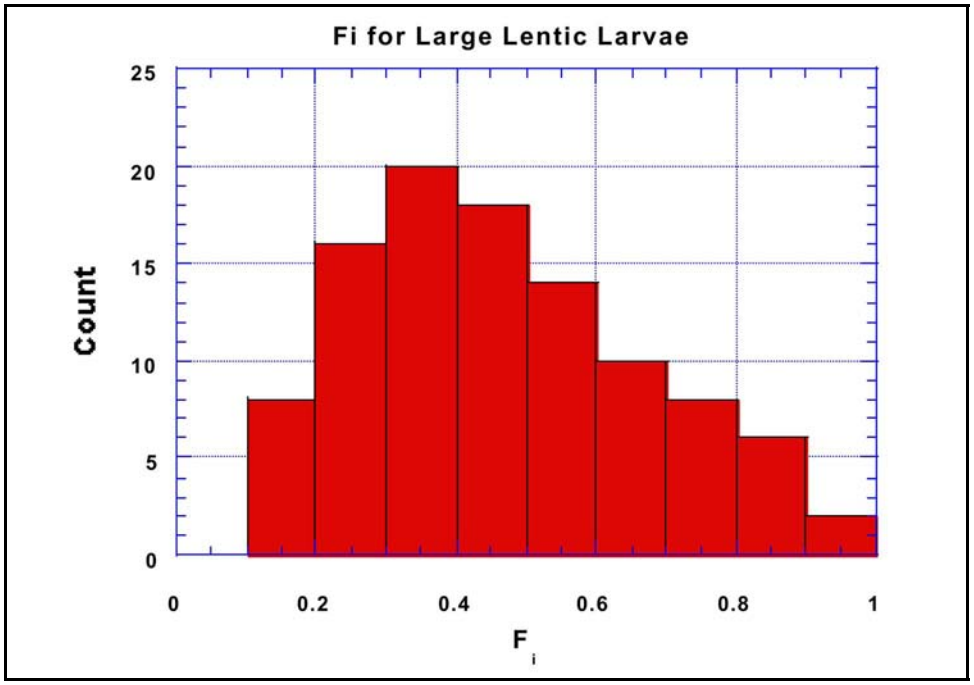

Figure 5. The distribution of f_i for large, lentic larvae (>10 mm in total length)

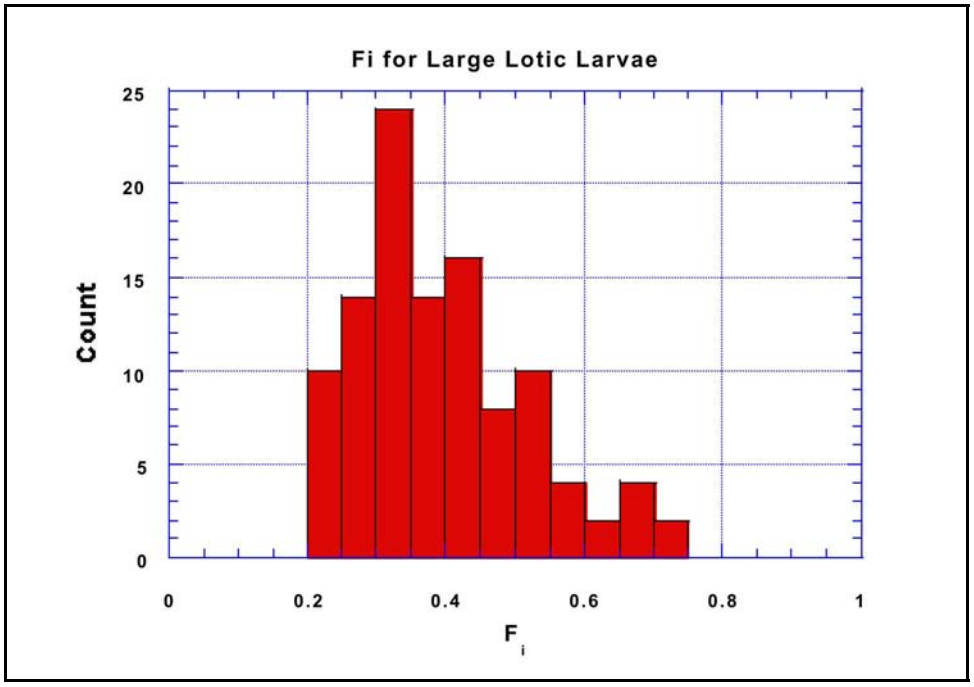

Figure 6. The distribution of f_i for large, lotic larvae (>10 mm in total length)

The CEM model can estimate the proportional mortality for three life stages of each species assessed: larvae, young-of-the-year, and adult fish. However, the Navigation Study Ecological Risk Assessment only addressed larval mortality for each species and traffic scenario. Larval entrainment data for selected power plants on the UMR-IWW System have been used to provide some context for evaluating the results of the CEM model calculations for commercial vessels. The cooling water intakes of power plants located on the UMR-IWW System are additional sources of larval entrainment mortality. Fish larvae are killed because they are entrained in or impinged on the power plant water intake structures. The increase in larval mortality that results from increased commercial traffic has been compared on a pool-by-pool basis to larvae entrained by power plants.

The calculated values of proportional mortality define an ecological effect of concern in assessing risks. Functions relating traffic intensity (i.e., vessels/day) to estimates of proportional mortality can be constructed using the model for specific traffic scenarios. More consistent with a probabilistic framework for risk, the uncertainties associated with the parameter values can be quantified and propagated through the calculations to estimate the likelihood that proportional mortality will exceed a specified value (e.g., 0.10).

In addition to directly examining the CEM estimates for different species, pools, and traffic scenarios, the results of the CEM model also serve as inputs to the EAL model. The EAL model extrapolates entrainment mortalities to estimates of the numbers of future individual adult fish that will be lost from the population as a result of a commercial vessel passage through a pool. Correspondingly, one method of integrating the effects of multiple vessels and pools lies in simply adding the number of future lost adults for each species and traffic scenario.

Equivalent Adults Lost model

Estimating the impacts of the incremental mortality of early life stages of fish in terms of losses in future adults is an important component of the Navigation Study Fish Ecological Risk Assessment. These losses were calculated using the Equivalent Adults Lost model (Horst 1975, Goodyear 1978). The EAL model translates the proportional mortalities estimated by the CEM model to numbers of lost future fish as the result of entrainment mortality suffered by larvae. The number of future adults lost due to larval entrainment mortalities was estimated using the equation:

$$EAL = L\left(\exp\left[-\sum_{i=1}^{3} Z_i t_i \right] - \exp\left[-\sum_{i=1}^{3} \left(Z_i + T_i \right) t_i \right] \right) \qquad \text{(Eq. 10)}$$

where,

i = 1 (larvae), 2 (young-of-the-year), or 3 (adult),

L = number of entrained and killed larvae,

t_i = duration of life stage i (days),

Z_i = non-tow (natural) mortality rate of life stage i, and

$T_i = n\ A\ R_i\ w_i f_i$ = tow-induced mortality rate of life stage i (see description of the CEM model).

Calculation of EAL requires estimates for the same parameters used in the CEM model (Boreman et al. 1981), together with estimates for the non-tow or natural mortality rates for each fish life stage. That is, the tow-induced mortalities are estimated using the CEM model. Natural mortality rates have been estimated for larvae, young-of-the-year, and adults for the 30 species of fish selected for the risk assessment. These mortality rates were obtained primarily through searching the technical literature, or where data were not available, professional judgement was used (e.g., Steve Gutreuter, U.S. Geological Survey, Upper Mississippi Science Center, pers. comm.). In many cases, species-specific data from other locations or data from similar species were used. Where necessary, daily mortality rates were estimated from reported annual mortality rates.

The calculated values of EAL are ecological effects of concern in assessing risks. Functions relating traffic intensity (i.e., vessels/day) to estimates of EAL can be constructed using the model for specific traffic scenarios. More consistent with a probabilistic framework for risk, the uncertainties associated with the parameter values can be quantified and propagated through the calculations to estimate the likelihood that EAL will exceed a specified value (e.g., 100 fish). Probabilistic estimation of risk is one objective of future refinement and expansion of the risk assessment of the effects of increased commercial navigation traffic.

Recruitment Forgone model

Jensen (1990) derived a model for estimating the effect of larval fish entrainment on the number of individual fish recruited into the fishery. The model is based on a description of the change in the size of a cohort subject to exponential mortality:

$$RF = L\ R_0/QN \qquad \text{(Eq. 11)}$$

where, RF is the estimate of the number of lost recruits, L is the estimated number of larvae killed by entrainment, and R_0 is the net reproductive rate (assumed = 1.0). The Q^N term (not to be confused with the entrainment Q) adjusts for natural mortality, growth, and fecundity from the time of egg hatching, through the larval, young-of-the-year, and juvenile life stages to the age of maturity (= assumed age of recruitment) according to the following (Jensen 1990):

$$Q' = H\ W_{INF}\ P_1\ P_2 \sum_{i=0}^{3} \frac{U_i \exp\left[-iK\left(x_M - x_o\right)\right]}{Z + iK} \left\{1 - \exp\left[-\left(Z + iK\right)\left(xv - x_M\right)\right]\right\} \qquad \text{(Eq. 12)}$$

where,

H = number of eggs produced per gram of female biomass;

W_{INF} = the asymptotic weight, g;

P_1 = fraction of eggs that hatch;

P_2 = fraction of females in the population;

K = annual growth coefficient, 1/year;

x_M = age at maturity, years;

x_0 = theoretical age when length equals zero, years;

x_v = the oldest age attainable, years;

U_i = 1, -3, 3, and -1 for i = 0, 1, 2, and 3, respectively; and

Z = instantaneous mortality rate for adults, 1/year.

In addition to estimates of the number of entrained larvae, the RF model parameters need only to be estimated for the recruited members of the population (Jensen 1990). This is the main advantage offered by the RF model. It is not necessary to estimate the abundance of fish in different life stages. Data describing fish abundance are largely not available for fish populations in the UMR-IWW System. The RF model simply estimates the number of fish that will not enter the fishery as a function of the number of fish larvae killed by entrainment.

Production Forgone model

The Production Forgone model was proposed by Rago (1984) as an alternative method for assessing the consequences of fish entrainment and impingement losses at water intakes for power plants. The future fish biomass (i.e., metric tons) that would have been produced by the larvae killed by entrainment is estimated by the PF model. Rago (1984) described mortality and growth using simple exponential equations that Ricker (1975) used in the original formulation of production. Jensen et al. (1988) developed a PF model based on the growth and mortality equations of the Beverton and Holt (1957) model wherein the life span of a fish was divided into four stages: larvae, young-of-the-year (age 0), juvenile, and adult. Our adaptation of Jensen et al.'s (1988) PF model is equated as:

$$PF = \sum_{i=1}^{3} \frac{G_i N_i W_i}{G_i - Z_i} \left[e^{(G_i - Z_i)t_i} - 1 \right] \qquad \text{(Eq. 13)}$$

where,

$N_i = N_{i-1}\exp(-Z_{i-1}t_{i-1})$ = number of life stage i individuals that are killed (i = 1,3),

$W_i = W_{i-1}\exp(G_{i-1}t_{i-1})$ = average weight of life stage i individuals (i = 1,3),

G_i = growth rate of life stage i,

Z_i = mortality rate of life stage i,

t_i = time duration of life stage i, and

i = 1 (larvae), 2 (young-of-year), 3 (adults).

As with the other models, necessary parameters were derived from existing data and information summarized in the technical literature. Growth rates required by the PF model also were be estimated using regressions of weight-length data (e.g., the von Bertalanffy growth equation) combined with estimates of fish length for each age class.

The PF as a result of entrained larval fish mortality was estimated for a number of alternative future traffic scenarios on the UMR-IWW System. These results may be particularly useful for assessing the ecological and economic significance of losses to forage fish species that are not of direct value to the commercial or sport fishery. Lost future biomass calculated using the PF model for species considered important to the commercial fishery was compared to commercial catch data compiled by the Upper Mississippi River Conservation Committee (UMRCC).

For all four models of impacts on fish, where particular interpretations or simplifying assumptions were necessary in using available data to estimate model parameter values, attempts were made to bias parameter values toward over-estimating potential impacts and risk. As an example, Table 2 lists the parameters for the four models for freshwater drum. In the future, distributions of parameters will be developed for those shown to contribute most to the model calculations.

Table 2
Fish Model Parameters for Freshwater Drum

Parameter	Parameter Value	References
Recruitment Forgone Model (Jensen 1990)		
Net reproductive rate (R_o)	1.0	Model assumption
Eggs/gram of female (H)	97.	Swedberg & Walburg 1970
Fraction of hatched eggs (p_1)	0.50	Professional judgment
Fraction of females in population (p_2)	0.50	Professional judgment
Asymptotic weight (g) (W_{INF})	6,803.	Rasmussen 1979
Age at time of egg hatching (years) (x_0)	0.42	Daiber 1953, Etnier & Starnes 1993, Scott & Crossman 1973, Becker 1983, Rasmussen 1979
Age at maturity (years) (x_m)	5	Daiber 1953, Rasmussen 1979
Lifespan (years) (x_v)	11	Pflieger 1997, Etnier & Starnes 1993
Adult mortality rate/year (Z)	0.30	Pauly 1980
Growth coefficient/year (K)	0.13	Pauly 1980
Production Forgone Model (Jensen et al. 1988)		
Initial weight larval stage (W_1)	0.00013	Swedberg & Walburg 1970, Holland-Bartels et al. 1990b, Dreves et al. 1996
Initial weight YOY (W_2)	0.0093	Swedberg & Walburg 1970, Etnier & Starnes 1993, Dreves et al. 1996
Initial weight adult (W_3)	15.	Butler & Smith 1950, Becker 1983, Dreves et al. 1996
Weight specific growth/day, eggs and larvae (G_1)	0.00025	Swedberg & Walburg 1970, Holland-Bartels et al. 1990b, Dreves et al. 1996
Weight specific growth/day, YOY (G_2)	0.046	Becker 1983, Dreves et al. 1996
Weight specific growth/day, adult (G_3)	0.80	Butler & Smith 1950, Becker 1983, Dreves et al. 1996
Natural mortality rate/day, eggs and larvae (Z_1)	0.23	Zigler & Jennings 1993
Natural mortality rate/day, YOY (Z_2)	0.007	Professional judgment
Natural mortality rate/day, adult (Z_3)	0.0007	Leidy & Jenkins 1977
Conditional Entrainment Mortality Model (Boreman et al. 1981) and Equivalent Adults Lost Model (Horst 1975, Goodyear 1978)		
Life stage duration (days), eggs and larvae (t_1)	37	Etnier & Starnes 1993, Becker 1983, Rasmussen 1979, Scott & Crossman 1973, Post et al. 1995
Life stage duration (days), YOY (t_2)	328	Etnier & Starnes 1993, Becker 1983, Rasmussen 1979, Scott & Crossman 1973, Post et al. 1995
Life stage duration (days), adult (t_3)	3,650	Pflieger 1997, Etnier & Starnes 1993
Ratio of the average concentration of the life stage in the entrained water to the average concentration in the river volume, eggs and larvae (w_1)	1.0	Littlejohn et al. 1985, Becker 1983, Holland & Sylvester 1983, Holland 1986, Pflieger 1997, Post et al. 1995, Conner et al. 1983, Holland et al. 1984, Brown & Coon 1994, Holland-Bartels et al. 1990b
Ratio of the average concentration of the life stage in the entrained water to the average concentration in the river volume, YOY (w_2)	0.50	Becker 1983, Pflieger 1997, Etnier & Starnes 1993, Rasmussen 1979, Scott & Crossman 1973
Ratio of the average concentration of the life stage in the entrained water to the average concentration in the river volume, adult (w_3)	0.50	Littlejohn et al. 1985, Pflieger 1997, Etnier & Starnes 1993, Becker 1983, Rasmussen 1979, Scott & Crossman 1973, Gutreuter et al. 1997

Fish Spawning Habitat Suitability Modeling

Another approach to assessing potential navigation impacts on fish populations is by addressing habitat degradation, alteration, or loss. Habitat models are based on the general assumption that a water body exhibits some carrying capacity for fish (Johnson 1993). The U.S. Fish and Wildlife Service has developed more than 150 HSI models for fish, including species that inhabit the UMR-IWW System (Johnson 1993). Habitat-based modeling approaches have been used to assess the potential impacts of increased traffic on the Ohio River using the Navigation Predictive Analysis Technique (NAVPAT) (USACOE 1994). The NAVPAT has been previously evaluated for Pool 13 of the UMR in potential support of the UMR-IWW System Navigation Study.

Parameter estimation in the habitat models refers mainly to model development and establishing the suitability indices for the habitat factors of interest. These indices may be developed in relation to field measurements or, in some cases, informed expert judgement. There have been attempts to incorporate uncertainty into assessments based on habitat evaluation (e.g., Ayyub and McCuen 1987). More recent advances include the use of GISs in addressing habitat suitability for fish (Martischang 1992).

The form, structure, and performance of habitat-based models have been reviewed extensively (e.g., Fausch et al. 1988). The primary challenge in applying these models lies in establishing reliable relationships between fish population dynamics and abiotic factors that are related to navigation impacts (e.g., physical habitat disruption, suspended sediment loads, increased sedimentation, etc.).

In the risk assessment, suitable spawning habitat for a particular fish species was evaluated. Fish spawning HSI models have been developed or are under development for 13 fish species representative of different spawning guilds for the UMR-IWW System (Tables 3 and 4). Models have been completed for ten species of fish. Spawning habitat models for northern pike, bullhead minnow, and channel catfish are still under consideration (Table 4).

The fish spawning HSI models are structured as a series of abiotic values describing different aspects of potential spawning habitat (Table 4). Values of the *SI* are specified over the [0,1] interval, with a value of 0 meaning unsuitable spawning habitat and a value of 1 corresponding to optimal spawning habitat. Habitat models can take the form of simple or multiple regression models, correlations, multivariate descriptions, or curvilinear relationships (Fausch et al. 1988). Equations for the fish spawning HSI models that have been developed thus far are listed below.

Table 3
Fish Species Selected to Assess the Effects Associated With the Incremental Increase in Commercial Navigation Traffic on Fish Spawning Habitat

Scientific Name	Common Name	Reproductive Guild (Balon 1975, Pitlo et al. 1995)	Definition of Guild (Balon 1975)
Family Acipenseridae - Sturgeons			
Acipenser fulvescens	Lake sturgeon	Litho-pelagophyl	Nonguarder, deposit eggs on a rock, rubble or gravel bottom, eggs and/or embryo become buoyant
Family Polyodontidae - Paddlefishes			
Polyodon spathula	Paddlefish	Litho-pelagophyl	Nonguarder, deposit eggs on a rock, rubble or gravel bottom, eggs and/or embryo become buoyant
Family Esocidae - Pikes			
Esox lucius	Northern pike	Phytophyl	Nonguarder, scatter or deposit eggs with an adhesive membrane that sticks to submerged, live or dead, aquatic plants, or to recently flooded terrestrial plants; sometimes they deposit eggs on logs and branches but never on the bottom
Family Cyprinidae - Minnows			
Notropis atherinoides	Emerald shiner	Pelagophyl	Nonguarder, non-adhesive eggs are released and scattered in open waters
Pimephales vigilax	Bullhead minnow	Phyto-lithophyl	Guarder, deposit eggs in relatively clearwater habitats, on submerged plants, if available, or on other submerged items such as logs, gravel, and rocks
Family Catostomidae - Suckers			
Ictiobus cyprinellus	Bigmouth buffalo	Phytophyl	Nonguarder, scatter or deposit eggs with an adhesive membrane that sticks to submerged, live or dead, aquatic plants, or to recently flooded terrestrial plants; sometimes they deposit eggs on logs and branches but never on the bottom
Family Ictaluridae - Catfishes			
Ictalurus punctatus	Channel catfish	Guarder/Nest Spawner (Cavity)/Lithophyl	Eggs are deposited in single-layer or multi-layer clutches on cleaned areas of rocks or pits dug in gravel
Family Centrarchidae - Sunfishes			
Micropterus punctulatus	Spotted bass	Guarder/Nest Spawner/ Lithophyl	Eggs are deposited in single-layer or multi-layer clutches on cleaned areas of rocks or pits dug in gravel
Micropterus salmoides	Largemouth bass	Guarder/Nest Spawner/ Phytophyl	Eggs are deposited in single-layer or multi-layer clutches on cleaned areas of rocks, pits dug in gravel, or on a soft muddy bottom
Pomoxis nigromaculatus	Black crappie	Guarder/Nest Spawner/ Phytophyl	Eggs are deposited in single-layer or multi-layer clutches on cleaned areas of rocks, pits dug in gravel, or on a soft muddy bottom
Family Percidae - Perches			
Stizostedion canadense	Sauger	Lithophyl	Nonguarder, deposit eggs on a rock, rubble, or gravel bottom where their embryos and larvae develop
Stizostedion vitreum	Walleye	Lithophyl	Nonguarder, deposit eggs on a rock, rubble, or gravel bottom where their embryos and larvae develop
Family Sciaenidae - Drums			
Aplodinotus grunniens	Freshwater drum	Pelagophyl	Nonguarder, non-adhesive eggs are released and scattered in open waters

Table 4
Status of Fish Spawning HSI Modeling and Physical Variables Included in Each Model

Fish Species	HSI Model Developed	Water Depth	Current Velocity	Water Level Fluctuation	Scour Depth	Tow Velocity	Substrate Size
Lake Sturgeon	x	x	x				x
Paddlefish	x	x	x			x	x
Northern Pike	a						
Emerald Shiner	x	x	x			x	x
Bullhead Minnow	a						
Bigmouth Buffalo	x	x	x	x			x
Channel Catfish	a						
Largemouth Bass	x	x	x	x		x	x
Spotted Bass	x	x	x			x	x
Black Crappie	x	x	x		x	x	x
Sauger	x	x	x		x	x	x
Walleye	x	x	x			x	x
Freshwater Drum	x	x	x			x	x

[a]Physical and hydrodynamic forces produced by commercial vessels do not appear relevant to reported spawning requirements.

Lake sturgeon

The spawning model for lake sturgeon is as follows:

Without traffic: $SI = Minimum\ of\ V5\ and\ (V6+V7+V8)/3$, (Eq. 14)

If $V6 \leq 0$, $V7 \leq 0$, or $V8 \leq 0$, then $SI = 0$,

Modified by each tow passage: $SI\ (MOD) = SI$, and
SI recovery rate = 0.0417 per hour,

where,

$V5$ = a modifier based on water temperature,

$V6$ = a modifier based on the ambient current,

$V7$ = a modifier based on the substrate size index, and

$V8$ = a modifier based on the water depth.

Assuming that there is no temperature limitation, $V5 = 1$.

V6 was defined according to the following values based on the ambient current velocity:

Ambient Current Velocity, *v* (cm/s)	*V6*
$0 < v \leq 15$	$2 * v/3$
$15 < v \leq 100$	1
$100 < v \leq 177$	$2.3 - 0.013 * v$
$v > 177$	0

The value of *V7* depends on the median substrate size (d_{50}) defined for the cell location and using the data summarized in Table 5:

Table 5
Relationship between Median Substrate Size (d_{50}, mm) and Fish Spawning Habitat Model Value

		d_{50}													
Fish Species	**Term**	**0.06**	**0.18**	**0.25**	**0.38**	**0.75**	**2.00**	**4.0**	**12.0**	**32.0**	**64.0**	**128**	**256**	**>1000**	**>2000**
Lake Sturgeon	*V7*	0.1	0.1	0.1	0.1	0.1	0.5	0.5	0.5	0.5	1.0	1.0	1.0	1.0	0.3
Paddlefish	*V1*	0	0.1	0.1	0.2	0.3	0.4	0.5	0.8	1.0	0.5	0.3	0.2	0.2	0.2
Emerald Shiner	*V2*	0	0	0	1.0	1.0	1.0	1.0	1.0	1.0	1.0	1.0	1.0	1.0	1.0
Largemouth Bass	*V15*	0.5	0.5	0.5	0.5	0.5	1.0	1.0	1.0	1.0	1.0	1.0	1.0	1.0	0.3
Spotted Bass	*V3*	0	0	0	0.2	0.3	0.55	0.8	1.0	1.0	1.0	1.0	1.0	1.0	1.0
Black Crappie	*V4*	0.15	0.75	0.80	0.85	1.0	0.85	0.65	0.6	0.55	0.53	0.5	1.0	0.4	1.0
Sauger	*V1*	0	0	0.2	0.4	1.0	1.0	0.4	0.8	1.0	1.0	1.0	0.8	1.0	1.0
Walleye	*V3*	0.4	0.4	0.4	0.4	0.4	0.9	0.9	0.9	0.9	1.0	1.0	1.0	0	0
Freshwater Drum	*V2*	0	0	0	1.0	1.0	1.0	1.0	1.0	1.0	1.0	1.0	1.0	1.0	1.0

V8 depends on the water depth as follows:

Water Depth, *d* (m)	*V8*
$0 < d \leq 0.3$	$1 * d/3$
$0.3 < d \leq 2$	1
$2 < d \leq 3$	$1.4 * d/10$
$3 < d \leq 6$	$1.1 * d/10$
$6 < d \leq 8$	$7/5 - 3 * d/20$
$8 < d \leq 18$	$-2 * d/100 + 0.36$
$d > 18$	0

Paddlefish

The spawning habitat model for paddlefish has the following form.

Without traffic: $SI = (V1 \times V2 \times V3)^{1/3}$, (Eq. 15)

Modified by each tow passage: *SI (MOD)* = *SI* x *V4*, and
SI recovery rate = 0.0417 per hour,

where,

V1 = a habitat suitability dependent on the substrate size index (Table 5),

V2 = a habitat suitability dependent on the ambient current,

V3 = a habitat suitability dependent on the water depth, and

V4 = a modifier dependent on the tow velocity.

V2 assumes the following values based on the ambient current velocity:

Ambient Current Velocity, *v* (ft/s)	*V2*
$v \leq 0.5$	0
$0.5 < v \leq 1$	$2 * v - 1$
$1 < v \leq 3$	1
$3 < v \leq 6$	$2 - 0.333 * v$
$v > 6$	0

V3 assumes the following values based on the water depth:

Water Depth, *d* (ft)	*V3*
$d \leq 1$	0
$1 < d \leq 6$	$0.2 * d - 0.2$
$d > 6$	1

V4 assumes the following values based on the tow velocity:

Tow Velocity, v_t (ft/s)	*V4*
$v_t \leq 3$	1
$3 < v_t \leq 6$	$2 - v_t/3$
$v_t > 6$	0

Emerald shiner

The fish spawning model for emerald shiner has the following form:

Without traffic: $SI = (V1 \times V2 \times V3)^{1/3}$, (Eq. 16)

Modified by each tow passage: *SI (MOD)* = *SI* x *V4*, and
SI recovery rate = 0.0417 per hour,

where,

V1 = a habitat suitability based on the water depth,

V2 = a habitat suitability based on the substrate size index (Table 5),

V3 = a habitat suitability based on the ambient current, and

V4 = a modifier based on the tow velocity (ft/s).

V1 assumes the following values for the various water depths:

Water Depth, *d* (ft)	*V1*
$d < 2$	$0.5 * d$
$d \geq 2$	1

V3 assumes the following values based on the ambient current velocity:

Ambient Current Velocity, *v* (ft/s)	*V3*
$v \leq 0.2$	1
$0.2 < v \leq 0.5$	$1.3 - 5 * v/3$
$0.5 < v \leq 1.2$	$0.8572 - 0.7143 * v$
$v > 1.2$	0

V4 assumes the following values based on the tow velocity:

Tow Velocity, v_t (ft/s)	*V4*
$v_t \leq 1$	1
$1 < v_t \leq 4$	$4/3 - v_t/3$
$v_t > 4$	0

Bigmouth buffalo

The spawning habitat mode for bigmouth buffalo is:

Without traffic: $SI = (V5^2 \times V6 \times V9^2 \times V11)^{1/6}$, (Eq. 17)

If $V5 \leq 0.4$, SI = *Minimum of SI and V5*,
If $V9 \leq 0.4$, SI = *Minimum of SI and V9*,

Modified by each tow passage: *SI (MOD)* = *SI*, and
SI recovery rate = 0.0417 per hour,

where,

V5 = a modifier based on the average maximum water temperatures in spawning habitat,

V6 = a modifier based on the minimum dissolved oxygen level during spawning,

V9 = a modifier based on the substrate composition, and

V11 = a modifier based on the water-level fluctuation.

Assuming no temperature and dissolved oxygen constraints yields *V5* = 1 and *V6* = 1. The substrate size index is assumed to be optimal for which *V9* = 0.8.

V11 assumes the following values based on the water-level fluctuations:

Water-Level Fluctuation, *w*	*V11*
$w < 0$	0.2
$w = 0$	0.7
$w > 0$	1

Largemouth bass

The spawning habitat model for largemouth bass is:

Without traffic: $SI = (V1 \times V9 \times V15 \times V17 \times V20)^{1/5}$, (Eq. 18)

Modified by each tow passage: $SI\ (MOD) = SI \times V6$, and
SI recovery rate = 0.0417 per hour,

where,

V1 = a modifier based on the percent pool and backwater area during summer flow,

V6 = a modifier based on the tow velocity,

V9 = a modifier based on the average weekly temperature in the pool,

V15 = a modifier based on the substrate size index (Table 5),

V17 = a modifier based on the water-level fluctuation, and

V20 = a modifier based on the ambient current.

V1 assumes the following values based on the percent pool and backwater area during summer flow:

% Pool and Backwater Area During Summer Flow, *p*	*V1*
$p \leq 15$	0
$15 < p \leq 60$	$0.0222 * p - 1/3$
$p > 60$	1

V6 assumes the following values based on the tow velocity:

Tow Velocity, v_t (ft/s)	*V6*
$v_t \leq 0.25$	1
$0.25 < v_t \leq 1$	$4/3 - 4 * v_t /3$
$v_t > 1$	0

Assuming that the average weekly temperature is not limiting, *V9* = 1.

V17 assumes the following values based on the water level fluctuations:

Water Level Fluctuation, *w* (m)	*V17*
$w \leq -8$	0
$-8 < w \leq 0$	$1 + w/8$
$0 < w \leq 10$	$1 - 0.03 * w$
$w > 10$	1

V20 assumes the following values based on the ambient current velocity:

Ambient Current Velocity, *v* (cm/s)	*V20*
$0 < v \leq 3$	1
$3 < v \leq 4$	$2.8 - 0.6 * v$
$4 < v \leq 10$	$2/3 - 0.0667 * v$
$v > 10$	0

Spotted bass

The spawning model for spotted bass is :

Without traffic: *SI = Minimum of (V1, V2, V3)*, (Eq. 19)

Modified by each tow passage:

*SI (MOD) = Minimum of (V1 * V4, V2, V3)*, and
SI recovery rate = 0.0417 per hour,

where,

V1 = a modifier based on the ambient current,

V2 = a modifier based on the water depth,

V3 = a modifier based on the substrate size index (Table 7), and

V4 = a modifier based on the tow velocity.

V1 assumes the following values based on the ambient current velocity:

Ambient Current Velocity, *v* (ft/s)	*V1*
$v \leq 1$	$1 - v$
$v > 1$	0

V2 assumes the following values for the various water depths:

Water Depth, *d* (ft)	*V2*
$d \leq 0.5$	0
$0.5 < d \leq 1$	$2 * d - 1$
$d \geq 1$	1

V4 assumes the following values based on the tow velocity:

Tow Velocity, v_t (ft/s)	*V4*
$0 < v_t \leq 1$	$1 - v_t$
$v_t > 1$	1

Black crappie

The black crappie spawning habitat model has the following form:

Without traffic: $SI = (V1 \times V2 \times V3 \times V4)^{1/4}$, (Eq. 20)

Modified by each tow passage:

SI (MOD) = SI x V5 x V6, and
SI recovery rate = 0.0417 per hour,

where,

V1 = 1, a modifier based on the structure,

V2 = a modifier based on the ambient current,

V3 = a modifier based on the water depth,

V4 = a modifier based on the substrate size (Table 5),

V5 = a modifier based on the scour depth, and

V6 = a modifier based on the tow velocity.

V2 assumes the following values based on the ambient current velocity:

Ambient Current Velocity, *v* (ft/s)	*V2*
$v \leq 0.1$	1
$0.1 < v \leq 0.5$	$2 * v - 1$
$v > 0.5$	0

V3 assumes the following values for the various water depths:

Water Depth, *d* (ft)	*V3*
$d \leq 0.5$	0
$0.5 < d \leq 1.5$	$1.5 * d - 0.5$
$d \geq 1.5$	1

V5 assumes the following values for various scour depths:

Scour Depth, d_s (inch)	*V5*
$d_s \leq 0.13$	1
$0.13 < d_s \leq 0.5$	$1.281 - 2.162 * d_s$
$0.5 < d_s \leq 1$	$0.4 - 0.4\ d_s$
$d_s > 1$	0

V6 assumes the following values based on the tow velocity:

Tow Velocity, v_t (ft/s)	*V6*
$v_t \leq 0.25$	1
$0.25 < v_t \leq 1$	$4/3 - 4 * v_t/3$
$v_t > 1$	0

Sauger

Equation 21 defines the form of the spawning habitat suitability model for sauger:

Without traffic: $SI = (V1 \times V2 \times V3)^{1/3}$, (Eq. 21)

Modified by each tow passage: *SI (MOD)* = *SI x V4 x V5*, and
SI recovery rate = 0.0417 per hour,

where,

V1 = a modifier based on the substrate size index (Table 5),

V2 = a modifier based on the ambient current,

V3 = a modifier based on the water depth,

V4 = a modifier based on the tow velocity, and

V5 = a modifier based on the scour depth.

V2 assumes the following values based on the ambient current velocity:

Ambient Current Velocity, *v* (ft/s)	*V2*
$v \leq 0.5$	0
$0.5 < v \leq 1$	$2 * v - 1$
$1 < v \leq 2$	1
$2 < v \leq 4$	$2 - 0.5 * v$
$v > 4$	0

V3 assumes the following values for the various water depths:

Water Depth, *d* (ft)	*V3*
$d \leq 0.25$	0
$0.25 < d \leq 1$	$4 * d/3 - 1/3$
$d \geq 1$	1

V4 assumes the following values based on the tow velocity:

Tow Velocity, v_t (ft/s)	*V4*
$v_t \leq 2$	1
$2 < v_t \leq 4$	$2 - 0.5 * v_t$
$v_t > 4$	0

V5 assumes the following values for various scour depths:

Scour Depth, d_s (inch)	*V5*
$d_s \leq 2$	$1 - 0.1 * d_s$
$2 < d_s \leq 3$	$1.5 - d_s/3$
$d_s > 3$	0.5

Walleye

The spawning habitat suitability model is formulated as follows:

Without traffic: SI = minimum ($V1$, $V2$, $V3$), (Eq. 22)

Modified by each tow passage:

$SI\ (MOD)$ = minimum $V1$, $V2$ x $V4$, $V3$, and
SI recovery rate = 0.0417 per hour,

where,

V1 = a habitat suitability based on water depth,

V2 = a habitat suitability based on water velocity,

V3 = a habitat suitability based on the substrate size index (Table 5), and

V4 = a modifier based on tow velocity.

V1 is obtained from the following table:

Water Depth, *d* (ft)	*V1*
$0 < d \leq 0.33$	$0.3636 * d$
$0.33 < d \leq 0.66$	$0.12 + (d - 0.33) * 0.88/0.33$
$0.66 < d \leq 1$	$1 - (d - 0.66) * 0.60/0.34$
$1 < d \leq 1.31$	$0.4 - (d - 1) * 0.40/0.33$
$d \geq 1.31$	0

V2 is related to the water current velocity as follows:

Water Current Velocity, *v* (ft/s)	*V2*
$0 < v \leq 0.5$	v
$0.5 < v \leq 2.46$	$0.5 + (v - 0.5) * 0.5/1.96$
$2.46 < v \leq 2.78$	$1 - (v - 2.46) * 0.75/1.32$
$2.78 < v \leq 3.12$	$0.25 - (v - 2.78) * 0.25/0.34$
$v > 3.12$	0

V4 is based on the tow velocity as follows:

Tow Velocity, v_t (ft/s)	*V4*
$v_t \leq 2.46$	1
$2.46 < v_t \leq 3.12$	$1 - (v_t - 2.46)/0.66$
$v_t > 3.12$	0

Freshwater drum

A spawning habitat suitability model for freshwater drum was developed using the emerald shiner model:

Without traffic: $SI = (V1 \times V2 \times V3)^{1/3}$, (Eq. 23)

Modified by each tow passage: $SI\ (MOD) = SI \times V4$, and
SI recovery rate = 0.0417 per hour,

where,

$V1$ = a habitat suitability based on the water depth,

$V2$ = a habitat suitability based on the substrate size index (Table 5),

$V3$ = a habitat suitability based on the ambient current, and

$V4$ = a modifier based on the tow velocity.

$V1$ assumes the following values for the various water depths:

Water Depth, d (ft)	$V1$
$d < 2$	$d/2$
$d \geq 2$	1

$V3$ assumes the following values based on the ambient current velocity:

Ambient Current Velocity, v (ft/s)	$V3$
$v \leq 0.2$	1
$0 < v \leq 0.5$	$1.3 - 10/6 * v$
$0.5 < v \leq 1.2$	$0.8572 - 0.7143 * v$
$v > 1.2$	0

$V4$ assumes the following values based on the tow velocity:

Tow Velocity, v_t (ft/s)	$V4$
$v_t \leq 1$	1
$1 < v_t \leq 4$	$4/3 - 1/3 * v_t$
$v_t > 4$	0

Model Application in Risk Assessment

The average Habitat Units over the spawning season for without-vessel impacts (i.e., baseline SI) and the decrease in Habitat Units caused by commercial vessels were calculated using the Suitability Index (SI) models (Figure 7). Each set of calculations addressed one pool, one traffic plan, years 2000 to 2050, all species of interest, and all GIS cells (potential spawning habitats) in the selected pool. However, only cells having sediment data and depth at high, medium, and low flows were used in the calculations. The computations were performed for each LTRMP Trend Pool.

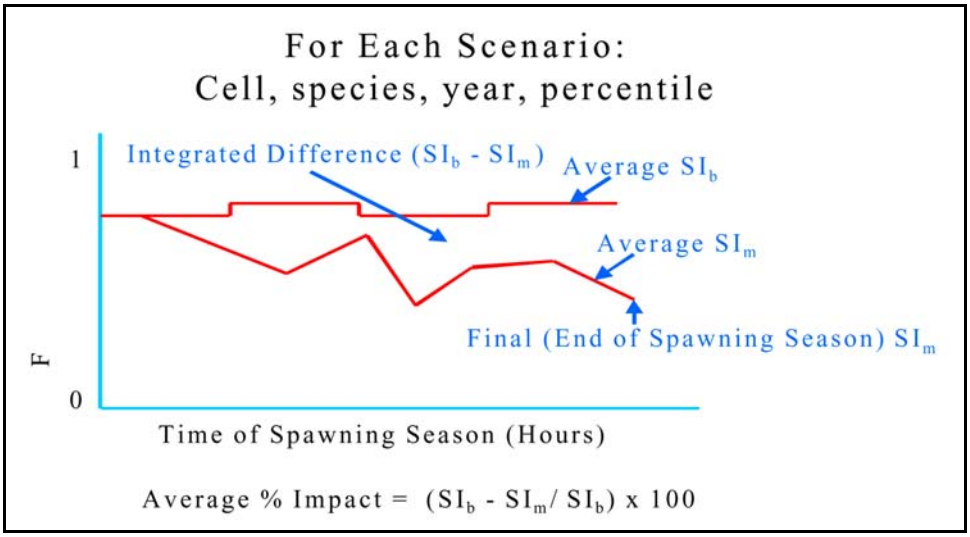

Figure 7. A graphical representation of the methodology for estimating the impacts of increased navigation traffic on fish spawning habitat, SI_b = *SI* baseline (due to traffic resulting without-project conditions) and SI_m = *SI* modified (due to traffic resulting from scenario)

For each pool, the day for the beginning and ending of the spawning season was determined for each species. The number of tows per day (TD),which varied by month, was input from the traffic file and the total number of tows during the spawning season was determined. The number of tows per day was also used to determine the average interarrival time (AIT) which also varied by month. AIT was 1/TD and had units of days.

The following computations were done for each cell in the pool:

1. NAVEFF results for the three stages were used to determine representative ambient velocity and depth. Representative ambient velocity V_a was determined for each month as

$$V_a = [V_a(high)\ (\%\ high\ flow) + V_a(medium)\ (\%\ medium\ flow) + V_a(low)\ (\%\ low\ flow)/100]$$

Representative depth for each month was determined in a manner similar to the ambient velocity calculations.

2. Monthly representative ambient velocity and depth were used along with substrate size to define the without tow SI for each month of the spawning season.

3. The distributions of the NAVEFF results for the 3 sailing lines, three stages, and 108 tow types was used to define the median values of maximum tow-induced velocity change (MVC) and maximum substrate scour (MSS) for each month of the spawning season. The MVC and MSS were used along with the

without tow SI to define the SI with tow for each month of the spawning season. A monthly DELSI was defined as (SI w/o tow) - (SI with tow) for each month of the spawning season.

4. The next step for each cell calculated the impacts of all tows during the spawning season to define the variation of SI throughout the spawning season. The without-tow SI for the first month of the spawning season defined the initial value for the SI calculations.

5. The calculations began with the first tow occurring at time 0000 on the first day of the spawning season. The next tow came AIT later with AIT varying depending on the month. Each tow caused the SI to drop by DELSI. The SI then recovered until the next tow arrived. The recovery rate was 1.0 SI/day, but the SI could not recover beyond the baseline SI value. The SI was also limited to greater than or equal to 0.0. Although the computations were done on a tow-by-tow basis, the date of the tow event was kept track of so that the appropriate monthly value of DELSI and AIT were used in the computations.

6. At the end of the loop on all tows during the spawning season, the average SI without tows and the average decrease in SI with tows was determined for the spawning season. The SI without tows and the average SI decrease with tows were multiplied by the area of the cell to provide Habitat Units (units of SI Acres) without tows and decrease in Habitat Units with tows.

7. These computations were made for years 2000 to 2050 and for each species before going to the next cell.

Breakage of Submerged Aquatic Plants

In the Navigation Study Submerged Aquatic Plant Ecological Risk Assessment, the potential ecological risks posed by commercial traffic resulting from various future traffic scenarios on submerged aquatic plants that grow in the main channel and main channel borders of the UMR-IWW System were assessed. Backwaters were not included in the risk assessment. Pool 13 is considered as the southern limit for maintaining viable populations of submerged aquatic plants in the main channel and main channel borders due to high turbidity in the lower pools. There are exceptions, however. Pool 19 supports populations of submerged aquatic plants and, in certain managed backwater areas in Pool 26, submerged aquatic vegetation can be found.

The threshold for plant breakage was set at a current velocity of $\geq$0.75 m/s (ambient plus velocity due to a passing tow) for the rule-based model (Figure 8). This value is somewhat lower than a velocity of 1.0 m/s, above which submerged aquatic plants rarely grow (Chambers et al. 1991, Biggs 1996), but higher than

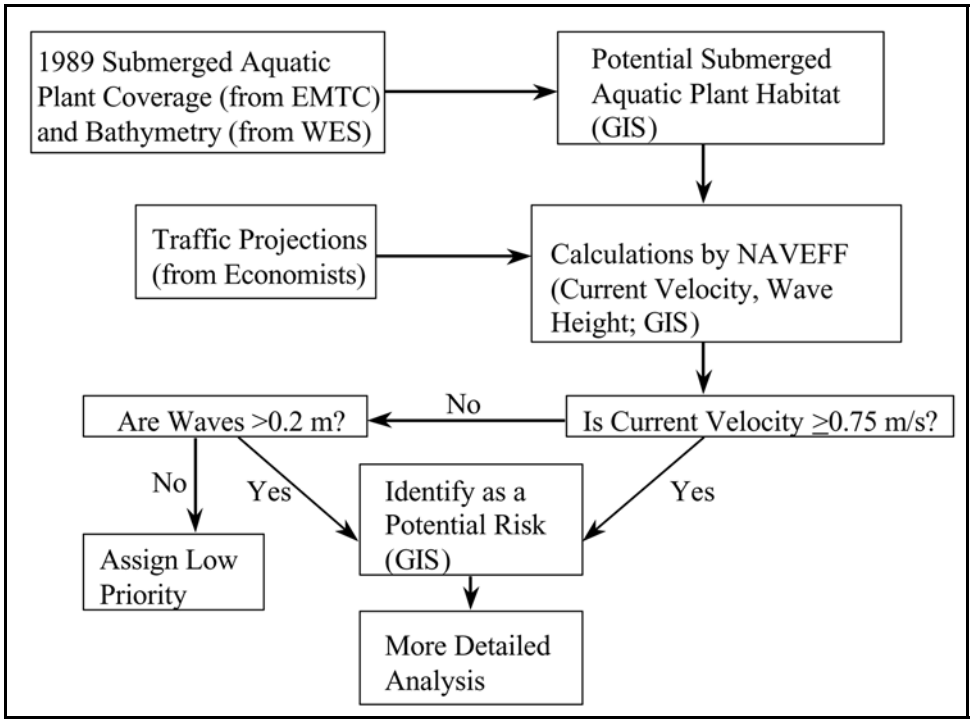

Figure 8. The rule-based model developed to assess the ecological effect of breakage of submerged aquatic plants due to the incremental increase in commercial navigation traffic; EMTC = Environmental Management Technical Center, WES = Waterways Experiment Station, and GIS = geographic information system

the value of 0.25 m/s, which was found as the breakage threshold for American wild celery and water milfoil (*Myriophyllum spicatum*) in a laboratory study by Stewart et al. (1997). Limitations associated with the study by Stewart et al. (1997) included the exclusive use of unidirectional waves and currents, a limitation imposed by the test flume capabilities, and the use of greenhouse-cultured plants, which were documented to be weaker and less resistant to tensile breakage than field-collected plants. Because of the limitations associated with Stewart et al.'s study (1997), the value of 0.25 m/s was appeared too low to use as the threshold in the rule-based model. The value of ≥0.75 m/s was selected as a compromise between the 0.25 and 1.0 m/s values.

A wave height threshold of >0.2 m, at a current velocity <0.75 m/s, was set for the rule-based model (Figure 8). This value was chosen because, at current velocities <0.75 m/s, waves higher than 0.2 m caused plant breakage resulting from entanglement due to current reversals in the passing wave series (Stewart et al. 1997). This value is consistent with observations that vegetation density and height is reduced at a wave height of 0.23 m (Coops and Van der Velde 1996).

Thresholds for current velocity and wave height were used as criteria for the rule-based model in order to evaluate the cells within the main channel and main channel borders of UMR Pools 4, 8, and 13 that had a mean depth of ≤1.5 m. These cells defined the area of existing (i.e., during 1989) submerged aquatic plant beds, previously recorded plant beds, or areas that offer habitat for future

plant beds. The number of these cells varied across the three stage heights that were examined.

Submerged Aquatic Plant Growth and Vegetative Reproduction

The estimated incremental impact of increased commercial navigation traffic on submerged aquatic plant growth and vegetative reproduction in the main channel and main channel borders is assessed using modifications of a physiological process model developed for hydrilla (*Hydrilla verticillata*), an introduced, nuisance submerged aquatic plant (Best and Boyd 1996, Boyd and Best 1996). The model (Figure 9) was modified for sago pondweed and wild celery, two species of submerged aquatic plants common to the UMR-IWW System. The models are identified as "POTAM" for sago pondweed and "VALLA" for wild celery. The models are used to estimate the risks of decreased plant growth and development of reproductive structures (e.g., tubers) due to the decrease in available underwater light in relation to increased suspended sediment concentrations that might result from increased commercial traffic. Nutrient relations have not yet been incorporated into these models due to lack of evidence for nutrient limitation in the water bodies concerned (Best and Boyd 1996, Boyd and Best 1996). These models have been previously published (Best and Boyd 1999a, 1999b, 1999c, 1999d).

Both species are rooted, tuber-forming, submerged aquatic plants native to the United States and have similar, important phases in their phenological cycles. However, they differ greatly in their geographical distribution and in their growth habits in terms of the vertical distribution of biomass within the water column. American wild celery occurs typically in relatively clear and cool, fresh, alkaline, or brackish waters of ponds, rivers, and estuaries. Wild celery occurs from Nova Scotia to northern parts of Mexico. Sago pondweed is common in fresh, alkaline, or saline waters of ponds, rivers, marshes, and ocean shores. It occurs from Newfoundland to South America, in Africa, and in parts of Asia. Sago pondweed can have over 60% of its biomass located in the upper third of the water column, where it forms a canopy-like cover near or at the water surface. In contrast to sago pondweed, wild celery has a basal rosette of leaves which may extend to the water surface but does not form a canopy. Canopy formation can be viewed as an optimum growth form for submerged aquatic plants on the basis of maximizing carbon gain in relation to light availability.

The models can be used to quantify the impacts of changes in important environmental factors on the dynamics of populations of submerged aquatic plant species, distinguished on the basis of their phenology and morphology. The effects on the following environmental factors can be tested: climate (site irradiance and air temperature), water depth, transparency, temperature, and wave action (removal of shoot biomass from water surface to a given water depth). Each model is equipped with input files containing plant characteristics and environmental conditions that can be changed by the user. Numeric model output is provided and can be easily viewed within a user-friendly shell, which

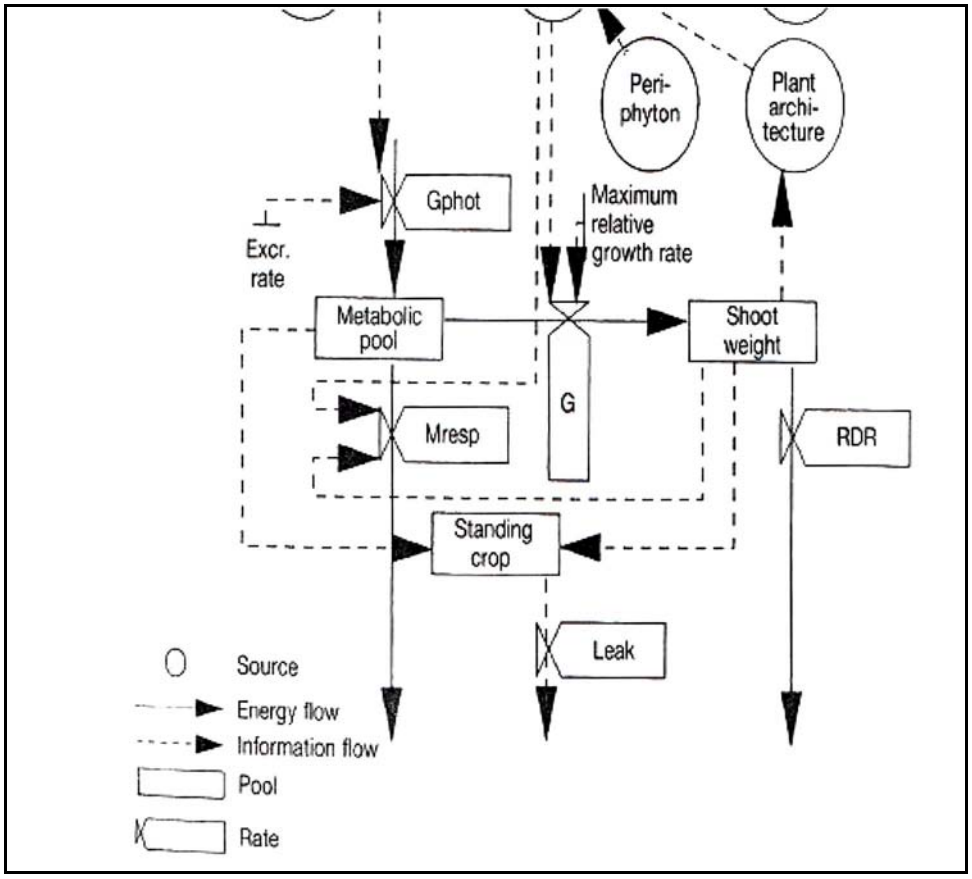

Figure 9. Flow diagram of a submerged macrophyte growth model pertaining to sago pondweed and wild celery

provides graphical output. The models have been published, and executable programs of the FORTRAN files and user manuals are available upon request (Best and Boyd 1999a, 1999b, 1999c, 1999d).

The models simulate growth of a monotypic (single species) submerged aquatic plant community, including roots and tubers. The modeled rate of dry matter accumulation is a function of irradiance, temperature, carbon dioxide (CO_2) availability, and plant growth characteristics. The rate of CO_2 assimilation (photosynthesis) of the plant community depends on the radiant energy absorbed by the shoots, which is a function of incident radiation, reflection at the water surface, attenuation by the water column, attenuation by the plant material, and leaf area of the community. The daily rate of gross CO_2 assimilation of the plant community is calculated as a function of the absorbed radiation, the photosynthetic characteristics of individual shoot tips, and the pH-determined CO_2 availability.

A fraction of the carbohydrates assimilated is allocated to maintain the existing plant biomass. The remaining carbohydrates are converted into structural dry matter (e.g., plant organs). In the process of conversion, part of the mass is lost in respiration. The dry matter produced is partitioned among the various plant organs using partitioning factors defined as a function of the phenological cycle of the species. The dry mass of the plant organs is obtained

by integration of their growth rates over time. The plant species winter either as a system composed of rooted plants and subterranean tubers, or as tubers alone. Environmental factors and plant growth characteristics vary with depth; therefore, the model partitions the water column and the associated growth-related processes into 0.1-m depth classes. All calculations are performed on a m^2 basis. The models run at daily time steps for periods of one to five years.

Development and phenological cycle

The phenology of the plant community is an ordered sequence of processes which take place over a period of time, punctuated by more or less discrete phenological events. The rate of phenological development is modeled as a function of temperature based on the degree-day hypothesis (Thornley and Johnson 1990a). Calibration according to this hypothesis allows for use of the model for the same plant species at other sites differing in temperature regimes.

Wintering, sprouting of tubers, and growth of sprouts to the water surface

Plant growth is initiated at a certain developmental phase, and a fixed number of plants develop through conversion of carbohydrates from hibernating tubers into plant material. The developmental phase and the plant density are species specific (Tables 6 and 7). Plant density is presumed to be constant throughout the year. This presumption is based on estimates of density of adolescent plants in the field, which indicate narrow density ranges for both species (Titus and Stephens 1983, Sher Kaul et al. 1995, Doyle 1999). It is possible that late in the growing season density increases somewhat through emergence of rosettes or shoots from stolons, but the role of these organs in biomass production and population survival is deemed negligible due to their low carbon gain (shaded by neighbor plants) and absence or low production of small-sized tubers. Small-sized tubers have low survival value for both species. The dormant period of the tubers appears to be far shorter in sago pondweed than in wild celery, providing a relatively longer period for new plant establishment for sago pondweed. Plant density for both species is 30 plants m^{-2} (Tables 6 and 7). Remobilization proceeds until a lower biomass limit is reached, equaling 10% of dry mass per tuber. Given the initial tuber mass, sprouts can only elongate a certain distance on these reserves. If net photosynthesis after this elongation period is negative for 23 days in wild celery or for 27 consecutive days in sago pondweed, the sprouts are presumed to die. The next tuber class can sprout subsequently, provided floral initiation has not yet been reached and temperature is within a range of 5-25 ^{o}C in wild celery and 5-28 ^{o}C in sago pondweed (Tables 6 and 7). In the elongation phase, shoot biomass is distributed equally over the successive 0.1-m depth layers, with each layer growing after the preceding layer achieves a minimum shoot biomass. After reaching maximum shoot height [water surface or $\leq$1.2 m for wild celery, water surface for sago pondweed (Best and Boyd 1996, 1999a, 1999c)], biomass is distributed following the species-specific spatial distribution (pyramid-type in wild celery, umbrella-type in sago pondweed).

Table 6
Parameter Values for VALLA; Values Listed are Those Used for Calibration, and Ranges are in Parentheses

Parameter	Abbreviation	Value	Reference
Morphology, Development, and Phenological Cycle			
First Julian day number	DAYEM	1	
Base temperature for juvenile plant growth	TBASE	3 ^{o}C	calibrated
Development rate as function of temperature	DVRVT* DVRRT	0.015 0.040	calibrated
Fraction of total dry matter increase allocated to leaves	FLVT	0.718	1, 2
Fraction of total dry matter increase allocated to stems	FSTT	0.159	1, 2
Fraction of total dry matter increase allocated to roots	FRTT	0.123	1, 2
Plant density	NPL	30. m^{-2}	1
Wintering and Sprouting of the Tubers			
Dormant tuber density	NDTUB	233 m^{-2}	3 (4)
Initial dry weight of a tuber	INTUB	0.090 g DW. $tuber^{-1}$ (0.002- 0.120)	3, 4
Relative death rate of tubers (on number basis)	RDTU	0.018 d^{-1} (0.015-0.021)	5
Growth of the Sprouts to the Water Surface			
Relation coefficient tuber weight-stem length	RCSHST	12 m g DW^{-1}	6, 7
Relative conversion rate of tuber into plant material	ROC	0.0576 g CH_2O. g DW^{-1} d^{-1}	6
Critical shoot weight per depth layer	CRIFAC	0.0091 g DW. 0.1 m plant $layer^{-1}$ (0.0091-0.041)	3, 4
Survival period for sprouts with negative net photosynthesis	SURPER	23 d	8,9
Light, Photosynthesis, Maintenance, Growth, and Assimilate Partitioning			
Potential CO_2 assimilation rate at light saturation for shoot tips	AMX	0.0165 g CO_2. g DW^{-1} h^{-1}	10
Conversion factor for translocated dry matter into CH_2O	CVT	1.05	11
Water depth	DEPTH	1 m	user def.
Initial light use efficiency for shoot tips	EE	0.000011 g CO_2 J^{-1}	11
Reduction factor to relate AMX to water pH	REDAM	1	
Thickness per plant layer	TL	0.1 m	12
Daytime temperature effect on AMX as function of DVS	AMTMPT*	0-1	10
Reflection coefficient of irradiance at water surface	RC	0.06	13
Plant species specific light extinction coefficient	K	0.0235 m^2 g DW^{-1}	10
Water type specific light extinction coefficient	L	0.43-0.80 m^{-1}	1
Reduction factor for AMX to account for senescence plant parts over vertical vegetation axis	REDF	1.0	user def.
Dry matter allocation to each plant layer	DMPC*	0-1	10
Daily water temperature (field site)	WTMPT	-, ^{o}C	user def.
Lag period chosen to relate water temp. to air temp., in case water temp. has not been measured	DELAY	1 d	user def.
Total live dry weight measured (field site)	TGWMT	-, g DM m^{-2}	user def.

(Continued)

Table 6 (Concluded)

Parameter	Abbreviation	Value	Reference
Induction and Formation of Tubers			
Translocation (part of net photosynthetic rate)	RTR	0.247	5
Critical tuber weight	TWCTUB	14.85 g DWm^{-2}	1, 3, 5
Tuber number concurrently initiated per plant	NINTUB	5.5 $plant^{-1}$ (0.002-15)	4, 1
Tuber density measured (field site)	NTMT	55-233 m^{-2}	4
Senescence			
Relative death rate of leaves (on DW basis; Q10 =2)	RDRT	0.021 d^{-1}	1
Relative death rate of stems and roots (on DW basis; Q10=2)	RDST	0.021 d^{-1}	1
Harvesting			
Harvesting	HAR	0 (0 or 1)	user def.
Harvesting day number	HARDAY	304 (1-365)	user def.
Harvesting depth (measured from water surface; 1-5 m)	HARDEP	0.1m<DEPTH	user def.

1. Titus & Stephens 1983; 2. Haller 1974; 3. Korschgen & Green 1988; 4. Korschgen et al. 1997; 5. Donnermeyer & Smart 1985; 6. Bowes et al. 1977; 7. Van der Zweerde 1981; 8. Titus & Adams 1979b; 9. Best 1987; 10. Titus & Adams 1979a; 11. Penning de Vries & Van Laar 1982a, 1982b; 12. Titus et al. 1975 ; 13. Golterman 1975 *Calibration function

Table 7
Parameter Values for POTAM; Values Listed are Those Used for Calibration, and Ranges are in Parentheses

Parameter	Abbreviation	Value	Reference
Morphology, Development, and Phenological Cycle			
First Julian day number	DAYEM	1	
Base temperature for juvenile plant growth	TBASE	3 °C	calibrated
Development rate as function of temperature	DVRVT* DVRRT	0.015 0.040	calibrated
Fraction of total dry matter increase allocated to leaves	FLVT	0.731	1
Fraction of total dry matter increase allocated to stems	FSTT	0.183	1
Fraction of total dry matter increase allocated to roots	FRTT	0.086	1
Plant Density			
Plant density	NPL	30 m^{-2}	2
Wintering and Sprouting of the Tubers			
Dormant tuber density	NDTUB	240 m^{-2}	1, 2
Initial dry weight of a tuber	INTUB	0.083 g DW. $tuber^{-1}$ (0.022- 0.155)	1 (3, 4)
Relative death rate of tubers (on number basis)	RDTU	0.026 d^{-1}	3
Growth of the Sprouts to the Water Surface			
Relation coefficient tuber weight-stem length	RCSHST	12 m. g DW^{-1}	5, 6
Relative conversion rate of tuber into plant material	ROC	0.0576 g CH_2O. g DW^{-1} d^{-1}	5
Critical shoot weight per depth layer	CRIFAC	0.0076 g DW. 0.1 m $plant\ layer^{-1}$	1, 5
Survival period for sprouts with negative net photosynthesis	SURPER	27 d	1

(Continued)

Table 7 (Concluded)			
Parameter	**Abbreviation**	**Value**	**Reference**
Light, Photosynthesis, Maintenance, Growth, and Assimilate Partitioning			
Potential CO_2 assimilation rate at light saturation for shoot tips	AMX	0.019 g CO_2. g DW^{-1} h^{-1}	7
Conversion factor for translocated dry matter into CH_2O	CVT	1.05	8
Water depth	DEPTH	1.3 m	user def.
Initial light use efficiency for shoot tips	EE	0.000011 g CO_2 J^{-1}	8
Reduction factor to relate AMX to water pH	REDAM	1	1
Thickness per plant layer	TL	0.1 m	9
Daytime temperature effect on AMX as function of DVS	AMTMPT*	0-1	1
Reflection coefficient irradiance at water surface	RC	0.06	10
Plant species specific light extinction coefficient	K	0.095m^2 g DW^{-1}	1
Water type specific light extinction coefficient	L	1.09 m^{-1}	1
Reduction factor for AMX to account for senescence plant parts over vertical vegetation axis	REDFT	1.0	user def.
Dry matter allocation to each plant layer	DMPC*	0-1	1
Daily water temperature (field site)	WTMPT	-, °C	user def.
Total live dry weight measured (field site)	TGWMT	-, g DM m^{-2}	user def.
Induction and Formation of Tubers			
Translocation (part of net photosynthetic rate)	RTR	0.19	1, 11
Critical tuber weight	TWCTUB	7.92 g DW m^{-2}	1,2,3,4,5
Tuber number concurrently initiated per plant	NINTUB	8 $plant^{-1}$ (7-12)	1 (4, 5)
Tuber density measured (field site)	NTMT	400-440 m^{-2}	3
Senescence			
Relative death rate of leaves (on DW basis; Q10 =2)	RDRT	0.047 d^{-1}	1
Relative death rate of stems and roots (on DW basis; Q10 =2)	RDST	0.047 d^{-1}	1
Harvesting			
Harvesting	HAR	0 (0 or 1)	user def.
Harvesting day number	HARDAY	304 (1-365)	user def.
Harvesting depth (measured from water surface; 1-5 m)	HARDEP	0.1m<DEPTH	user def.

1. Best 1987; 2. Sher Kaul et al. 1995; 3. Van Wijk 1989; 4. Spencer & Anderson 1987; 5. Bowes et al. 1977; 6. Van der Zweerde 1981; 7. Van der Bijl et al. 1989; 8. Penning de Vries & Van Laar 1982a, 1982b; 9. Titus et al. 1975; 10. Golterman 1975; 11. Wetzel & Neckles 1986 *Calibration function

Light, photosynthesis, and growth

The measured daily total irradiance (wavelengths of 300-3,000 nm) and the maximum/minimum temperatures of the site are used as input for the model in the form of a separate weather data file. Only half of the irradiance reaching the water surface is presumed to be photosynthetically active radiation (PAR), and 6% of the PAR is presumed to be reflected by the water surface (Best and Boyd 1996, Boyd and Best 1996).

In the models, daily irradiance within the water column is attenuated following the Lambert-Beer law. Although subsurface irradiance is attenuated by both color and particles within the water column, no distinction between either of these factors has been made, and one site-specific light extinction coefficient accounts for subsurface attenuation. The vertical profiles of light

within the vegetation layers are also characterized, and the light absorbed by each horizontal vegetation layer is derived using these profiles. The plant community-specific extinction coefficient, *K*, is assumed to be constant throughout the year and is 0.0235 m^2 g DW^{-1} for wild celery (Titus and Adams 1979a) and 0.095 m^2 g DW^{-1} for sago pondweed (Best 1987).

Instantaneous gross photosynthesis (*FGL* expressed in g CO_2 m^{-2} h^{-1}) in the models depends on the standing crop per depth layer *i* (SC_i in g DW m^{-2} layer $^{-1}$), the photosynthesis light response of individual shoot apices at ambient temperature (*AMAX* in g CO_2 g DW^{-1} h^{-1}), the initial light use efficiency (*EE* in g CO_2 J^{-1} absorbed), the absorbed light energy ($IABSL_i$ in J m^{-2} s^{-1}), and temperature (*AMTMPT*). The photosynthesis light response of leaves is described by the following exponential function.

$$FGL = SC_i \ AMAX \ (1 - exp \ [- EE \ IABSL_i \ 3600 / AMAX \ SC_i] \qquad \text{(Eq. 24)}$$

For photosynthetic activity at light saturation and optimum temperature (*AMX*), the values of 0.0165 g CO_2 g DW^{-1} h^{-1} for wild celery (Titus and Adams 1979a) and 0.019 g CO_2 g DW^{-1} h^{-1} for sago pondweed (Van der Bijl et al. 1989) were used. The photosynthetic activity at ambient temperature (*AMAX*) is calculated proportionally from that at optimum temperature using a relative function fitted to data for wild celery (Titus and Adams 1979a) and sago pondweed (Best 1987). For photosynthetic light use efficiency (*EE*), a value of 11 x 10^{-6} g CO_2 J^{-1}, typical for C_3 plants, is used (Penning de Vries and Van Laar 1982a). Substituting the appropriate value for the absorbed PAR yields the assimilation rate for each specific shoot layer.

The instantaneous rate of gross assimilation over the height of the vegetation is calculated by relating the assimilation rate per layer to the community-specific biomass distribution and by subsequent integration of all 0.1-m-high vegetation layers. The daily rate of gross assimilation is calculated by using a 3-point Gaussian integration method (Goudriaan 1986, Spitters 1986).

Maintenance costs are calculated based on the chemical composition characteristic for the plant organs, ranging from 0.010 to 0.016 g CH_2O g $AFDW^{-1}$ (Penning de Vries and Van Laar 1982b). Maintenance costs for the dormant tubers are negligible. A temperature increase of 10 ^oC is assumed to increase maintenance respiration by a factor of about 2 (with a reference temperature of 30 ^oC) (Penning de Vries and Van Laar 1982b).

Assimilates in excess of maintenance costs are converted into structural plant material. Growth efficiency and concomitant CO_2 evolution (equal growth respiration) are accounted for by using the assimilate requirement for growth. The assimilates required to produce one unit weight of plant organ are calculated from its chemical composition, and typical values are 1.46 g CH_2O g DW^{-1} for leaves, 1.51 for stems, and 1.44 for roots (Penning de Vries and Van Laar 1982b, Griffin 1994).

As summarized in Equation 25 below, plant growth (*GTW* expressed as g DW m^{-2} d^{-1}) equals remobilized carbohydrates (*REMOB* in g DW m^{-2} d^{-1}, converted to

g CH_2O m^{-2} d^{-1} by multiplication with *CVT,* a conversion factor of translocated dry matter into glucose) augmented with gross photosynthesis (*GPHOT*) and decreased by downward translocation (*TRANS1*) and maintenance respiration (*MAINT*), all expressed as g CH_2O m^{-2} d^{-1}, divided by the assimilate requirement for plant biomass production (*ASRQ*, expressed as g CH_2O g DW^{-1}):

$$GTW = ((REMOB \cdot CVT)+(GPHOT - TRANS1 - MAINT) / ASRQ \qquad \text{(Eq. 25)}$$

The assimilate allocation pattern in plants (excluding tubers) is proportional to the biomass distribution pattern and depends on the physiological age. The typical patterns are followed when shoots have reached their maximum height and are 72% to leaves, 16% to stems, and 12% to roots in wild celery (Haller 1974, Titus and Stephens 1983), and 73% of the total to leaves, 18% to stems, and 9% to roots in sago pondweed (Best 1987).

The vertical shoot biomass distribution within the water column follows typical patterns, being pyramid-shaped in wild celery with 78% of the shoot biomass in the lower 0.5 m of the water column (Titus and Adams 1979a), and umbrella-shaped in sago pondweed with 78% of the shoot biomass in the upper 0.5 m of the water column (Best 1987). This entails the distribution of shoot biomass in the upper (sago pondweed) or lower (wild celery) five 0.1-m vegetation layers according to a specific fitted function (*DMPC*) based on the respective species-specific shapes, followed by equal distribution of the remaining biomass over the remaining 0.1-m layers up to a total biomass share of 5% per layer and proportional distribution of the then-remaining biomass over all 0.1-m vegetation layers. A species-specific share of total biomass is allocated to the roots presumed to be situated in the upper 0.1 m of the sediment layer. The vertical biomass distribution pattern is recalculated and redistributed by the models when a rooting (equal water) depth other than the nominal one is chosen.

Flowering, translocation, tuber formation, and senescence

Flowering affects metabolic activity of the modeled plants by initiating substantial downward translocation of assimilates to form tubers in both sago pondweed and wild celery. Translocation and tuber formation have been formulated similarly for both species, but the parameter values are species specific. In wild celery, translocation occurs after flowering is initiated, at a day length <14.7 hours (Titus and Stephens 1983, Donnermeyer and Smart 1985), and at a temperature between 5 and 25 ^{o}C (Donnermeyer and Smart 1985). Wild celery tubers grow with a maximal rate of 24.7% of net production per day (Donnermeyer and Smart 1985). Translocation continues as long as plant biomass is greater than 0. In sago pondweed, translocation occurs after flowering is initiated, at a day length <16 hours (Best 1987), and at a temperature between 5 and 28 ^{o}C (Van Vierssen et al. 1994). Sago pondweed tubers grow at a maximal rate of 19% of net production per day (Wetzel and Neckles 1986, Best 1987), with remaining assimilates available for other processes.

Tuber production is based on the hypothesis that plants produce the largest possible tubers at their ambient light levels, because large tubers have the largest potential to survive future adverse low temperatures, low irradiance, and a short

growth season. This hypothesis is supported by field data on sago pondweed (Van Dijk et al. 1992) and experimental data on sago pondweed and wild celery (Doyle 1999). The variation in tuber size found in the field is attributed to the inability of the plants to complete the last tuber class with such a large tuber size of the season. In the models, after reaching a given tuber size, all concurrently initiated tubers of that "class" are added to the tuber bank, and a new tuber class is initiated. A fixed, linear relationship was found in both species, indicating that the tuber number concurrently initiated increases with tuber size, with a larger range for sago pondweed than for wild celery.

Senescence is modeled by defining a death rate as a certain fraction of plant biomass per day when the conditions for growth deteriorate. The timing and the values of relative death rates for plants have been derived from field observations on shoot biomass for wild celery by Titus and Stephens (1983) and for sago pondweed by Best (1987). The timing was found by running the model repeatedly with different development rates and different base and reference temperatures, until a realistic timing of decreasing shoot biomass occurred. Values for the relative death rate were found by applying the same differential equation that is commonly used for simple exponential growth to describe exponential decrease in biomass after flowering, with a negative specific decrease rate (Hunt 1982, Thornley and Johnson 1990b). Following this approach, relative death rates of 0.021 g DW g DW^{-1} d^{-1} for wild celery and 0.047 g DW g DW^{-1} d^{-1} for sago pondweed were calculated. The timing and values of the relative death rates for the tubers have been derived similarly from published data on tuber bank dynamics (Titus and Stephens 1983, Van Wijk 1989). Thus, relative death rates of 0.021 d^{-1} for wild celery and 0.026 d^{-1} for sago pondweed were calculated.

Model application in risk assessment

To assess potential commercial navigation impacts on plant growth and vegetative reproduction, traffic events were simulated for pools with known plant beds (LTRMP trend pools: Pools 4, 8, and 13) in relation to the projected number of vessels/day for a number of alternative future traffic scenarios. Each simulated vessel was identified as one of the 108 possible combinations of vessel types, three water discharge regimes, and three sailing line positions by sampling from a cumulative density function describing the relative distribution of vessel types, discharge regimes, and sailing line positions for the pool and month being evaluated. Physical forces models (NAVEFF, NAVSED) estimated the alterations in suspended sediment concentrations as a function of vessel configuration. A cumulative distribution function of the sediment concentrations was developed by repeated simulation of the physical forces models by randomly sampling the vessel configuration. From annual projections of traffic events, daily projections of interarrival times (e.g., the average time between successive tows passing any reference location within a pool) of the vessels were simulated using an exponential queuing model with the exponent defined as an inverse function of the interarrival time. These interarrival times represent the sequence of tow events for Pools 4, 8, and 13 in the UMR-IWW System. Using 10^{th}, 50^{th}, and 90^{th} percentile values from the cumulative distribution function of the sediment concentrations and the sequence of tow events, projections of daily distribution of sediment concentrations were made for three representative GIS

cells within each pool at the 10th, 50th, and 90th percentile levels. For each percentile, the representative cells were those that contained the maximum monthly sediment concentrations in a pool for cells <0.5 m in depth, between 0.5 and 1.0 m in depth, and between 1.0 and 1.5 m in depth. These sediment concentrations were then used to estimate the likelihood of reductions in plant growth and vegetative reproduction (e.g., POTAM, VALLA) resulting from various traffic scenarios at the 10th, 50th, and 90th percentile levels.

For the estimation of the impacts of traffic on the growth and vegetative reproduction of wild celery and sago pondweed in each cell (not the representative cell) $\leq$1.5 m depth in each of the three LTRMP trend pools, Pools 4, 8, and 13, a multi-step approach was adopted. A sediment index was calculated for each cell in the trend pool for each of the three percentiles of sediment concentrations as the ratio of the measured sediment concentration in that cell to the sediment concentration in the representative cell (cell that contained the maximum sediments for that cell class). For the three cells (representing each cell class) with the maximum sediment concentration, the light extinction coefficients were estimated for each of the 6 years of interest (2000, 2010, ..., 2050) by combining the sediment concentration data with the interarrival times of the tows passing in the vicinity of actual or potential plants beds. The growth and vegetative reproduction obtained for the representative cells represents the minimum growth possible in a pool (for a particular cell class and sediment concentration percentile). For both species, vegetative reproduction was not affected in the maximum cells for any traffic scenario; therefore, vegetative reproduction was excluded from any further analysis.

To estimate the growth in the other cells (non-representative cells) of the trend pool, the growth of the two plant species in a pristine cell (cell without traffic and near-zero sediment concentrations and with the same climatic conditions as the trend pool under consideration) for each of the three cell classes was first estimated. This growth represented the maximum growth possible in a cell with zero sediment concentrations and growing in climatic conditions similar to that of the trend pool under consideration. Using this maximum growth for each cell class (sediment index = 0), the minimum growth for that cell class and for each sediment concentration percentile (representative cell sediment index = 1), calculated as explained earlier, and the sediment index value for each (non-representative) cell in the cell class under consideration, the growth for the cell was estimated as a linearly interpolated value function of the sediment index.

This exercise was repeated for each of the three trend pools for each traffic scenario. The incremental effect of increased traffic resulting from each alternative scenario was then estimated as the normalized percent difference between the value of the growth metric (i.e., total live biomass, total biomass) for the without-project conditions and the value of the growth metric for the alternative traffic scenario under consideration. The value of the growth metric for the without-project conditions was used as the normalization parameter. This calculation was conducted for each of the three trend pools, for each of the three cell classes, and for each of the three sediment concentration percentiles. Thus, for Pool 4, for 0.5-m depth class, and 50% sediment concentration, the percent reduction in the total biomass of wild celery would be calculated for a particular traffic scenario as described below.

$$\text{Percent reduction in total biomass} = \frac{total\ biomass_{without\ project} - total\ biomass_{traffic\ scenario}}{total\ biomass_{without\ project}} \quad \text{(Eq. 26)}$$

To estimate the growth in cells in the non-trend pools (Pools 5, 5A, 6, 7, 9, 10, 11, and 12), growth in the cells with the maximum sediment concentration in the three trend pools was used as the starting point. First, the cell with the maximum sediment concentration was identified for each non-trend pool for each cell class and for each of the three percentiles. Next, sediment ratios for the other cells were calculated in the manner described for the trend pools. Interpolations of growth for each traffic scenario for cells with maximum sediment concentrations in Pools 5, 5A, 6, and 7 were conducted using growth estimates of maximum sediment concentration cells from Pools 4 and 8, while interpolations for Pools 9, 10, 11, and 12 were conducted using growth estimates from Pools 8 and 13. A linear interpolation scheme based on distance from the two adjacent trend pools was used to estimate the growth in non-trend pools. For interpolation purposes, Pools 5, 5A, 6, and 7 were assumed to be placed equally apart from each another and Pools 4 and 8 in a sequential manner; similarly, Pools 9, 10, 11 and 12 were assumed to be placed equally apart from each another and Pools 8 and 13 in a sequential manner. This simplified interpolation was used because the results from Pools 4, 8, and 13 indicated that the growth continuously decreased from the upper (northern) to lower (southern) pools even for the pristine case. Another reason was that the maximum sediment concentrations did not indicate any discernible patterns from the upper to lower pools, which could be used to justify or perform interpolation based on sediment concentrations in trend and non-trend pools.

In order to address the uncertainty associated with the interarrival times and the sediment concentration for each tow, the entire sequence described above up to the growth estimation was conducted in a Monte Carlo framework using 500 simulations of interarrival times and sediment concentrations for the representative cells. The interarrival times for each simulation run were sampled from an exponential distribution. The sediment concentration for each realization was based on sampling the cumulative distribution function of the sediment concentrations generated from NAVEFF simulations using a stratified random (i.e., Latin Hypercube) sampling method. Thus, 500 alternate simulations of the growth of live and total biomass were calculated for each representative cell of the trend pools for the with and without-traffic scenarios.

Growth and Reproduction of Freshwater Mussels

To assess the effects of increased navigation traffic on the growth and reproduction of freshwater mussels, a bioenergetics model for the threeridge mussel was developed and implemented for locations of known mussel beds in the UMR-IWW System. The threeridge mussel is one of the most common species and is widespread throughout the UMR-IWW System (USGS 1999). The overall methodology for the Navigation Study Freshwater Mussel Ecological Risk Assessment is summarized in Figure 10.

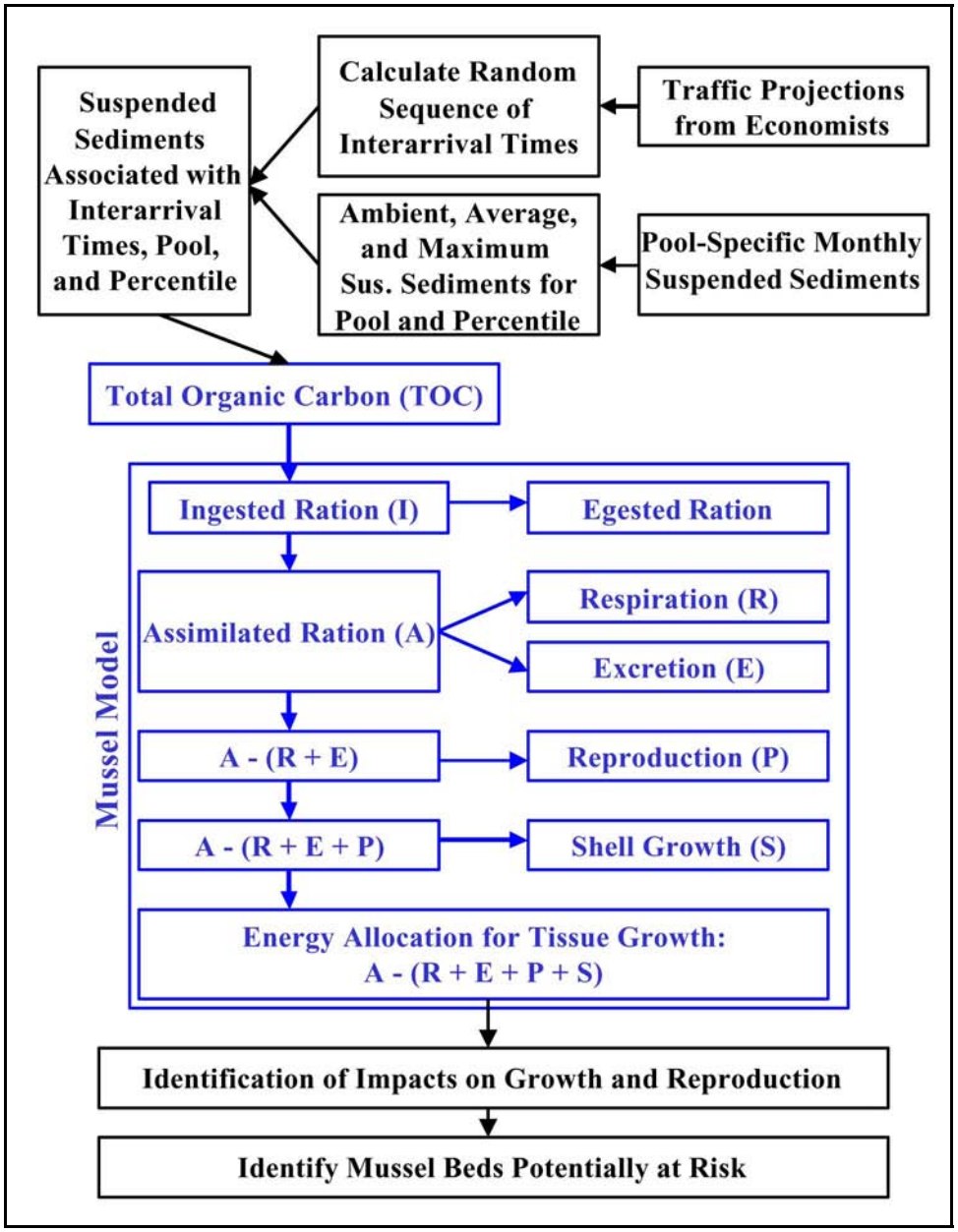

Figure 10. Schematic of the freshwater mussel risk assessment methodology

Mussel bioenergetics model description

A bioenergetics model developed for the threeridge mussel is summarized below; this model is a modification of the bioenergetics model originally developed by Schaeffer et al. (1998). Modifications were developed in consideration of the bioenergetics model described by Bayne and Newell (1983). The conceptual model is shown in blue in Figure 10 and was adapted for our model from the flow diagram also presented in Bayne and Newell (1983). Components of the flow diagram are described in the following. Ingested ration (*I*) includes all filtered material. In this model, it is assumed that a fraction of this material is absorbed and assimilated for use by the mussel and that the remaining proportion is rejected as pseudofeces (material that is filtered by the

mussel but not ingested by the mussel). Energetic gains and losses include gains obtained from the assimilated material (A) and losses resulting from respiration (R), excretion (E), reproduction (P), and shell growth (S). A hierarchy of energy allocation is assumed, where the costs of both respiration and excretion are met before energy is allocated to somatic or gametic growth. For sexually mature mussels, it is assumed that reproductive costs are met before energetic allocation to tissue or shell growth occurs.

Although this physiological hierarchy of allocation has not been examined for threeridge, the following has been observed. For some mollusks, reproductive onset does not occur until the cessation of somatic growth, while for others, growth continues after the age of maturity with an increasing proportion of surplus energy allocated to reproduction (Calow 1983). Animals that never allow reproduction to detract from somatic processes have been defined as *reproductively restrained*, while animals that reproduce at the expense of somatic requirements have been defined as *reproductively reckless* (Calow 1983). Calow (1983) conjectures that reproductively restrained organisms consist of those organisms subjected to environmental conditions in which survival of the offspring is not favorable as compared to that of the parents, for example intertidal marine environments in which wave action causes continuous disturbances and in which competition for space is high because space on stable substrate is limited. Reproductively reckless organisms consist of those organisms found in areas in which environmental conditions are favorable to the survival of the offspring, for example well-established freshwater systems in which space is not limited, natural disturbances are infrequent (Calow 1983), and resource availability is consistent. Because the UMR-IWW System is a well-established, fairly stable ecosystem containing mussel beds miles long, and because threeridge is one of the most abundant and robust species in the URM-IWW System, it seems reasonable to assume that threeridge follows a predominantly reproductively reckless strategy in which energy is allocated to reproduction before growth for sexually mature mussels.

Mussel model formulation

The bioenergetics model was developed to simulate tissue growth, shell growth, and reproductive effort via changes in tissue and shell energy. Hourly changes in tissue and shell energy determine the total, overall growth of threeridge mussels. Equations [adapted from Schaeffer et al. (1998)] describing the energy present in tissue and shell at time t are given by the following:

$$dE_t/dt = A - (R + E + P + S) \quad \text{(Eq. 27)}$$

$$dE_s/dt = S \quad \text{(Eq. 28)}$$

where, E_t (kJ) is the tissue energy at time t, E_s (kJ) is the shell energy at time t, A (kJ/hour) is assimilation, R (kJ/hour) is respiration, E (kJ/hour) is excretion, P (kJ/hour) is reproduction, and S (kJ/hour) is shell growth. Tissue and shell energies are converted to tissue dry weight [W_t (g)] and shell dry weight [W_s (g)], enabling the calculation of total dry weight [W_T (g)]. The conversion equations and the total dry weight equation are:

$$W_t = E_t \times k_1 \quad \text{(Eq. 29)}$$

$$W_s = E_s \times k_1 \quad \text{(Eq. 30)}$$

$$W_T = W_t + W_s \quad \text{(Eq. 31)}$$

where, k_1 is 22.5 g/kJ and is the conversion constant. Using the above equations, changes in tissue dry weight, shell dry weight, and total dry weight are calculated for an individual mussel between the ages of one and ten.

Because mussels do not internally regulate their body temperature, periods of activity and inactivity are primarily defined by environmental conditions. For mussels found in temperate environments, winter conditions generally lead to temporary food shortages and temperature decreases, resulting in the cessation of filtration, hence assimilation and growth. Observations made by Isely (1914) for unionids in various rivers in Oklahoma indicated that, for the threeridge mussel, virtually all growth (weight gain and shell growth) occurred between early April and late September (summer months). In addition, between late September and early April (winter months), mussels either maintained their end-of-summer-season weight or lost weight. Similar observations were made by Bayne and Worrall (1980) for the blue mussel (*Mytilus edulis*) and by Van der Schalie and Van der Schalie (1950) for unionids. Temperatures at which filtration ceased or resumed were not recorded for unionids by either Isely (1914) or Van der Schalie and Van der Schalie (1950). For zebra mussels (*Dreissena polymorpha*), the lower optimal temperature for filtration was reported to be approximately 12.0 °C (Schneider 1992). For pocketbook mussels (*Lampsilis ventricosa*), it was observed that mantle flap contractions increased two-fold between temperatures of 14.5 °C and 22.5 °C (Grier 1926). Drew Miller (USACOE, WES, Vicksburg, MS, pers. comm.) indicated that for freshwater mussels in the UMR-IWW System, activity was inhibited at temperatures below 12.0 to 15.0 °C and resumed above those temperatures. In addition, temperatures in the upper 30 °Cs could result in the cessation of filtering. Assuming that temperature dictates mussel activity, we defined two distinctive periods: one of activity and one of inactivity. Periods of activity occur when temperatures are greater than 12.0 °C and less than 36.0 °C. These periods are characterized by growth in which all physiological processes (assimilation, basal and active respiration, excretion, reproduction, and shell growth) occur. The governing equation for energy exchange during active periods is given by Equation 27 above. Periods of inactivity are defined by temperatures below 12.0 °C or above 36.0 °C and are characterized by maintenance processes in which the mussel loses tissue mass. All processes except for basal respiration are assumed to be arrested during this period. Thus, all components in Equation 27 except basal respiration become zero, and the governing equation during inactive periods is $dE_t/dt = -R$. Using professional judgement, we decided that maximal weight loss during inactive periods was no greater than 15% of the end-of-summer-season weight, which may be an underestimate for threeridge mussels (Drew Miller, USACOE, WES, Vicksburg, MS, pers. comm.). Substantially greater weight losses have been observed for some marine species (Bayne and Newell 1983).

Assimilation. Assimilation is the hourly energy gain obtained from the proportion of filtered material metabolized by the mussel. It is modeled as a function of ingestion (I in g/hour), where ingestion is the amount of material filtered by the mussel and is a function of filtration rate, food availability, and temperature. The equations describing ingestion and assimilation are as follows:

$$I = \begin{cases} K_a W_t^{ba} \times C \times p(t) \times f_r(T) & T \geq 12.0\ ^\circ C \\ 0.0 & T < 12.0\ ^\circ C \end{cases} \quad \text{(Eq. 32)}$$

$$A = AE \times I \times k_a \quad \text{(Eq. 33)}$$

where, $K_a W_t^{ba}$ is the weight-dependent filtration rate of the mussel in mL/hour, and K_a is the filtration rate in mL/g/hour of a one-gram mussel at 20 °C. This value was obtained from results reported in Table 10 in Payne et al. (1997) for threeridge mussels under conditions of infrequent exposure to turbulence and suspended solids. The original value of 0.088±0.007 was expressed in terms of mg/g/hour and was converted to units used in the bioenergetics model via the conversion used by Schaeffer et al. (1998). The conversion factor used for this value was 1000 mL/5 mg, yielding a value of 19.0 mL/g/hour.

The reliance of the filtration rate on the weight of the mussel is given by b_a. We were unable to find literature values for b_a for unionid mussels. Schaeffer et al. (1998), however, reported that values for other suspension feeding mollusks ranged from 0.462-0.820 (Wilbur 1983) and used these values to calibrate the growth rate of the modeled mussel to actual growth rate data obtained for the ebonyshell mussel (*Fusconaia ebena*) (Payne and Miller 1989). Calibrations performed by Schaeffer et al. (1998) found b_a to be 0.637. This value was used for our simulations.

AE represents the assimilation efficiency and is the proportion of filtered material converted to energy useable by the mussel. Schaeffer et al. (1998) set this value to 0.54, the mean value for efficiencies reported for suspension feeding mollusks by Wilbur (1983). *C* represents the total organic carbon (TOC) in g/mL and is a function of the day of the year. The proportion of total suspended sediments (TSS) that is TOC was estimated to be 0.0896. This value was determined from unpublished data from the LTRMP [Dave Soballe, Environmental Management Technical Center (EMTC), Upper Mississippi Science Center, Onalaska, WI, pers. comm.] for the ratios of particulate organic matter (POM) to TSS (0.28) and TOC to POM (0.32). Daily *C* values were determined by first multiplying monthly mean, pool-specific TSS values (unpublished data from the LTRMP) by 0.0896 and then linearly interpolating these values to obtain daily, baseline TOC values for pools 13, 26, and LaGrange under without project conditions. Underlying TOC estimates determined in this manner is the assumption that mussel growth is limited by ambient suspended sediment and food concentrations in their respective environments. Thus, mussels in areas where TOC concentrations are low will tend to be smaller compared to mussels growing in areas where TOC concentrations are higher. This trend has been observed by Whitney et al. (1997a) for unionids found throughout the IWW.

Increased sediment loads due to increased traffic on the UMR-IWW System were accounted for in the model by diluting the energetic value of the threeridge mussel's food supply. Dilution (*D*) was determined by the following equation:

$$D = TOC/(TOC + ssed) \quad \text{(Eq. 34)}$$

where, *ssed* (g/mL) is the suspended sediments resulting from a tow. Final dilution of the carbon supply was determined via the following equation:

$$C = TOC \times D \times fctr \quad \text{(Eq. 35)}$$

where, *fctr* (nondimensional) is a scaling constant. For our calculations, the value of *fctr* was set to 1.0. Clearly, when *ssed* is zero, *D* is one, and the food supply is the baseline TOC available to the mussel in the without project scenario. As tow-induced suspended sediment concentrations increase, the value of D decreases and C is correspondingly diluted. For the purpose of this conservative risk assessment, it was further assumed that the sediments resuspended by passing commercial vessels comprised 100% inorganic materials (i.e., zero food quality for filter feeding organisms).

Unpublished studies on filtration activity indicate that threeridge mussel filters approximately 60% of the time (D. Miller, USACOE, WES, Vicksburg, MS, pers. comm.). Thus, *p(t)* is estimated by selecting a uniform random number between 0 and 1 at each model time step (1 h). If the random number is less than 0.6, *p(t)* is assigned a value of zero and the mussel does not filter; for random numbers equal to or greater than 0.6, p(t) is defined as 1.0 and the mussel filters during that time step. Studies performed by Payne et al. (1997) in which shell gape behavior of threeridge was monitored *in situ* in the East Channel of the Mississippi River at Prairie du Chien indicated that threeridge regularly cycles between 100% and 50% open and experiences periods of closure several times an hour for five minutes or less. This same study indicated that although some of the mussels monitored did in fact close their shells during vessel passage (commercial and pleasure), the length of time these mussels remained closed was not out of character with what they naturally experience.

The $f_r(T)$ term is the temperature-dependent filtration rate multiplier. Using the optimal temperature filtration range discussed previously and values reported by Schneider (1992) for the zebra mussel, filtration rate multipliers were determined via the temperature algorithm described in Thornton and Lessem (1978). Pool-specific daily water temperature values were determined by linearly interpolating average weekly values reported in data provided by Dan Wilcox (USACOE, St. Paul District, St. Paul, MN, pers. comm.) for Pools 13 and 26. Daily water temperature values for the LaGrange Pool were determined by averaging daily values reported for all years at all sites. Linear interpolation was used to fill in missing values. Data for the LaGrange Pool were provided by Clinton Beckert (USACOE, Rock Island District, Moline, IL, pers. comm.) and were taken from the EMTC database. Pool-specific daily water temperature values used in this manner inherently dictate through model calibrations that the simulated mussel becomes acclimated to the local temperature regime.

The constant, k_a, converts the proportion of filtered material useable by the mussel into assimilated energy. Its value is 20.0 kJ/g (Lucas 1996.)

Respiration. Respiration is modeled as a function of basal respiration and assimilation. The equation is given by the following:

$$R = R_b + R_a \times A \qquad \text{(Eq. 36)}$$

where, R_b (kJ/hour) is the age-specific basal (or standard) metabolic rate representing costs associated with maintenance during both active and inactive periods. Basal metabolism, in the absence of food, is described by Bayne and Newell (1983) as indicating the rate of weight loss as energy reserves are utilized to maintain the body in a viable condition. Estimates for R_b were determined by back-calculating from pool-specific data coupled with the 15% maximum weight loss assumption during inactive periods. It was assumed that the basal metabolic rate in effect during inactive periods held for the duration of the growing season and changed at the onset of the following year, after growth occurred. Values for R_b for unionids were not found in the literature, and a 15% maximum weight loss during inactive periods was assumed (Drew Miller, USACOE, WES, Vicksburg, MS, pers. comm.).

R_a (dimensionless) represents the age(size)-specific metabolic costs associated with assimilation. After age-specific values for R_b were estimated, initial estimates for R_a were determined again by back-calculating and using pool-specific data. Final model calibration was done by adjusting initial R_a estimates so that the yearly tissue dry weight values calculated by the model were within ±20.0% of yearly tissue dry weight values yielded by pool-specific regression equations (see the section on "Shell Growth" for pool-specific regression equations). Metabolic costs modeled in this way (as a function of assimilation) inherently account for respiration dependence on weight.

Excretion. Excretion is the energy loss due to the production of non-metabolized material. It is modeled as a function of the assimilation rate and is given by the following equation:

$$E = k_e \times A \qquad \text{(Eq. 37)}$$

where, k_e is the proportion of material not fully metabolized by the mussel. Values of k_e were not found in the literature for unionids. Bayne and Newell (1983), however, report that excreta comprises 1-10% of the total energy budget for the blue mussel. Using professional judgement, we assumed that 10% of the absorbed ration is excreted as unmetabolized products for the threeridge mussel.

Reproduction. Reproductive requirements are modeled as a function of glochidial weight, glochidial numbers, and brood time. The equation is given by the following:

$$P = \begin{cases} (G \times N \times k_p)/B & T \geq 21.0\ ^{\circ}C \text{ and } W_t \geq 0.9g \\ 0.0 & T < 21.0\ ^{\circ}C \text{ or } W_t < 0.9g \end{cases} \quad \text{(Eq. 38)}$$

where, G is the weight of a single glochidia, estimated by Stein (1973) to be 1.6×10^{-7} g for the threeridge mussel. N represents the number of glochidia per brood, found to be approximately 1.71×10^5 for threeridge mussels (Stein 1973). k_p is the value of 22.5 kJ/g and is the conversion constant, converting the weight of the glochidia into the energetic equivalent of reproduction. B is the brood time over which a single brood is produced and is given by Stein (1973) as 24 days.

Reproduction commences when the threeridge mussel reaches sexual maturity and environmental temperatures are suitable. Sexual maturity is assumed to depend on size. Although this assumption is not supported by documented evidence, it was reasoned that threeridge would need to reach a size large enough to accommodate brood chambers. Additionally, it was observed via field studies that the ebonyshell mussel (which is similar in size to threeridge), on average, did not develop gonadal tissue until its tissue dry weight (W_t) was approximately 0.9g (Payne and Miller 1989). Due to the lack of information for threeridge, this value was used as the minimal threshold value after which modeled threeridge can reproduce. Suitable environmental conditions occur when temperatures are greater than or equal to 21.0 $^{\circ}$C, a value reported for threeridge mussels by Stein (1973).

Shell growth. Shell growth (S) is modeled as a function of tissue energy available from the previous time step and tissue energy available at the current time step after energy has been allocated to respiration, excretion, and reproduction. Shell growth occurs only when the tissue index is greater than the optimum tissue index, and the mussel is in an active growth period. The equation is as follows:

$$S = \begin{cases} max(0, ((Et(t) - R + E + P)) + Et(t-1))) & T \geq 12.0\ ^{\circ}C \text{ and } TI \geq OTI \\ 0.0 & T < 12.0\ ^{\circ}C \text{ or } TI < OTI \end{cases} \quad \text{(Eq. 39)}$$

where, TI (nondimensional) is the tissue index and is the calculated ratio of dry tissue weight to dry shell weight for the mussel at the current time step. OTI represents the optimum tissue index and is the ratio of the dry tissue weight to dry shell weight of the mussel calculated using the pool-specific equations given below.

The following equations were determined by using regression plots and regression formulas calculated from tissue dry weight and shell dry weight measurements determined by weighing sampled species to the nearest 0.01g (Whitney et al. 1997b). Age of each of these sampled mussels was determined by first counting growth rings and then using a thin radial cross section of the shell and hinge ligament (Whitney et al. 1997b). Ages determined by these methods were comparable and fell within ±1 year (Whitney et al. 1997b).

For Pool 13, the equations were taken from Whitney et al. (1997b) and are given by:

$$W_t = 0.0015 \times (SL^{2.6419}) \times 0.03 \quad \text{(Eq. 40)}$$

$$W_s = 0.0015 \times (SL^{2.5620}) \quad \text{(Eq. 41)}$$

$$SL = 0.0068550 \times Age^3 - 0.4318429 \times Age^2 + 9.7916577 \times Age + 3.2610581 \quad \text{(Eq. 42)}$$

where, *SL* is the length of the shell in mm, and *Age* is the age of the mussel in years. For Pool 26, the equations were taken from Whitney et al. (1997a) and are given below.

$$W_t = 0.00202084 \times (SL^{2.55148}) \times 0.03 \quad \text{(Eq. 43)}$$

$$W_s = 0.00227046 \times (SL^{2.4551}) \quad \text{(Eq. 44)}$$

$$SL = 0.0140520 \times Age^3 - 0.8170876 \times Age^2 + 16.2119671 \times Age - 6.1828848 \quad \text{(Eq. 45)}$$

For the LaGrange Pool, the equations were taken from Whitney et al. (1997a) and are given below.

$$W_t = 0.00202084 \times (SL^{2.55148}) \times 0.03 \quad \text{(Eq. 46)}$$

$$W_s = 0.00227046 \times (SL^{2.4551}) \quad \text{(Eq. 47)}$$

$$SL = 0.0081078 \times Age^3 - 0.5345261 \times Age^2 + 13.5837809 \times Age - 2.9339400 \quad \text{(Eq. 48)}$$

Live weight regression equations reported for mussels were used in the calculations. Drew Miller (USACOE, WES, Vicksburg, MS, pers. comm.) indicated that, on average, dry tissue weight is approximately 3.0% of live weight (wet tissue and wet shell weight) but is variable between individuals. This value was used to calculate the percentage of tissue dry weight from the live weight equations.

Parameters for the threeridge mussel bioenergetics model were developed for each pool of interest. As of this writing, mussel beds in UMR Pool 13 and 26 and the IWW LaGrange Pool have been evaluated. The model parameters for Pool 13 are presented in Table 8 as an example.

Table 8
Model Parameters for the Threeridge Mussel for Pool 13 in the UMR-IWW System

Parameter	Definition	Value	Units	Reference
Et_0	Initial tissue energy	0.56	kJ	Calculated from initial conditions
Wt_0	Initial tissue dry weight	0.0250	g/dry weight	Calculated from initial conditions
Es_0	Initial shell energy	22.61	kJ	Calculated from initial conditions
Ws_0	Initial shell dry weight	1.00	g/dry weight	Calculated from initial conditions
SL_0	Initial shell length	12.63	mm	Whitney et al. 1997a
K_a	Filtration rate at 20 °C	19.0	mL/g/hours	Payne et al. 1997
b_a	b_a in filtering rate equation	0.634	nondimensional	Schaeffer et al. 1998
AE	Assimilation efficiency	0.54	nondimensional	Schaeffer et al. 1998
k_a	Conversion constant – food to energy	20.0	kJ/g dry weight	Lucas 1996
G	Weight of a single glochidia	1.60E-7	g	Stein 1973
N	Number of glochidia/brood	1.71E+5	nondimensional	Stein 1973
B	Brood time	24.0	days	Stein 1973
k_p	Conversion constant – glochidia to energy	22.5	kJ/g	Schaeffer et al. 1998
k_e	Proportion of assimilated material that is excreted eetededeted	0.10	nondimensional	Professional judgement

4 Model Verification, Calibration, and Evaluation

This section includes an evaluation of each of the models used in the ecological risk assessments. Included in the evaluation of each model are the assumptions and limitations. When possible, verification and calibration of each model is also presented.

Evaluation of Larval Fish Models

In the paragraphs below are evaluations, assumptions, and limitations of the four larval fish impact models used in the Navigation Study Fish Ecological Risk Assessment.

Conditional Entrainment Mortality model

Evaluation. The CEM model has proven useful in assessing the potential impacts of fish entrainment by power plant water intake structures (Boreman and Goodyear 1988). However, it will prove nearly impossible to directly evaluate the accuracy or precision of calculated larval entrainment mortalities in relation to baseline traffic or projected traffic increases as part of the Navigation Study. The logistical problems associated with mark-recapture approaches that introduce fish larvae adjacent to a passing vessel (e.g., the bow of the vessel), and the subsequent capture of larvae behind the vessel appear insurmountable with existing technologies. This problem is exacerbated by the number of recaptured larvae required to achieve reasonable statistical power in analyzing data from this kind of experiment. Nevertheless, results of the larval entrainment calculations can be compared with existing power plant water intake fish entrainment mortality data to evaluate the reasonableness of the CEM model used in the Navigation Study Fish Ecological Risk Assessment.

Assumptions and limitations. The main assumptions of the CEM model are that: (1) the data describing the spatial-temporal location of the organisms are accurate, (2) the entrainment impacts do not alter the distribution of organisms within the water body, (3) natural mortality is uniform throughout a given life stage, and (4) density-dependent responses are not important (Boreman and Goodyear 1988).

Equivalent Adults Lost model

Evaluation. The nature of the model projections (i.e., future fish lost) makes it difficult to evaluate the performance and reliability of the EAL model. Its validity is influenced not only by the assumptions and limitations specific to this model, but also by the accuracy and precision of the estimates of CEM that serve as a primary input to the EAL model. The main utility of the EAL model is to put any suspected increase in mortality rate into more concrete terms (i.e., numbers of fish) that can then be used to assess significance and to develop mitigation alternatives. Calculations (future fish lost) resulting from the EAL model for species considered important to the commercial fishery can also be compared to commercial catch data compiled by the UMRCC to evaluate the reasonableness of the larval entrainment estimates and to assess the possible significance of lost future adults.

Assumptions and limitations. The key assumption underlying the EAL model is that the fish population of interest is essentially in a steady-state, with individuals only replacing themselves throughout their life span (Horst 1975, Goodyear 1978). Limitations in the EAL projections parallel those of the CEM model given the structural and functional interrelations between the two models. In addition, direct extrapolation of the CEM model results using the EAL calculations assumes that all other conditions that potentially influence fish population dynamics remain unchanged during the period of extrapolation. It should be recognized that the EAL model provides a first approximation to the severity of potential losses; the model does not necessarily give insights concerning the long-term viability of the impacted population.

Recruitment Forgone model

Evaluation. Jensen (1990) used the RF model to estimate RF for a population of yellow perch (*Perca flavescens*) in the western basin of Lake Erie; these fish were subject to entrainment by the Monroe Power Plant water intake, Monroe, Michigan. However, the projections of RF were not evaluated in relation to any field measurements. As with the EAL model, validation of future projections from the RF model is possible for the UMR-IWW System. This would require a substantial investment in monitoring of recruitment classes of the species and pools of interest.

Assumptions and limitations. The main assumption of the RF model is that the population is at equilibrium with a net reproductive rate of one. One limitation is that for populations that are rapidly increasing, the assumption of $R_o = 1.0$ can lead to the underestimation of RF (Jensen 1990).

Production Forgone model

Evaluation. Jensen et al. (1988) applied the PF model to a population of gizzard shad subject to entrainment by a power plant water intake in western Lake Erie. Extensive sensitivity analysis of the model demonstrated that estimated survival rate of first-year fish was a critical model parameter.

Assumptions and limitations. The key assumption of this modeling approach is that the population's short-term future growth will be similar to its

recent history. Thus, mortality and growth schedules inferred from current population structure will likely apply over future time periods.

Submerged Aquatic Vegetation Growth Model Calibration and Validation

The submerged aquatic vegetation models (VALLA and POTAM) can be used for a variety of simulation experiments. Parameter values used in calibration runs of VALLA and POTAM are listed in Tables 5 and 6. The first example consists of the results of calibration and allows for the comparison with measured biomass data. The second example illustrates model performance using the same physiological parameter values as input but with weather data from a different location (latitude). Weather data for the second example are from Minneapolis/St. Paul, Minnesota, representative for the UMR (10-year average, 1985-94). The third example illustrates the effects of water transparency values, representative for Pool 4 of the UMR (5-year average; 1991-96, growth season values only) on plant biomass and tuber formation, using the same Minneapolis/St. Paul weather data as for the second example.

VALLA

The simulated plant biomass of wild celery was similar to that found in Chenango Lake, New York in 1983 (Titus and Stephens 1983) (Figure 11). Peak biomass occurred at the same time and was somewhat lower in the simulation than actually measured, possibly as an artifact of the rather low frequency of field measurements. The simulated tuber number was well within the measured tuber number range.

Using the same parameter values as input for a simulation of biomass dynamics in the UMR, located at a higher latitude than Chenango Lake, model simulations yielded higher plant biomass and tuber numbers (three instead of two tuber classes were completed), largely as a consequence of higher irradiance (Figure 12). Extending the duration of the simulation to two years indicated that, under such conditions, a stable population could exist, with the end-of-year tuber numbers equaling 267 m^{-2}.

A simulation of a wild celery community at a more shallow rooting depth of 1 m, but at water transparency values representative of Pool 4 of the UMR, indicated that these environmental conditions inhibit biomass and tuber production to such an extent that the population becomes extinct after one year. Extinction in this case means that the population is not capable of completing any tuber class, because the plant biomass itself is very low. However, a lower tuber density of 10 m^{-2} allowed larger individual plants to develop, due to less self-shading. The latter plants were able to complete a tuber class composed of a lower number and lighter tubers (3.3 tubers of 0.06 g DW per plant) and, in doing so, increased the tuber bank density. Although smaller tubers are less likely to give rise to viable new shoots in deep, turbid water, they may generate

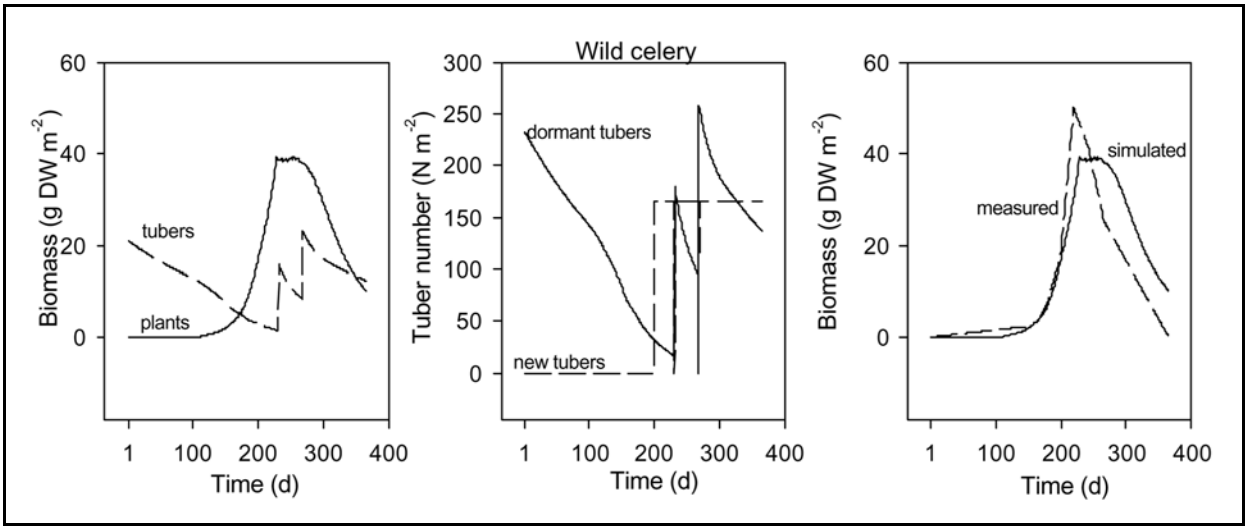

Figure 11. The simulated biomass of plants, dormant and new tuber numbers, and measured plant biomass of a wild celery community in Chenago Lake, New York. Field data from Titus and Stephens (1983); climatological data pertaining to Binghamton, New York, 1987; longitude 75°50'E, latitude 42°15'N; water depth 1.4 m; light extinction coefficient 0.43 m^{-1}

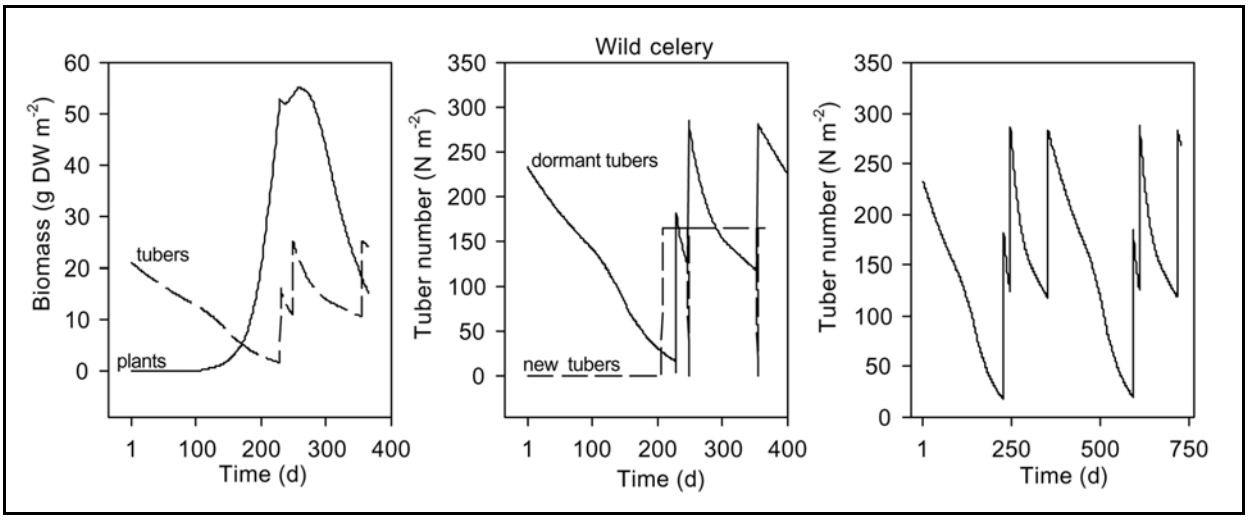

Figure 12. The simulated biomass of plants, dormant tuber numbers, and new tuber numbers of a wild celery community in the UMR. The same parameter values as in Figure 11 are used. Climatological data pertaining to St. Paul, Minnesota, 10-year average (1985-1994); longitude 93°E, latitude 45°N; water depth 1.4 m; light extinction coefficient 0.43 m^{-1}

viable plants under temporary clear-water conditions at the same rooting depth or under the pertinent turbid water conditions at a more shallow rooting depth. Smaller tubers can, therefore, still be important for system-wide persistence (in contrast to local persistence) of a population in a given water body. At a more shallow depth of 0.5 m, substantial biomass and tuber formation proved possible, with two tuber classes being completed and an end-of-year tuber number of 134 m^{-2} (Figure 13).

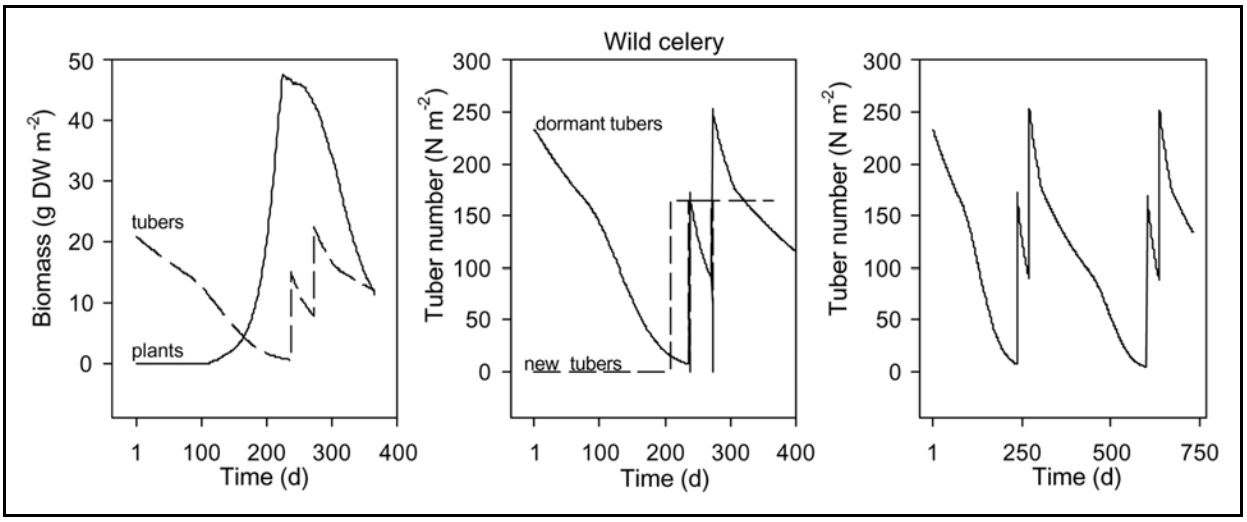

Figure 13. The simulated biomass of plants, dormant tuber numbers, and new tuber numbers of a wild celery community in UMR Pool 4. The same parameter values as in Figure 11 are used. Climatological data pertaining to St. Paul, Minnesota, 10-year average (1985-1994); longitude 93°E, latitude 45°N; water depth 0.5 m; light extinction coefficient 2.0-3.173 m^{-1} (5-year average UMR Pool 4, 1991-1996)

Although the simulated plant biomass production was substantial at rooting depths between 0.5 and 1.0 m, it was considerably less than reported for a depth range of 0.5 to 1.3 m with a minimum of 0.3 m in Pool 9 of the UMR (Donnermeyer and Smart 1985). At the shallow depth of 0.5 m, there may be too much uprooting by wave exposure to permit permanent plant establishment. However, the simulated biomass for the minimum rooting depth of 0.3 m was within the reported range (105 g DW m^{-2}), and five tuber classes were completed, confirming similarity between simulated and measured biomass data.

Wild celery tubers, as well as sago pondweed tubers, are an important food source for waterfowl, such as canvasback ducks (Korschgen et al. 1988), and herbivory may significantly reduce tuber bank density. A simulation starting from an initial, reduced, dormant tuber density of 10 tubers m^{-2} indicated that wild celery behaves similar to sago pondweed under these conditions: relatively heavier plants are formed due to decreased self-shading, and the equilibrium tuber density is gradually restored over the years.

POTAM

The simulated plant biomass of sago pondweed was similar to that found in the Zandvoort Canals, The Netherlands in 1987 (Best 1987) (Figure 14). Peak biomass occurred somewhat later and was higher in the simulation than measured values, possibly as an artifact of the rather low frequency of field measurements. The simulated tuber number was well within the measured tuber number range; the end-of-year tuber number was 64 m^{-2}.

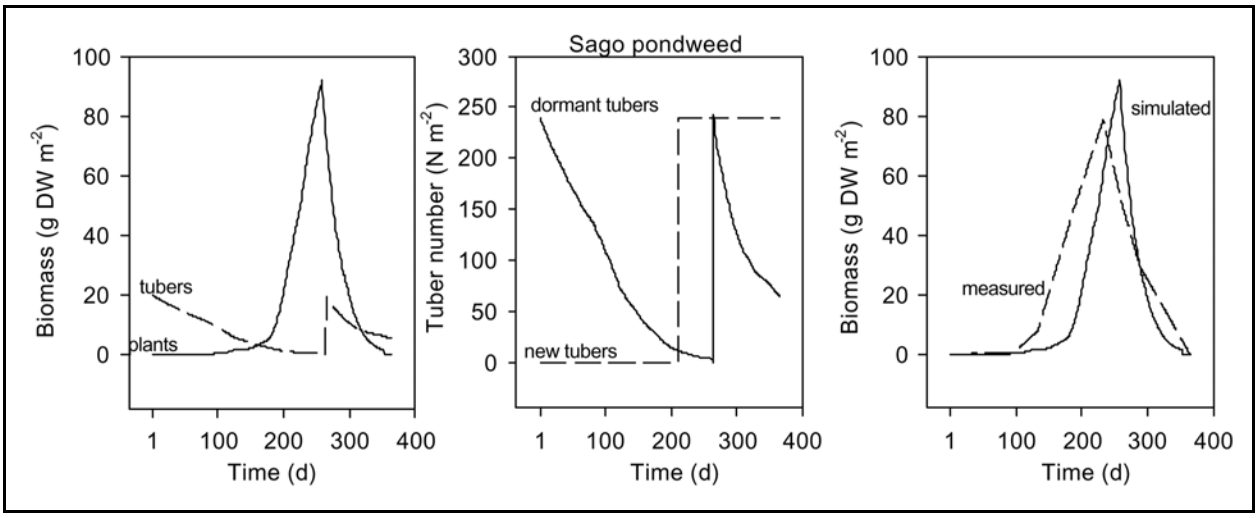

Figure 14. The simulated biomass of plants, dormant and new tuber numbers, and measured plant biomass of a sago pondweed community in Zandvoort Canals, The Netherlands. Field data from Best (1987); climatological data pertaining to De Bilt, The Netherlands, 1987; longitude 5°11'E, latitude 52°6'N; water depth 1.3 m; light extinction coefficient 1.07 m^{-1}

Using the same parameter values as input for a simulation of biomass dynamics in the UMR, located at a lower latitude than Zandvoort, yielded a somewhat higher plant biomass and far higher tuber numbers than in Zandvoort (Best 1987) (Figure 15). The higher tuber numbers were largely attributed to the higher irradiance and considerably longer window for tuber formation in the UMR. Extending the duration of the simulation to two years indicated that, in such conditions, a stable population could exist, with the end-of-year tuber numbers equaling 130 tubers m^{-2}.

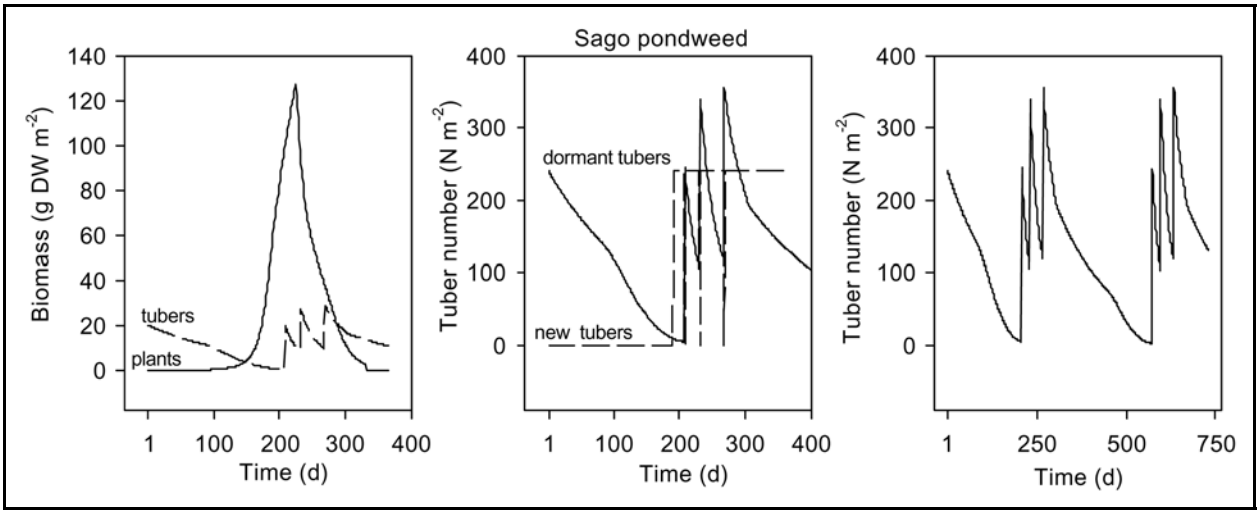

Figure 15. The simulated biomass of plants, dormant tuber numbers, and new tuber numbers of a sago pondweed community in the UMR. The same parameter values as in Figure 14 are used. Climatological data pertaining to St. Paul, Minnesota, 10-year average (1985-1994); longitude 93°E, latitude 45°N; water depth 1.3 m; light extinction coefficient 1.07 m^{-1}

Simulation of a sago pondweed community at a more shallow rooting depth of 1.0 m, but at water transparency values representative of Pool 4 of the UMR, indicated that biomass and tuber production are inhibited under these environmental conditions, since lower values were computed (Figure 16). Only two tuber classes were completed in this case, where formerly three tuber classes were produced in the less turbid, but deeper, water. However, by extending the duration of the simulation to two years, it was observed that this plant population also was stable, with tuber numbers equaling 62 tubers at the end of the year. Sago pondweed data relevant to the UMR are not available; therefore, comparisons between simulated and measured data were not possible.

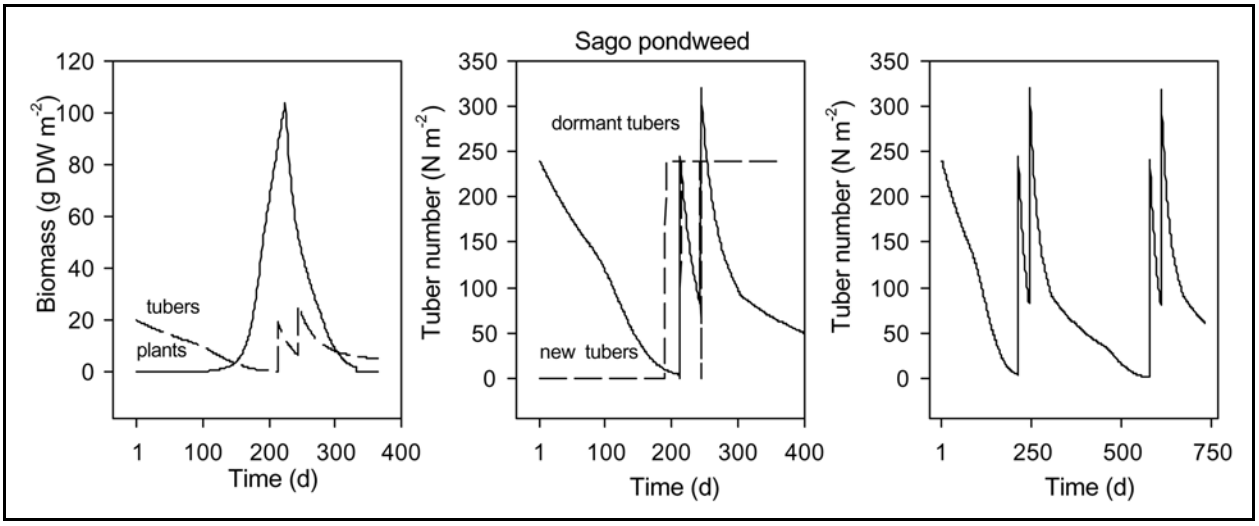

Figure 16. The simulated biomass of plants, dormant tuber numbers, and new tuber numbers of a sago pondweed community in UMR Pool 4. The same parameter values as in Figure 14 are used. Climatological data pertaining to St. Paul, Minnesota, 10-year average (1985-1994); longitude 93°E, latitude 45°N; water depth 1.0 m; light extinction coefficient 2.0-3.173 m^{-1} (5-year average UMR Pool 4, 1991-1996)

Conditions that could endanger the persistence of sago pondweed populations in the UMR were investigated by performing various simulations using POTAM. An increase in the light extinction coefficient of the water column to 3.0 m^{-1} during the whole year combined with weather data of a cold year (1992) caused a relatively small decrease in peak biomass. However, these conditions allowed only one tuber class to be completed. Nevertheless, although the end-of-year tuber numbers were relatively low (37 m^{-2}), the population was still viable. Sago pondweed tubers are a popular food source for waterfowl, and an already sparse population of 37 tubers m^{-2} can easily be cropped to 10 m^{-2} (Bick and Van Schaik 1980, Dirksen 1982). Herbivory could effectively eliminate the diminished population. However, running POTAM with an initial tuber density of 10 m^{-2} demonstrated that more biomass per plant was formed due to less self-shading, and four tuber classes were completed, restoring the tuber density to 61 m^{-2} at the end of the year.

VALLA and POTAM Model validation simulation results

From the simulations performed for model validation, it appears that both plant populations can persist in monotypic stands at a rooting depth of 1.0 m or less at current water transparency levels in the UMR. Under the turbid conditions, sago pondweed benefits from its canopy-type growth form, which maximizes light interception and carbon gain near or at the water surface. Wild celery is in a less advantageous position due to its pyramid-type growth form, which allows less light interception in the deeper water and, consequently, less carbon gain. In addition, sago pondweed shoots appear to benefit from a longer establishment period during the spring and persist for a longer time span without photosynthetic net carbon gain than wild celery. This results in stable population dynamics for sago pondweed, while wild celery experiences population fluctuations.

Increasing turbidity and herbivory will cause local decreases in tuber densities. Populations which have a low-density tuber bank have the ability to survive and return to normal tuber densities under average weather and water level conditions. This ability is more pronounced for sago pondweed than for wild celery. However, populations with a low-density tuber bank are at risk of becoming locally extinct under unfavorable weather or high water level conditions. It may be possible for locally-extinct populations to be restored by propagule imports from elsewhere, provided that the sources are nearby and that conduits between the propagule source and the site of local extinction exist. In addition, prerequisites for recolonization include (1) presence of propagules, (2) sufficient light, (3) suitable substrate, (4) tolerable current velocities and waves, (5) sufficient nutrients, and (6) minimal herbivory. Two periods appear to be critical for the persistence of local populations: (1) early spring during the initial elongation of the sprouts, and (2) the latter part of summer during tuber formation. The prerequisites for local persistence of populations with low-density tuber banks are the ability of the new shoots to reach a maximum attainable height in the water column where they can generate a positive carbon gain and the ability of full-grown plants to complete one large-size tuber class. The models can be used to calculate the timing of these sensitive periods for any combination of locations, rooting depth, and water transparency and can serve as important tools for developing water management strategies concerning submerged aquatic plant populations.

Evaluation of the Mussel Bioenergetics Model

The calibration, behavior, assumptions, and limitations of the mussel bioenergetics model are presented in the following paragraph.

Mussel bioenergetics model calibration

The mussel model was calibrated in the following way. Active respiration rate values for each modeled year 1-10 were adjusted so that tissue dry weight from the model was within ±20% of the tissue dry weight values obtained for each corresponding age from the pool-specific regression equations (equations 40-48) reported by Whitney et al. (1997a and 1997b). When modeled tissue dry weight fell within these ranges, modeled shell dry weight fell within ±22% of the values obtained from the regression equations for shell dry weight in equations 14-22. Calibration results are shown in Tables 9 through 11 for both tissue dry weight (TDM) and shell dry weight (SDM) for Pools 13, 26, and the LaGrange Pool, respectively.

Table 9
Calibration Results Showing Tissue Dry Weight (TDM) and Shell Dry Weight (SDM) in Grams as Compared to Data TDM and SDM of a Mussel (Age 1 to 10) Growing in Pool 13

Age (Years)	Model TDM	Data TDM	Model SDM	Data SDM
1	0.0566	0.0552	1.673	1.484
2	0.1231	0.1241	3.505	3.256
3	0.3220	0.2848	8.831	7.285
4	0.4865	0.5112	13.29	12.85
5	1.055	1.013	28.37	24.93
6	1.298	1.272	34.47	31.11
7	1.643	1.660	43.42	40.25
8	2.025	1.932	52.88	46.64
9	2.267	2.287	59.17	54.93
10	2.983	3.016	77.43	71.83

Table 10
Calibration Results Showing Tissue Dry Weight (TDM) and Shell Dry Weight (SDM) in Grams as Compared to Data TDM and SDM of a Mussel (Age 1 to 10) Growing in Pool 26

Age (Years)	Model TDM	Data TDM	Model SDM	Data SDM
1	0.0182	0.0176	0.5940	0.5318
2	0.1780	0.1826	5.347	5.052
3	0.5480	0.5463	15.81	14.50
4	1.059	1.089	29.76	28.16
5	1.744	1.767	48.00	44.88
6	2.513	2.531	68.41	63.42
7	3.349	3.333	90.09	82.65
8	4.193	4.131	111.6	101.6
9	4.840	4.892	128.4	119.6
10	5.551	5.591	146.3	136.0

Table 11
Calibration Results Showing Tissue Dry Weight (TDM) and Shell Dry Weight (SDM) in Grams as Compared to Data TDM and SDM of a Mussel (Age 1 to 10) Growing in the LaGrange Pool

Age (Years)	Model TDM	Data TDM	Model SDM	Data SDM
1	0.0652	0.0715	2.063	2.050
2	0.2475	0.2994	7.526	8.132
3	0.6470	0.6995	18.79	18.40
4	1.233	1.261	34.53	32.43
5	1.917	1.957	53.19	49.51
6	2.774	2.760	75.71	68.92
7	3.680	3.640	99.71	89.95
8	4.577	4.567	122.7	112.0
9	5.542	5.514	147.3	134.1
10	6.419	6.461	170.1	156.3

Mussel bioenergetics model behavior

Figures 17-22 present the accumulation of tissue dry weight and shell dry weight, and the cumulative energetic allocations to assimilation, respiration, excretion, and reproduction over a ten year period of growth for a young mussel (age 1 to 10) in Pool 13 in the absence of traffic under constant environmental conditions. Pool 13 was used as an example, but behavior for all pools is similar. For sexually mature mussels, plateaus and decreases in tissue dry weight accumulation during active periods represent periods in which the mussel's reproductive effort is highest (Figure 17). Observe that energy allocation for reproduction does not occur until approximately the fourth year for mussels in Pool 13 (Figure 18). The onset of reproduction varies by pool. (Recall from the section on "Reproduction" that reproductive onset in the model occurs when tissue dry weight is greater than 0.9 grams and temperature conditions are suitable). Discontinuities visible in shell dry weight accumulation during active periods also represent periods in which energy allocation to reproductive effort is highest (Figure 19). Recall that the model assumes a hierarchal allocation of energy, first to respiration and excretion, then to reproduction for sexually mature mussels, and finally to shell growth (Figure 10). This hierarchal allocation is most clearly demonstrated in Figure 19. Respiration and excretion follow assimilation as expected (Figures 20 through 22).

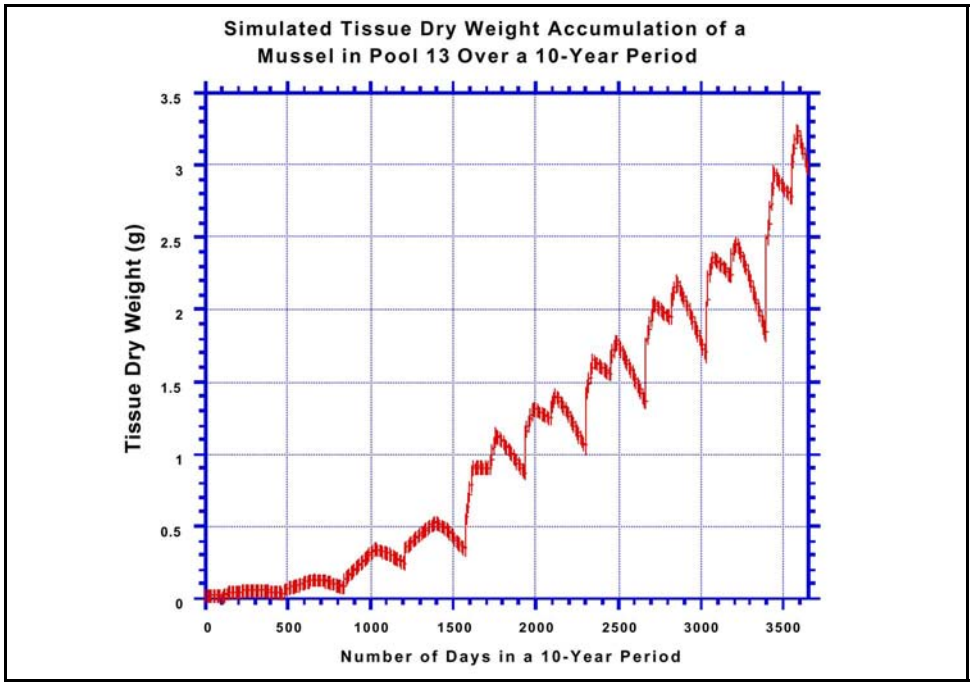

Figure 17. Simulated tissue dry weight accumulation of a threeridge mussel in Pool 13 over a 10-year period in the absence of traffic

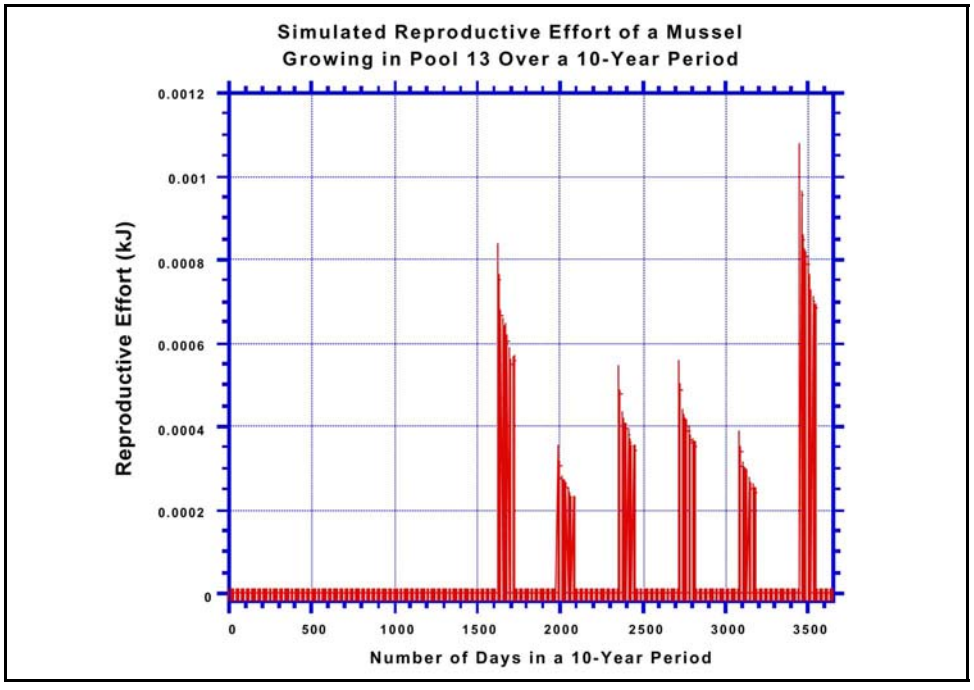

Figure 18. Simulated reproductive effort of a threeridge mussel growing in Pool 13 over a 10-year period in the absence of traffic

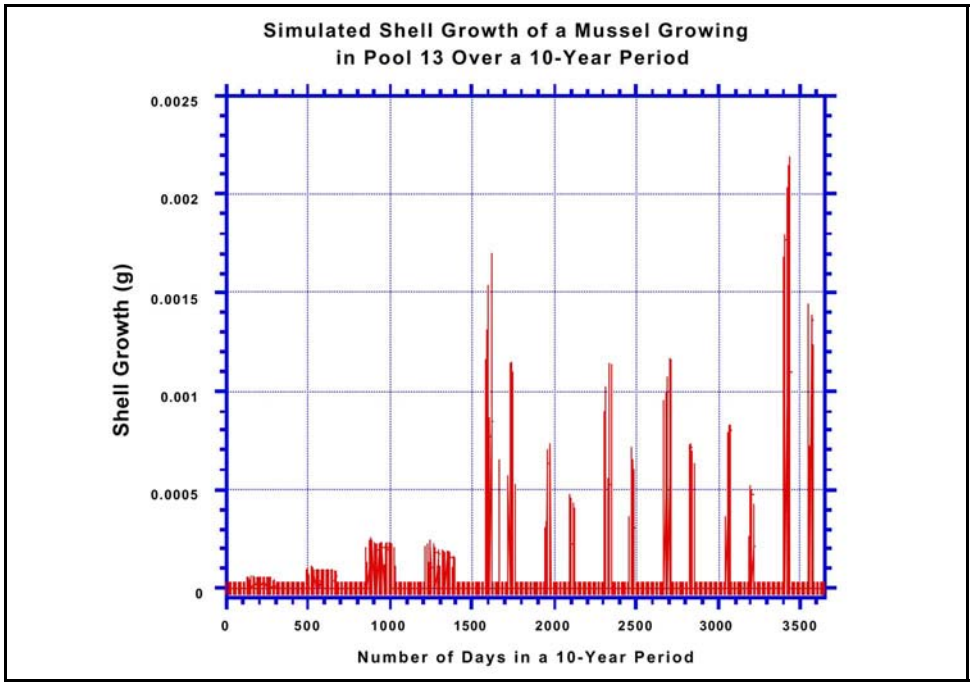

Figure 19. Simulated shell growth of a threeridge mussel growing in Pool 13 over a 10-year period in the absence of traffic

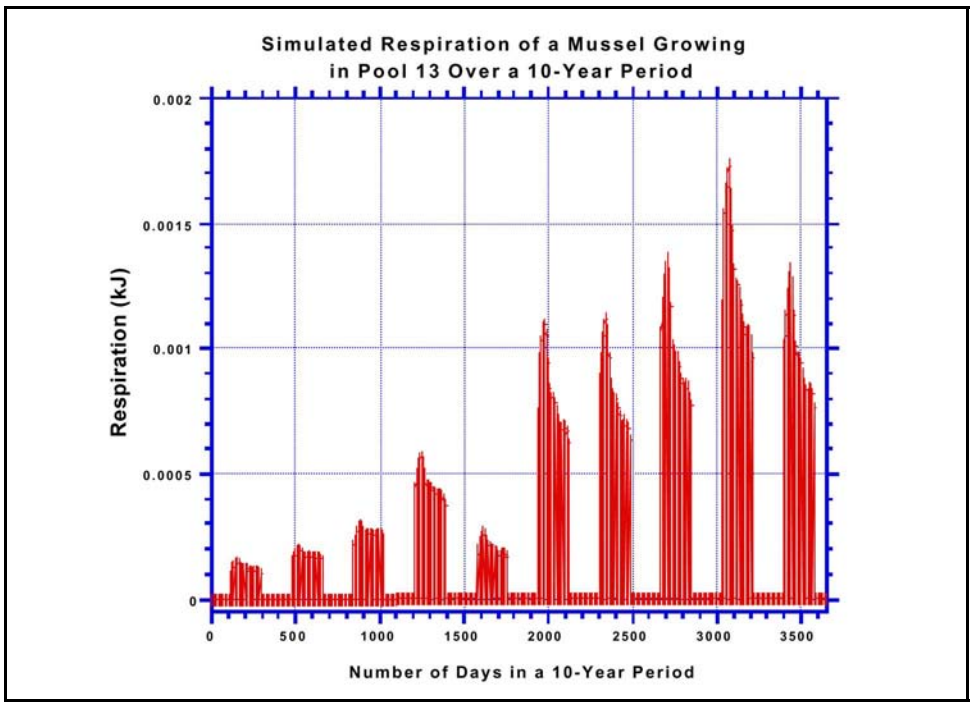

Figure 20. Simulated respiration of a threeridge mussel growing in Pool 13 over a 10-year period in the absence of traffic

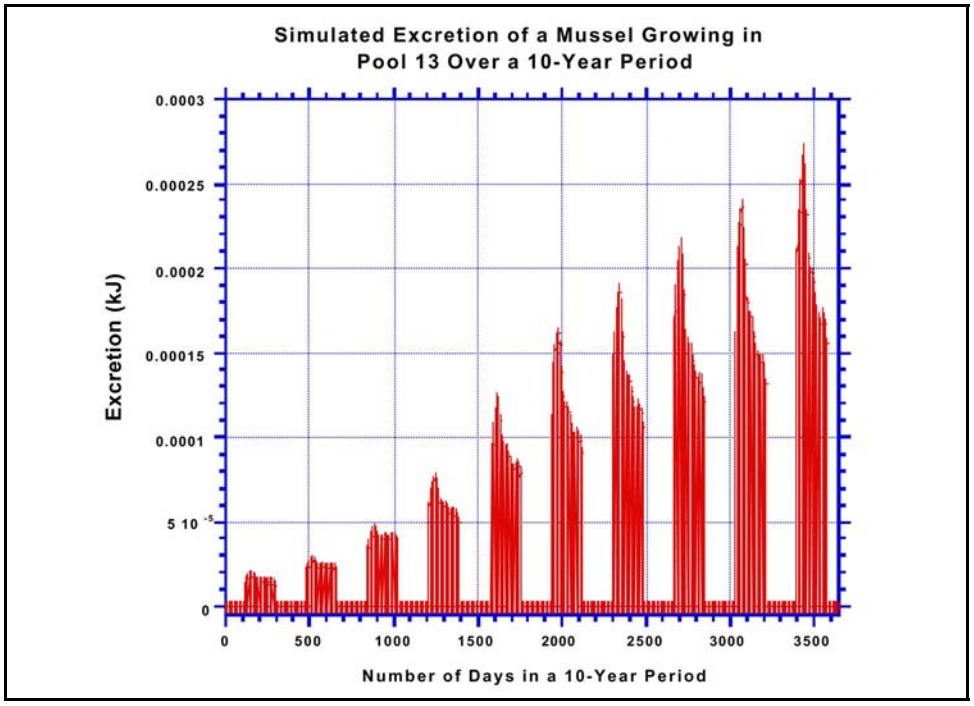

Figure 21. Simulated excretion of a threeridge mussel growing in Pool 13 over a 10-year period in the absence of traffic

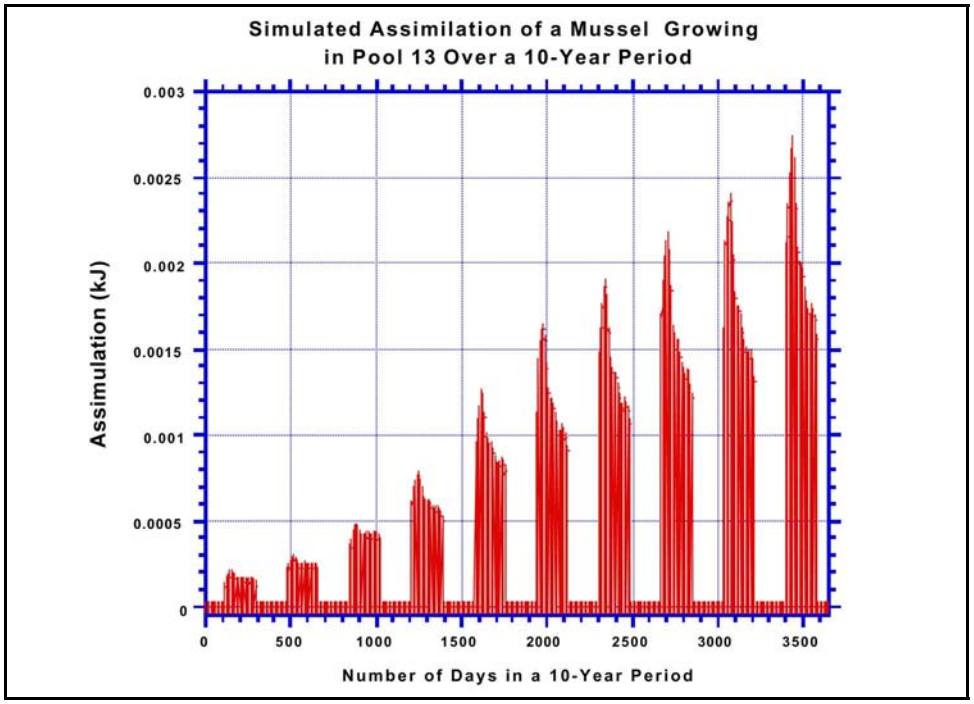

Figure 22. Simulated assimilation of a threeridge mussel growing in Pool 13 over a 10-year period in the absence of traffic

Mussel bioenergetics model assumptions and limitations

As with all models, the threeridge mussel model is limited by its assumptions and the accuracy of model parameter values. Many of the model assumptions and data limitations have been discussed previously. However, a summary list is presented as follows:

- The model presented here has been developed and parameterized (to the extent allowable by available information) for the threeridge mussel. Threeridge is a hearty, robust mussel found in abundance throughout the UMR-IWW System, and at present is not threatened or endangered. Because of this, caution is advised when extrapolating results from this model to other, perhaps more sensitive, species.

- Every attempt was made to estimate model parameters from data collected from studies performed on threeridge. However, information on physiological rates for threeridge was sufficiently sparse that values were derived from other freshwater species residing in the UMR-IWW System and in other aquatic systems. In some cases, data for marine species were used. Additionally, information for estimating some parameter values was simply not available. In such cases, we based our estimates on discussions with mussel biologists and ecologists . These informed estimates or educated guesses are labeled as "opinion in the absence of empirical data". The relative importance of these parameter values in influencing the model results has been addressed through extensive sensitivity analyses.

- For sexually mature mussels, a hierarchy of energy allocation is assumed to occur, energy being allocated first to respiration and excretion, then to reproduction, then to tissue and shell growth. Because information concerning resource allocation to reproduction is lacking for threeridge, this assumption was speculative. Under conditions of increasingly continuous disturbance (i.e., continuous sediment resuspension) during the reproductive period, the model will correspondingly allocate less energy to reproduction.

- In its current formulation, filtration rates of the mussel model are dependent only on the size of the mussel. While this is a well documented phenomena (see Bayne and Newell 1983, and Burky 1983 for a review of the literature), it has also been observed that filtration rates also depend on suspended particle concentrations and decrease or level off as suspended particle concentrations increase above some threshold (Bayne and Newell 1983, and Burky 1983). Given the current model structure, filtration and ingestion will continue even when suspended particle concentrations may rise above levels that might realistically cause threeridge to stop filtering. However, this model bias influences both the baseline simulations and simulations involving increased tow-induced sediment resuspension. The incremental impact, which is the endpoint in this assessment, will be less influenced by this bias.

- The probability (i.e., 0.6) that the mussel is filtering is constant in the current deterministic version of the model, although we have developed a distribution for this probability that is used in our Monte Carlo version of the mussel model. In field studies performed by Payne et al. (1997) it was found that considerable variability in shell gape behavior exists between individuals exposed to both commercial and pleasure boat passages. These results were obtained from a relatively small sample of mussels (six), so that generalizations as to the behavior of threeridge under periodic exposure could not be made so that this parameter contains a great deal of uncertainty. If data become available to define the probability of mussels remaining open as a function of disturbance frequency (i.e., tow passage events) , the corresponding modification can be made to the mussel growth model.

- Sexual maturity in the model is assumed to be dependent on size only. Based on the observations of Payne and Miller (1989) for the ebonyshell mussel, this value was set to 0.9g. However, the development of gonadal tissue in mussels is a complex process and is most likely dependent on internal factors specific to the individual (i.e., variation in biological processes), and external factors specific to the individual's microenvironment (i.e., suspended particle concentrations and frequency of disturbance). As additional information describing sexual maturity becomes available for the threeridge or other unionid mussels, this model assumption might need to be revised.

- Acclimation to ambient suspended sediment concentrations and average temperature regimes was assumed for mussels in each pool. Underlying this assumption is the idea that mussels will grow only to the extent allowable by food concentrations in their environments.

- Sediment resuspension due to increased traffic was assumed to affect growth through dilution of the food supply. It has been observed that for some unionids if suspended sediment concentrations are sufficiently high (650.0 and 700.0 mg/L under frequent and infrequent turbulence, respectively), the filtering rate can also be affected (Aldridge et al. 1987), but that under lower suspended sediment concentrations (20.0 and 120.0 mg/L under frequent and infrequent turbulence, respectively), the decrease in the filtering rate is minimal (Payne et al. 1997). Research is currently being conducted to determine whether or not further refinements in this aspect of the model are required.

- A maximum overwinter weight loss of 15% was assumed and was used to theoretically determine age-specific basal respiration values. Drew Miller (USACOE, WES, Vicksburg, MS, pers. comm.) has indicated that overwinter weight loss experienced by threeridge mussels might exceed this value.

- Age-specific basal respiration values determined for periods of inactivity were assumed to carry over through periods of activity. This may or may not be the case since basal respiration depends on the size of the mussel.

- Active respiration was assumed to be dependent only on assimilation. It has been observed by Bayne and Newell (1983) that pseudofeces production may contribute to metabolic energy allocations. This may need to be considered in future model refinements.

- Shell length, tissue dry weight, and shell dry weight used to calculate optimum tissue index are from the same data set used to calibrate the model. This was unavoidable since an alternative data set was not available.

Scale and Extrapolation

The ecological models have been developed largely on the basis of the comparatively extensive data available from the LTRMP trend pools, Pools 4, 8, 13, and 26 on the UMR and the LaGrange Pool on the IWW. These pools have also been the focus of detailed hydrodynamic and hydraulic model applications that calculate the physical forces required by the ecological models. Unfortunately, extensive data that describe the physics, sediments, and biology are not readily available for the remaining pools on the system. Therefore, methods for extrapolating effects estimated for the trend pools to non-trend pools were developed to complete a comprehensive assessment for the entire UMR-IWW System. The specific details for interpolations and extrapolations of impacts estimated for the trend pools are described in the technical reports pertaining to the separate assessments for fish, mussels, and submerged aquatic plants.

5 Ecological and Physical Forces Model Integration

The complex and diverse nature of the modeling components that constitute the overall assessment requires a plan for organization and integration. The anticipated result of implementing the plan will be a general system model that will facilitate the timely and efficient evaluation of ecological risks posed by future commercial traffic scenarios for the UMR-IWW System.

This chapter briefly describes the models used to estimate hydraulic conditions characteristic of selected pools, the physical forces produced by commercial vessels, and vessel-induced sediment resuspension and movement. The operational (i.e., data and information) connections that will integrate the models are also listed.

Physical and Hydrodynamic Forces Models

Several hydrodynamic and hydraulic models have been developed or implemented from existing models to support the Navigation Study ecological risk assessments. These models are briefly described in the following section. More detailed descriptions are presented in other reports in the Navigation Study technical publications series. Emphasis is placed primarily on model results that are needed by the ecological models (Chapter 3) to calculate ecological impacts and risk.

NAVEFF

The NAVEFF model estimates the "far-field" changes in current velocity and return currents produced by a passing commercial vessel (Maynord 1999). The model derives from the analysis of large-scale laboratory experiments performed using scaled-down physical replicas of selected UMR-IWW System river segments and scale models of commercial vessel and barge configurations. Physically moving the model vessel through the instrumented model channel provides for direct measurement of current velocities and wave heights induced by the moving vessel. Repeated experiments with scale models of different river segments generated data sets that were used to develop the NAVEFF computer model. The physical forces generated by the NAVEFF have been estimated for all 108 possible traffic configurations. The results have been stored as GIS coverages for all the cells in each pool.

DIFFLARV

The physical mixing model, DIFFLARV, estimates the time and distance between successive commercial vessels required for complete mixing of the river channel for varying vessel configurations, discharge regimes, and channel bathymetry (Holley 1997). The CEM model assumes complete mixing between vessel passages, and DIFFLARV serves as a tool to evaluate this important assumption. The DIFFLARV model also includes the Blau and van der Kaa equations that calculate the rate of water entrainment (m^3/s) through the propeller jet for the different vessel configurations, channel bathymetry, and flow conditions. The entrainment rate is the basis for estimates of CEM for larval fish in the Navigation Study Fish Ecological Risk Assessment.

NAVSED

The time series of suspended sediment concentrations produced by a passing commercial vessel was simulated using the NAVSED model (Copeland et al. 1999). This model is a modification of the NAVEFF that incoporates an algorithm for estimating sediment resuspension in relation to vessel characteristics, sediment type, and hydraulic conditions at the main channel border. Sediment concentration time series were calculated for all 108 vessel configurations under conditions of low, medium, and high discharge, beginning with the LTRMP trend pools. Sediment time series were also being simulated given different probabilities of vessel location in the navigation channel (i.e., sailing line).

RMA-2

The RMA-2 model simulates detailed ambient current velocities for selected pools of the UMR-IWW System. Initial efforts focused on UMR Pools 4, 8, 13 and 26, the IWW LaGrange Pool, and the open river (e.g., River Miles 30-80). The model uses a detailed grid of river bathymetry and river discharge to simulate current velocities in the main channel, side channels, and backwaters.

HIVEL

The HIVEL model has been applied to selected segments of the UMR-IWW System in order to simulate the “near-field” impacts of moving commercial vessels in producing current velocities and sediment resuspension in the immediate vicinity of the vessel. The HIVEL also models the transport and deposition of suspended sediments.

Model Integration

The following discussion briefly outlines the integration of the physical forces models with the biological models developed for the Navigation Study ecological risk assessments.

NAVEFF

The wave heights and current velocities generated by the NAVEFF serve as input data for the fish spawning habitat models and the rule-based model for physical breakage of submerged aquatic vegetation.

DIFFLARV

There is no direct interconnection between the DIFFLARV and the ecological models. The model exists to separately and independently evaluate the assumption of complete mixing between successive vessel passages within a pool. For computational purposes, it proved convenient to code the entrainment velocity equations into a separate program that produces an input data file for the CEM model.

NAVSED

The NAVSED model was used to estimate sediment resuspension by commercial vessels. The time series of sediment concentrations for appropriate cells in the LTRMP trend pool GIS coverages were input to the plant growth models to estimate reductions in growth and vegetative reproduction. These suspended sediment concentrations were also used to estimate commercial traffic impacts on freshwater mussel bioenergetics, growth, and reproduction.

RMA-2

Ambient current velocities are needed for the physical forces screening calculations of submerged aquatic vegetation breakage, for sediment suspension calculations, for NAVEFF calculations, and fish spawning habitat suitability models. The RMA-2 model provided detailed simulations of current velocities for selected portions of several pools in the UMR-IWW System.

HIVEL

The results of the HIVEL can provide additional information concerning the concentration of suspended sediments for portions of the river where, for example, mussel beds might be located. These sediment concentrations in relation to hydraulic and hydrodynamic conditions and vessel configuration can also be used to develop rule-based models to assist in extrapolating the impacts of commercial vessels to other river segments that are not directly modeled.

System Model Structure

The system model developed in support of the Navigation Study will be a distributed modeling system. It will not likely exist as a single computer program. The operational objective is to develop a set of interactive hydrodynamic, hydraulic, and ecological models that can share data and results in the assessment of commercial navigation impacts on ecological resources, as well as other navigation-related issues (e.g., bank erosion and backwater sedimentation). Most of the existing codes have been developed in FORTRAN or BASIC and establishing the operational linkages among the models will be

fairly straightforward: the file of hydraulic or hydrodynamic results can be automatically formatted as input to the ecological models. To facilitate model integration, it has proven effective and economical to store the results of model calculations (e.g., NAVEFF results) as "data layers" in a GIS. Using this approach, the ecological effects models can retrieve the necessary results without necessarily having to re-run the physical forces model.

6 Risk-Based Decision Making

Ultimately, the results of the risk assessments will be used in a decision-making context. Risks will have to be evaluated in terms of their significance. The set of decisions will likely include alternative approaches for avoiding, if possible, impacts and risks. For situations where avoidance is not feasible or realistic, selecting among alternatives for minimizing and/or mitigating impacts or risks will be necessary. The system model that essentially captures and operationally summarizes the overall assessment will provide a scientifically-defensible approach for decisions that economically and effectively reduce risks.

Importantly, upon completion of the Navigation Study ecological risk assessments, a set of integrated physical forces and ecological models will have been developed, implemented, and evaluated for the UMR-IWW System. This integrated system model will provide USACOE planning personnel, resource managers, and decision makers with additional capabilities to characterize ecological impacts and risks. The system model will also help address questions concerning site-specific modifications or additions of navigation infrastructure, exploration of alternative plans for operation and maintenance, and other resource management challenges.

7 Bibliography

Aldridge, D. W., Payne, B. S., and Miller, A. C. (1987). "The effects of intermittent exposure to suspended solids on three species of freshwater mussels," *Environmental Pollution* 45, 17-28.

Ayyub, B. M., and McCuen, R. H. (1987). "Quality and uncertainty assessment of wildlife habitat with fuzzy sets," *Journal of Water Resources Planning and Management* 113, 95-109.

Balon, E. K. (1975). "Reproductive guilds of fishes: a proposal and definition," *Journal of the Fisheries Research Board of Canada* 32, 821-864.

Bartell, S. M. (1996). "Ecological/environmental risk assessment: principles and practices," *in* Kolluru, R. V., Bartell, S. M., Pitblado, R. M., Stricoff, R. S., Editors, *Risk Assessment and Management Handbook*, McGraw-Hill, Inc., New York, NY, 10.3-10.59.

Bartell, S. M., Gardner, R. H., and O'Neill, R. V. (1992). *Ecological Risk Estimation*, Lewis Publishers, Chelsea, MI.

Bayne, B. L., and Newell, R. C. (1983). "Physiological energetics of marine molluscs," *in The Mollusca. Volume 4*. Academic Press, New York, NY, pp. 207-515.

Bayne, B. L., and Worrall, C. M. (1980). "Growth and production of mussels, Mytilus edulis from two populations. *Marine Ecology Progress Series* 3, 317-328.

Becker, G. C. (1983). *Fishes of Wisconsin*. The University of Wisconsin Press, Madison, WI.

Best, E. P. H. (1987). "Characteristic photosynthesis and respiration rates under laboratory conditions, and in situ biomass production of *Elodea nuttallii* and *Potamogeton pectinatus* (Unpublished)," Centre for Agrobiological Research, Wageningen, The Netherlands.

Best, E. P. H., and Boyd, W. A. (1996). "A simulation model for growth of the submersed aquatic macrophyte hydrilla (*Hydrilla verticillata* (L.F.) Royle," Technical Report A-96-8, U.S. Army Corps of Engineers, Waterways Experiment Station, Vicksburg, MS. 43 p. + app.

Best, E. P. H., and Boyd, W. A. (1999a). "A simulation model for growth of the submersed aquatic macrophyte sago pondweed (*Potamogeton pectinatus* L.) (Draft)," Technical Report A-99-x, U.S. Army Corps of Engineers, Waterways Experiment Station, Vicksburg, MS.

Best, E. P. H., and Boyd, W. A. (1999b). "POTAM (Version 1.0): A simulation model for growth of sago pondweed (Draft)," Instruction Report A-99-x, U.S. Army Corps of Engineers, Waterways Experiment Station, Vicksburg, MS.

Best, E. P. H., and Boyd, W. A. (1999c). "A simulation model for growth of the submersed aquatic macrophyte wild celery (*Vallisneria americana* Michx.) (Draft)," Technical Report A-99-x, U.S. Army Corps of Engineers, Waterways Experiment Station, Vicksburg, MS.

Best, E. P. H., and Boyd, W. A. (1999d). "VALLA (Version 1.0): A simulation model for growth of wild celery (Draft)," Instruction Report A-99-x, U.S. Army Corps of Engineers, Waterways Experiment Station, Vicksburg, MS.

Beverton, R. J. H., and Holt, S. J. (1957). *On the Dynamics of Exploited Fish Populations*. Fish. Invest. Series 2, Ministry of Agriculture, Fisheries, and Food, London.

Bick, H., and Van Schaik, A. W. J. (1980). "Oecologische visie randmeren," Advies van de Natuurwetenschappelijke Commissie van de Natuurbeschermingsraad, 291 pp. (In Dutch).

Biggs, B. J. F. (1996). "Hydraulic habitat of plants in streams," *Regulated Rivers: Research and Management* 12, 131-144.

Boreman, J., and Goodyear, C. P. (1988). "Estimates of entrainment mortality for striped bass and other fish species inhabiting the Hudson River Estuary," *American Fisheries Society Monograph* 4, 152-160.

Boreman, J., Goodyear, C. P., and Christensen, S. W. (1981). "An empirical model for estimating entrainment losses at power plants sited on estuaries," *Transactions of the American Fisheries Society* 110, 253-260.

Boyd, W. A., and Best, E. P. H. (1996). "HYDRIL (Version 1.0): A simulation model for growth of hydrilla," Instruction Report A-96-1, U.S. Army Corps of Engineers, Waterways Experiment Station, Vicksburg, MS. 30 p.

Bowes, G., Van, T. K., Garrard, L. A., and Haller, W. T. (1977). "Adaptation to low light levels by hydrilla," *Journal of Aquatic Plant Management* 15, 32-35.

Brown, D. J., and Coon, T. G. (1994). "Abundance and assemblage structure of fish larvae in the Lower Missouri River and its tributaries," *Transactions of the American Fisheries Society* 123, 718-732.

Butler, R. L., and Smith Jr., L. L. (1950). "The age and rate of growth of the sheepshead, *Aplodinotus grunniens* Rafinesque, in the Upper Mississippi

River navigation pools," *Transactions of the American Fisheries Society* 79, 43-54.

Calow, P. (1983). "Life-cycle patterns and evolution," *in The Mollusca. Volume 6*. Academic Press, New York, NY, pp. 649-678.

Campbell, K. R., and Bartell, S. M. (1998). "Ecological models and ecological risk assessment," *in* Newman, M. C. and Strojan, C. L., Editors, *Risk Assessment: Logic and Measurement*, Ann Arbor Press, Chelsea, MI, 69-100.

Chambers, P. A., Prepas, E. E., Hamilton, H. R., and Bothwell, M. L. (1991). "Current velocity and its effect on aquatic macrophytes in flowing waters," *Ecological Applications* 1, 249-257.

Conner, J. V., Pennington, C. H., and Bosley, T. R. (1983). "Larval fish of selected aquatic habitats on the Lower Mississippi River," Technical Report E-83-4, U.S. Army Engineer Waterways Experiment Station, Vicksburg, MS.

Coops, H., and Van der Velde, G. (1996). "Effects of waves on helophyte stands: mechanical characteristics of stems of *Phragmites australis* and *Scirpus lacustris*," *Aquatic Botany* 53, 175-185.

Copeland, R. R., Abraham, D. D., Nail, G. H., Seal, R., and Brown, G. L. (1999). "Sedimentation study, numerical model investigation (Draft)," ENV Report No. 25, U.S. Army Corps of Engineers, Waterways Experiment Station, Vicksburg, MS.

Daiber, F. C. (1953). "Notes on the spawning population of the freshwater drum (*Aplodinotus grunniens* Rafinesque) in Western Lake Erie," *The American Midland Naturalist* 50(1), 159-171.

Dirksen, S. (1982). "The importance of pondweed for Bewicks swans in the Lauwersmeer," *Limosa* 55, 30-31 (In Dutch).

Donnermeyer, G. N., and Smart, M. M. (1985). "The biomass and nutritive potential of *Vallisneria americana* Michx in Navigation Pool 9 of the Upper Mississippi River," *Aquatic Botany* 22, 33-44.

Doyle, R. D. (1999). "Effects of waves on the early growth of *Vallisneria americana*," ENV Report 12, U.S. Army Corps of Engineers, Waterways Experiment Station, Vicksburg, MS.

Dreves, D. P., Timmons, T. J., and Henson, J. (1996). "Age, growth, and food of freshwater drum, *Aplodinotus grunniens* (Sciaenidae), in Kentucky Lake, Kentucky/Tennessee," *Transactions of the Kentucky Academy of Science* 57(1), 22-26.

Etnier, D. A., and Starnes, W. C. (1993). *The Fishes of Tennessee*. University of Tennessee Press, Knoxville, TN.

Fausch, K. D., Hawkes, C. L., and Parsons, M. G. (1988). "Models that predict standing crop of stream fish from habitat variables: 1950-85," General Technical Report PNW-GTR-213, Portland, OR, US Department of Agriculture, Forest Service, Pacific Northwest Research Station. 52 p.

Fremling, C. R., and Claflin, T. O. (1984). "Ecological history of the Upper Mississippi River," *in* Wiener, J. G., Anderson, R. V., and McConville, D. R., Editors, *Contaminants in the Upper Mississippi River*. Butterworth Publishers, Boston, MA.

Golterman, H. L. (1975). *Physiological Limnology. An Approach to the Physiology of Lake Ecosystems*, Elsevier Scientific Publishing Company, Amsterdam, Holland. 489 p.

Goodyear, C. P. (1978). "Entrainment impact estimates using the equivalent adult approach," Report FWS/OBS-78/65, U.S. Fish and Wildlife Service, Office of Biological Service, Washington, DC.

Goudriaan, J. (1986). "A simple and fast numerical method for the computation of daily totals of crop photosynthesis," *Agricultural and Forestry Meteorology* 38, 251-255.

Grier, N. M. (1926). "Notes on the naiades of the upper Mississippi drainage: III. On the relation of temperature to the rhythmical contractions of the "mantle flags" in *Lampsilis ventricosa*," *The Nautilus* 39,111-114.

Griffin, K. L. (1994). "Caloric estimates of construction cost and their use in ecological studies," *Functional Ecology* 8, 551-562.

Gutreuter, S. (1997). "Fish monitoring by the long term resource monitoring program on the Upper Mississippi River System: 1990-1994," Technical Report 97-T004, U.S. Geological Survey, Onalaska, WI,

Gutreuter, S., Burkhardt, R. W., Stopyro, M., Bartels, A., Kramer, E., Bowler, M. C., Cronin, F. A., Soergel, D. W., Petersen, M. D., Herzog, D. P., Irons, K. S., O'Hara, T. M., Blodgett, K. D., and Raibley, P. T. (1997). "1992 Annual Status Report: A summary of fish data in six reaches of the Upper Mississippi River System," Program Report 97-P006, U.S. Geological Survey, La Crosse, WI,.

Haller, W. T. (1974). "Photosynthetic characteristics of the submersed aquatic plants hydrilla, southern naiad, and Vallisneria," Ph.D. Thesis, University of Florida, Gainesville, FL. 88 p.

Holland, L. E. (1986). "Distribution of early life history stages of fishes in selected pools of the Upper Mississippi River", *Hydrobiologia* 136, 121-130.

Holland, L. E., and Sylvester, J. R. (1983). "Distribution of larval fishes related to potential navigation impacts on the Upper Mississippi River, Pool 7," *Transactions of the American Fisheries Society* 112, 293-301.

Holland, L., Hornung, T., Huston, M., and Duval, M. (1984). *Analysis of Existing Information on Ichthyoplankton Drift Through Dams on the Upper Mississippi River*. U.S. Fish and Wildlife Service, La Crosse, WI.

Holland-Bartels, L.E., Dewey, M.R., and Zigler, S.J. (1990a). "Pilot study of spatial patterns of ichthyoplankton among river reaches and habitats of the Upper Mississippi River System," U.S. Fish and Wildlife Service, La Crosse, WI.

Holland-Bartels, L.E., Littlejohn, S.K., and Huston, M.L. (1990b). *A Guide to Larval Fishes of the Upper Mississippi River*. United States Fish and Wildlife Service, La Crosse, WI.

Holley E. R. (1997). "Computer model for transport of larvae between barge tows in rivers (Draft Report)," ENV Report 26, U.S. Army Corps of Engineers, Waterways Experiment Station, Vicksburg, MS.

Horst, T. J. (1975). "The assessment of impact due to entrainment of ichthyoplankton," *in* Saila, S. R., Editor, *Fisheries and Energy Production: A Symposium*, Lexington Books, Lexington, MA, 107-118.

Hunt, R. (1982). *Plant Growth Curves*, Arnold, London.

Isely, F. B. (1914). "Experimental study of the growth and migration of fresh–water mussels. Appendix III," Report, U.S. Commissioner of Fisheries, 24 p.

Jensen, A. L. (1990). "Estimation of recruitment forgone resulting from larval fish entrainment," *Journal of Great Lakes Research* 16, 241-244.

Jensen, A. L., Reider, R. H., and Kovalak, W. P. (1988). "Estimation of production forgone," *North American Journal of Fisheries Management* 8, 191-198.

Johnson, B. L. (1993). "Review of existing models for evaluating fish population changes relative to environmental impacts." EMTC 93-S005, U.S. Fish and Wildlife Service, National Fisheries Research Center, La Crosse, WI, Environmental Management Technical Center, Onalaska, WI, 25 p.

Kaplan, S., and Garrick, B. J. (1981). "On the quantitative definition of risk," *Risk Analysis* 1, 11-27.

Killgore, K. J., Maynord, S. T., Chan, M. D., and Morgan, II, R. P. (1997). "Effects of propeller entrainment on riverine ichthyoplankton (Draft)." ENV Report 2, U.S. Army Corps of Engineers, Waterways Experiment Station, Vicksburg, MS.

Korschgen, C. E., George, L. S., and Green, W. L. (1988). "Feeding ecology of canvasbacks staging on Pool 7 of the Upper Mississippi River," *in* Weiler, M. W., Editor, *Waterfowl in Winter*, University of Minnesota Press, Minneapolis, MN, 237-249.

Korschgen, C. E., and Green, W. L. (1988). "American wild celery (*Vallisneria americana*): ecological considerations for restoration," Fish and Wildlife Technical Report 19, U.S. Department of the Interior Fish and Wildlife Service, Washington, DC.

Korschgen, C. E., Green, W. L., and Kenow, K. P. (1997). "Effects of irradiance on growth and winter bud production by *Vallisneria americana* and consequences to its abundance and distribution," *Aquatic Botany* 58, 1-9.

Leidy, G. R., and Jenkins, R. M. (1977). "The development of fishery compartments and population rate coefficients for use in reservoir ecosystem modeling," Contract Report Y-77-1.

Littlejohn, S., Holland, L., Jacobson, R., Huston, M., and Hornung, T. (1985). "Habits and habitats of fishes in the Upper Mississippi River," U.S. Fish and Wildlife Service, La Crosse, WI.

Lucas, A. (1996). *Bioenergetics of aquatic animals*. Taylor and Francis, Inc., Bristol, PA.

Martischang, M. F. (1992). "Using an address matching approach to represent locations of fish habitat in a geographic information system," *in* Greer, J. D., Editor, *Remote Sensing & Natural Resource Management,* American Society for Photogrammetry and Remote Sensing. Bethesda, MD, 355-369.

Maynord, S. (1999). "Comparison of NAVEFF model to field return velocity and drawdown data," ENV Report 14, U.S. Army Corps of Engineers, Waterways Experiment Station, Vicksburg, MS.

Pauly, D. (1980). "On the interrelationships between natural mortality, growth parameters, and mean environmental temperature in 175 fish stocks," *Journal Du Conseil. Conseil International Pour L'Exploration De La Mer* 39(2), 175-192.

Payne, B. S., and Miller, A. C. (1989). "Growth and survival of recent recruits to a population of *Fusconaia ebena* (Bivalvia: Unionidae) in the lower Ohio River," *The American Midland Naturalist* 121, 99-104.

Payne, B. S., Miller, A. C., and Shaffer, L. (1997). "Physiological effects on freshwater mussels (Family: Unionidae) of intermittent exposure to physical effects of navigation traffic (Draft)," ENV Report 6, U.S. Army Engineer Waterways Experiment Station, Vicksburg, MS.

Penning de Vries, F. W. T., and Van Laar, H. H. (1982a). "Simulation of growth processes and the model BACROS. Simulation of plant growth and crop production," Pudoc, Wageningen, 99-102.

Penning de Vries, F. W. T., and Van Laar, H. H. (1982b). "Simulation of growth processes and the model BACROS, Simulation of plant growth and crop production," Pudoc, Wageningen, 114-131.

Pflieger, W. L. (1997). *The Fishes of Missouri*. Revised edition. Missouri Department of Conservation, Jefferson City, MO.

Pitlo Jr., J., Van Vooren, A., and Rasmussen, J. (1995). "Distribution and relative abundance of Upper Mississippi River fishes," Upper Mississippi River Conservation Committee, Rock Island, IL.

Post, J. R., Rudstam, L. G., and Schael, D. M. (1995). "Temporal and spatial distribution of pelagic age-0 fish in Lake Mendota, Wisconsin," *Transactions of the American Fisheries Society* 124, 84-93.

Rago, P. J. (1984). "Production forgone: an alternative method for assessing the consequences of fish entrainment and impingement losses at power plants and other water intakes," *Ecological Modelling* 24, 79-111.

Rasmussen, J. L. (1979). "A compendium of fishery information on the Upper Mississippi River," Upper Mississippi River Conservation Committee, Rock Island, IL.

Ricker, W. E. (1975). *Computation and Interpretation of Biological Statistics of Fish Populations*. Fisheries Research Board of Canada Bulletin 191, Fisheries and Marine Service, Ottawa.

Schaeffer, D. J., Martin, J. A., Brent, R., Tompkins, M., and Hauser, T. (1998). "Effects of commercial navigation traffic on freshwater mussels in the Upper Mississippi River System." Draft Technical Report, EcoHealth Research, Inc., Champaign, IL.

Schneider, D. W. (1992). "A bioenergetics model of zebra mussel, *Dreissena polymorpha*, growth in the Great Lakes," *Canadian Journal of Fish and Aquatic Science* 149, 1406-1416.

Scott, W. B., and Crossman, E. J. (1973). *Freshwater Fishes of Canada*. Bulletin 184, Fisheries Research Board of Canada, Ottawa.

Sher Kaul, S., Oertli, B., Castella, E., and Lachavanne, E. (1995). "Relationship between biomass and surface area of six submerged aquatic plant species," *Aquatic Botany* 51, 147-154.

Spencer, D. F., and Anderson, L. W. J. (1987). "Influence of photoperiod on growth, pigment composition and vegetative propagule formation for *Potamogeton nodosus* and *Potamogeton pectinatus* L.," *Aquatic Botany* 28, 103-112.

Spitters, C. J. T. (1986). "Separating the diffuse and direct component of global radiation and its implications for modeling canopy photosynthesis. II. Calculation of canopy photosynthesis," *Agricultural and Forestry Meteorology* 38, 231-242.

Stein, C. B. (1973). "The life history of *Amblema plicata*, the three ridge naiad," Ph.D. Dissertation, Ohio State University.

Stewart, R. M., McFarland, D. G., Ward, D. L., Martin, S. K., and Barko, J. W. (1997). "Flume study investigation of the direct impacts of navigation-generated waves on submersed aquatic macrophytes in the Upper Mississippi River," ENV Report 1, U.S. Army Corps of Engineers, Waterways Experiment Station, Vicksburg, MS.

Swedberg, D. V., and Walburg, C. H. (1970). "Spawning and early life history of the freshwater drum in Lewis and Clark Lake, Missouri River," *Transactions of the American Fisheries Society* 99(3), 560-570.

Thornley, J. H. M., and Johnson, I. R. (1990a). "Development," *in Plant and Crop Modelling. A Mathematical Approach to Plant and Crop Physiology*, Clarendon Press, Oxford, 139-144.

Thornley, J. H. M., and Johnson, I. R. (1990b). "Plant growth functions," *in Plant and Crop Modelling. A Mathematical Approach to Plant and Crop Physiology*. Clarendon Press, Oxford, 74-89.

Thornton, K. W., and Lessem, A. S. (1978). "A temperature algorithm for modifying biological rates," *Transactions of the American Fisheries Society* 107(2), 284-287.

Titus, J., Goldstein, R. A., Adams, M. A., Mankin, J. B., O'Neill, R. V., Weiler, P. R., Shugart, H. H., and Booth, R. S. (1975). "A production model for *Myriophyllum spicatum* L.," *Ecology* 56, 1129-1138.

Titus, J., and Adams, M. A. (1979a). "Coexistence and the comparative light relations of the submersed macrophytes *Myriophyllym spicatum* L. and *Vallisneria americana* Michx.," *Oecologia (Berlin)* 40, 273-286.

Titus, J. E., and Adams, M. A. (1979b). "Comparative carbohydrate storage and utilization patterns in the submersed macrophytes, *Myriophyllym spicatum* and *Vallisneria americana*," *The American Midland Naturalist* 102, 263-272.

Titus, J. E., and Stephens, M. D. (1983). "Neighbor influences and seasonal growth patterns for *Vallisneria americana* in a mesotrophic lake," *Oecologia* 56, 23-29.

U.S. Army Corps of Engineers (USACOE). (1994). "Navigation predictive analysis technique (NAVPAT) pilot application for Pool 13, Upper Mississippi River." U.S. Army Corps of Engineers, Louisville District, Louisville, KY.

U.S. Environmental Protection Agency (USEPA). (1998). "Guidelines for ecological risk assessment." PA/630/R-95/002F, U.S. Environmental Protection Agency, Risk Assessment Forum, Washington, DC.

U.S. Geological Survey (USGS). (1999). "Ecological status and trends of the Upper Mississippi River System 1998: A report of the Long Term Resource Monitoring Program," LTRMP 99-T001, U.S. Geological Survey, Upper Midwest Environmental Sciences Center, La Crosse, WI.

Van der Bijl, L., Sand-Jensen, K., and Hjermind, A. L. (1989). "Photosynthesis and canopy structure of a submerged plant, *Potamogeton pectinatus*, in a danish lowland stream," *Journal of Ecology* 77, 947-962.

Van der Schalie, H., and Van der Schalie, A. (1950). "The mussels of the Mississippi River," *The American Midland Naturalist* 44, 448–466.

Van der Zweerde, W. (1981). "Research of the influence of light intensity and day length on the formation of turions in the aquatic macrophyte *Hydrilla verticillata* Royle," Student Report, Centre for Agrobiological Research, Wageningen (In Dutch).

Van Dijk, G. M., Breukelaar, A. W., and Gijlstra, R. (1992). "Impact of light climate history on seasonal dynamics of a field population of *Potamogeton pectinatus* L. during a three-year period (1986-1988)," *Aquatic Botany* 43, 17-41.

Van Vierssen, W., Mathies, A., and Vermaat, J. E. (1994). "Early growth characteristics of *Potamogeton pectinatus* L.: the significance of the tuber," *in* van Vierssen, W., Hootsmans, M., and Vermaat, J., Editors, *Lake Veluwe, A Macrophyte-dominated System under Eutrophication Stress*. Kluwer Academic Publishers, Dordrecht, Boston, London, 135-144.

Van Vooren, A. (1983). "Distribution and relative abundance of Upper Mississippi River fishes," Upper Mississippi River Conservation Commission, Fish Technical Section, Rock Island, IL.

Van Wijk, R. J. (1989). "Ecological studies on *Potamogeton pectinatus* L. I. General characteristics, biomass production and life cycles under field conditions," *Aquatic Botany* 31, 211-258.

Wetzel, R. L., and Neckles, H. A. (1986). "A model of *Zostera marina* L. photosynthesis and growth: simulated effects of selected physical-chemical variables and biological interactions," *Aquatic Botany* 26, 307-323.

Whitney, S. D., Blodgett, K. D., and Sparks, R.E. (1997a). "A comprehensive mussel survey of the Illinois River, 1993–1995," Draft Technical Report, Illinois Natural History Survey, Champaign, IL.

Whitney, S. D., Blodgett, K. D., and Sparks, R. E. (1997b). "A comprehensive evaluation of three mussel beds in Reach 15 of the Upper Mississippi River," Report Reprint 97–R022, U.S. Geological Survey, Environmental Management Technical Center, Onalaska, WI.

Wilbur, K. M. (Editor) (1983). *The Mollusca*. Volumes 2, 4, 5, 6, and 7. Academic Press, New York, NY.

Zigler, S. J., and Jennings, C. A. (1993). "Mortality rates of early developmental stages of freshwater drum and sunfish in the Upper Mississippi River System," EMTC 93-S019, National Biological Survey, National Fisheries Research Center, La Crosse, WI.

REPORT DOCUMENTATION PAGE

Form Approved
OMB No. 0704-0188

1. REPORT DATE *(DD-MM-YYYY)*	2. REPORT TYPE	3. DATES COVERED *(From - To)*
September 2003	Interim report	

4. TITLE AND SUBTITLE

Ecological Models and Approach to Ecological Risk Assessments

5a. CONTRACT NUMBER

5b. GRANT NUMBER

5c. PROGRAM ELEMENT NUMBER

6. AUTHOR(S)

Steven M. Bartell, Kym Rouse Campbell, Erin M. Miller, Shyam K. Nair, Elly P. H. Best, and David J. Schaeffer

5d. PROJECT NUMBER

5e. TASK NUMBER

5f. WORK UNIT NUMBER

7. PERFORMING ORGANIZATION NAME(S) AND ADDRESS(ES)

The Cadmus Group, Inc., 136 Mitchell Road, Oak Ridge, TN 37830;
U.S. Army Engineer Research and Development Center, Environmental Laboratory, 3909 Halls Ferry Road, Vicksburg, MS 39180-6199;
EcoHealth Research, Inc., 701 Devonshire Driver, Champaign, IL 61820

8. PERFORMING ORGANIZATION REPORT NUMBER

ENV Report 38

9. SPONSORING / MONITORING AGENCY NAME(S) AND ADDRESS(ES)

See reverse

10. SPONSOR/MONITOR'S ACRONYM(S)

11. SPONSOR/MONITOR'S REPORT NUMBER(S)

12. DISTRIBUTION / AVAILABILITY STATEMENT

Approved for public release; distribution is unlimited.

13. SUPPLEMENTARY NOTES

14. ABSTRACT

The Navigation Study being performed by the U.S. Army Corps of Engineers is assessing the potential environmental impacts associated with anticipated increases in commercial navigation traffic on the Upper Mississippi River-Illinois Waterway System. Each Navigation Study ecological risk assessment addresses a time period beginning with the present condition (defined as 2000) and continuing through the year 2050, in 10-year increments. Upon completion, the assessments will fulfill a requirement of the National Environmental Policy Act of 1969, and a subsequent Environmental Impact Statement, summarizing the results of each risk assessment, will be prepared. This report describes the overall approach adopted for performing the environmental assessments and presents several ecological models that were instrumental in their completion. The report also briefly outlines several hydraulic and hydrodynamic models necessary for the assessments and discusses their integration with the ecological models to estimate ecological impacts. Specific assessment results for each of the component ecological risk assessments (fish, submerged aquatic plants, and freshwater mussels) for future traffic scenarios are presented in separate reports of the Navigation Study series of technical publications.

15. Subject Terms

See reverse

16. SECURITY CLASSIFICATION OF:			17. LIMITATION OF ABSTRACT	18. NUMBER OF PAGES	19a. NAME OF RESPONSIBLE PERSON
a. REPORT	b. ABSTRACT	c. THIS PAGE			19b. TELEPHONE NUMBER *(include area code)*
UNCLASSIFIED	UNCLASSIFIED	UNCLASSIFIED		108	

9. SPONSORING / MONITORING AGENCY NAME(S) AND ADDRESSES (Concluded).

U.S. Army Engineer District, Rock Island, Clock Tower Building, P.O. Box 2004, Rock Island, IL 61204-2004

U.S. Army Engineer District, St. Louis, 1222 Spruce Street, St. Louis, MO 63103-2833

U.S. Army Engineer District, St. Paul, Army Corps of Engineers Centre, 190 5th Street East, St. Paul, MN 55101-1638

15. SUBJECT TERMS

Ecological risk assessment
Ecological impacts of commercial navigation
Larval fish entrainment
Submersed aquatic plant growth
Fish spawning habitat
Unionid mussel growth and reproduction
Uncertainty analysis